UNIVERSITY OF BELGRADE

SCHOOL OF ELECTRICAL ENGINEERING

MOHAMED B. JANNAT

ANALYSIS OF OPTIMAL SIZING AND LOCATION OF SHUNT CAPACITORS IN ACTIVE DISTRIBUTION NETWORKS

Doctoral Dissertation

Belgrade, 2018

UNIVERZITET U BEOGRADU
ELEKTROTEHNIČKI FAKULTET

MOHAMED B. JANNAT

ANALIZA OPTIMALNE SNAGE I LOKACIJE OTOČNIH BATERIJA KONDENZATORA U AKTIVNIM DISTRIBUTIVNIM MREŽAMA

Doktorska Disertacija

Beograd, 2018

PODACI O MENTORU I ČLANOVIMA KOMISIJE

Mentor:

Dr Željko Đurišić, docent

(Univerzitet u Beogradu, Elektrotehnički fakultet)

Članovi komisije:

Dr Željko Đurišić, docent

(Univerzitet u Beogradu, Elektrotehnički fakultet)

Dr Zlatan Stojković, redovni profesor

(Univerzitet u Beogradu, Elektrotehnički fakultet)

Dr Čedomir Zeljković, docent

(Univeritet u Banja Luci, Elektrotehnički fakultet)

Dr Nikola Rajaković, redovni profesor u penziji

(Univerzitet u Beogradu, Elektrotehnički fakultet)

Dr Aleksandar Savić, docent

(Univerzitet u Beogradu, Elektrotehnički fakultet)

Datum usmene odbrane:_____

List of Contents

List of Figures

List of Tables

Author's publications

Papers published in international scientific journals:

1. **Mohamed B. Jannat**, Aleksandar S. Savić, Optimal capacitor placement in distribution networks regarding uncertainty in active power load and distributed generation units production, IET Generation, Transmission & Distribution, 2016, Volume 10, Issue 12, pp. 3060 - 3067, DOI: 10.1049/iet-gtd.2016.0192 ISSN 1751-8695, IF 1,576, (M22).

Papers published in international scientific conferences:

1. **Mohamed Jannat**, Aleksandar Savić, Jamal Abdulmalek, " Using of Genetic Algorithms (GAs) to find the optimal power flow Case study (the 23 bus Serbian system) ", 2nd International Conference on Automation, Control, Engineering & Computer Science, March 2015, Tunisia, (M33).

Papers published in domestic scientific conferences:

1. **Mohamed Jannat**, Aleksandar Savić, " Calculation of optimal power flow by using a genetic algorithm ", Energija, ekonomija, ekologija, pp. 107-111, No. 3-4, XVII, Mart 2015, ISSN br. 0354-8651, (M51).

2. Jelena Kušić, **Mohamed Jannat**, Aleksandar Savić, " Calculation of the available transmission capacity using the sensitivity method and the Monte Carlo simulation ", Energija, ekonomija, ekologija, pp. 222-226, No. 1-2, XVIII, Mart 2016, ISSN br. 0354-8651, (M51).

ANALYSIS OF OPTIMAL SIZING AND LOCATION OF SHUNT CAPACITORS IN ACTIVE DISTRIBUTION NETWORKS

Abstract

The increase in power demand requires an increase in the number of feeder or feeder capacity, more generation and expand the network by increasing substation capacity as well as equipment capacity. These options are expensive. In addition, the flow of reactive power in distribution systems increases the losses and reduces the line voltages particularly at heavy loads where the voltage at buses reduces when moved away from the substation, and the losses are high. In order to minimise those losses and to maintain the voltage profile within acceptable limits, reactive power compensation is used. Reactive power compensation can be beneficial if they are correctly applied by choosing the correct location and size of the compensation. Commonly, the capacitors are used for the reactive power compensation.

Shunt capacitors are used for a voltage profile improvement, maximise transmitted power flowing through the networks and improving the efficiency of distribution systems. There are many ways to install shunt capacitors, but it is very difficult to determine the best locations and size of shunt capacitors. In addition, the stochastic nature of loads in systems makes the placement becomes more complicated.

The aim of this thesis is to introduce a new method for finding the optimal size and location of the shunt capacitors using multiobjective optimisation. The proposed method, based on the application of the Monte Carlo Simulation methods, respects the uncertainties associated with load demand and renewable sources power production. In addition, this method takes into account the correlation between sets of random variables.

Active power consumption for the distribution network has been modeled by using one-year measurements at the feeding transformer station. The measured data converted to the load duration curve then the load duration curve was modeled by the multistep load model by applying clustering technique. For wind turbines, data on wind speed have been obtained by the measurements taken at the analyzed location for the period of one year. The Weibull PDF (Probability Density Function) adequately models the measured wind data thus the parameters of Weibull PDF were calculated. In the

same time, Beta PDF appropriately models the random variations of the solar radiation. On the basis of the measured data, the shape parameters of Beta PDF were obtained.

The optimisation problem was modeled by two objective functions with the aim of improving voltage profile in a network by optimal selection of the locations and installed powers of the shunt capacitors. The first objective function aims to improve voltage profile of the network by minimising the sum of square deviations of the expected voltage value from the reference value. The goal of the second objective function is minimisation the sum of installed powers of shunt capacitors. Here, if the installed power of the shunt capacitors is small, this will result in a slight voltage profile improvement and vice versa. Therefore, the two objective functions are contradictory. The suggested objective functions were optimised simultaneously by applying the Non-dominated Sorting Genetic Algorithm II (NSGA-II). NSGA-II algorithm was chosen because it represents one of the standard procedures for solving multiobjective optimisation problems. In addition, NSGA-II algorithm has been widely used for solving the problem of optimum placement of shunt capacitors.

The proposed method was applied to a real medium voltage distribution network supplying several small communities. Despite the production from renewable energy sources in this distribution network, there are significant voltage drops in the network and considerable active power losses. By applying this method to the distribution network in three scenarios, a set of optimal solutions was obtained for every scenario. Every solution gives specific powers and locations to install the shunt capacitors in the analyzed network. A set of optimal solutions generally gives more a complete description of the optimisation problem. In addition, because there are more compromise optimal solutions, more freedom in choosing the final solution will be given where the best suits solution can be chosen from the offered set of solutions.

The first and the second scenarios contained the installation of only one and two shunt capacitors respectively with and without taking into account the correlation between the random variables. The third scenario analyzed the installation of three shunt capacitors with taking into account the correlation between the random variables. With some comparisons, resulting in one scenario has been taken for further analysis. All obtained solutions are optimal therefore an additional analysis is required. To choose the best solution or the solution that contains the least violations of the permitted

limits, this thesis proposed comparing the minimum and maximum expected voltage values of the complete set of optimum solutions for the highest and the lowest load levels. Also, the expected active power and energy losses prior to and after building-in shunt capacitors were calculated to determine the expect annual active energy saving by the chosen solution. The cost of the expected annual energy saving and the cost of building-in shunt capacitors have been shown and compared to verify whether the building-in shunt capacitors from the chosen solution is a good economic investment.

Keywords: Optimal size and location of shunt capacitors, Multi-criteria optimisation, NSGA-II, Uncertainty in load demand and renewable sources generation, Correlation between random variables.

Scientific field: Technical science – Electrical engineering.

Specific scientific field: Power systems.

UDK: 621.3

ANALIZA OPTIMALNE SNAGE I LOKACIJE OTOČNIH BATERIJA KONDENZATORA U AKTIVNIM DISTRIBUTIVNIM MREŽAMA

Rezime

Povećanje potražnje za električnom energijom zahteva povećanje broja grana u mreži, povećanje proizvodnje, potrebu za proširenjem mreže, povećanje kapaciteta transformatorskih stanica kao i ostalih elemenata mreže. Ove aktivnosti su u suštini veoma skupe. Pored toga, protok reaktivne snage u distributivnim sistemima dodatno povećava gubitke i smanjuje napone u mreži. Ovo je posebno izraženo kod velikih opterećenja gde se naponi značajno smanjuju sa udaljenošću od transformatorske stanice. Pri tome i gubici u mreži se povećavaju. Kako bi se smanjili gubici i održao profil napona u prihvatljivim granicama, koristi se kompenzacija reaktivne snage. Kompenzacija reaktivne snage može biti korisna ako se pravilno izabere optimalna lokacija i snaga uređaja za kompenzaciju. Obično se za kompenzaciju reaktivne snage koriste otočni kondenzatori.

Otočni kondenzatori se koriste za poboljšanje naponskog profila, povećanje snage koja se može preneti kroz mrežu i poboljšanje efikasnosti distributivnih sistema. Postoje mnogi načini za instaliranje otočnih kondenzatora, ali je veoma teško odrediti najbolje lokacije i snage otočnih kondenzatora. Pored toga, stohastička priroda opterećenja u distributivnom sistemu dodatno komplikuje ovaj zadatak.

Cilj ove doktorske disertacije je uvođenje nove metode za pronalaženje optimalne veličine i lokacije otočnih kondenzatora primenom višekriterijumske optimizacije. Predloženi metod, zasnovan na primeni Monte Carlo simulacije, uvažava neizvesnosti vezane za snage potrošnje u čvorovima i snage proizvodnje obnovljivih izvora. Pored toga, ovaj metod uzima u obzir korelaciju između skupova slučajnih promenljivih.

Poštrošnja aktivne snage u distributivnoj mreži modelovana je na osnovu jednogodišnjih merenja u napojnoj transformatorskoj stanici. Izmereni podaci su konvertovani u krivu trajanja opterećenja, nakon čega je kriva trajanja opterećenja modelovana višestepenom krivom opterećenja primenom tehnike klasterovanja. Za vetrogeneratore, podaci o brzini vetra dobijeni su na osnovu merenja na analiziranoj lokaciji za period od jedne godine. Izmereni podaci su modelovani primenom Weibull-

ove raspodele gustine verovatnoće koja je standardna raspodela za ove svrhe. Slučajne varijacije sunčevog zračenja su modelovane Beta raspodelom gustine verovatnoće. Na osnovu izmerenih podataka na analiziranoj lokaciji određeni se parametri ove raspodele.

Optimizacioni problem je modelovan pomoću dve kriterijumske funkcije s ciljem poboljšanja naponskog profila u mreži optimalnim izborom lokacije i instalisane snage otočnih kondenzatora. Cilj prve kriterijumske funkcije je unapređenje naponskog profila mreže minimizacijom sume kvadrata odstupanja očekivane vrednosti napona od referentne vrednosti. Cilj druge kriterijumske funkcije je minimizacija ukupne instalisane snage otočnih kondenzatora. Jasno je da ako je instalisana snaga otočnih kondenzatora mala, to će rezultirati manjim poboljšanjem profila napona i obrnuto. Prema tome, ove dve kriterijumske funkcije su kontradiktorne. Predložene kriterijumske funkcije su simultano optimizovane primenom genetičkog algoritma sa sortiranjem prema nedominaciji (algoritam NSGA-II). Algoritam NSGA-II izabran je zato što predstavlja jednu od standardnih procedura za rešavanje problema višekriterijumske optimizacije. Pored toga, algoritam NSGA-II se često koristi za rešavanje problema optimalne loakcije otočnih kondenzatora.

Predloženi metod je primenjen na realnoj distributivnoj mreži srednjeg napona koja snabdeva nekoliko manjih mesta. Uprkos proizvodnji snage iz obnovljivih izvora, u ovoj distributivnoj mreži se imaju značajni padovi napona i znatni gubici aktivne snage. Primenom predložene metode na distributivnu mrežu za tri različita scenarija, dobijena su optimalna rešenja za svaki od scenarija. Svako rešenje daje snage i lokacije za ugradnju otočnih kondenzatora u analiziranoj mreži. Set optimalnih rešenja generalno daje bolje informacije o problema optimizacije. Pored toga, kada postoji više kompromisnih optimalnih rešenja, ima se veća sloboda u izboru konačnog rešenja, jer se najbolje rešenje može izabrati iz ponuđenog skupa rešenja.

Kod prvog i drugog scenarija analizirana je instalacija jednog, odnosno dva otočna kondenzatora, sa i bez uzimanja u obzir korelacije između slučajnih promenljivih. Kod trećeg scenarija analizirana je instalacija tri otočna kondenzatora sa uvažavanjem korelacije između slučajnih varijabli. Uz odgovarajuća poređenja odabran je jedan scenario za dalju analizu. Pošto su sva dobijena rešenja optimalna, izbor konačnog rešenja zahtevao je dodatnu analizu. Da bi se izabralo najbolje rešenje ili rešenje koje najmanje narušava dozvoljene granice, u tezi je predloženo upoređivanje

minimalnih i maksimalnih očekivanih vrednosti napona kompletnog seta optimalnih rešenja za najviše i najniže nivoe opterećenja. Za izabrano rešenje izračunati su očekivani gubici aktivne snage i energije pre i nakon ugradnje otočnih kondenzatora kako bi se utvrdila očekivana godišnja ušteda aktivne energije. Pored ušteda aktivne energije, za izabrano rešenje su izračunati troškovi ugradnje kondenzatora. Poređenjem ušteda i troškova pokazano je da ugradnja kondenzatora ima pun ekonomski smisao.

Ključne reči: Optimalna snaga i lokacija otočnih kondenzatora, višekriterijumska optimizacija, NSGA-II, neodređenost snage potrošnje i generisanja obnovljivih izvora, korelacija između slučajnih promenljivih.

Naučna oblast: Tehničke nauke – Elektrotehnika.

Uža naučna oblast: Elektroenergetski sistemi.

UDK: 621.3

Acknowledgement

First of all, I would like to thank Allah, the most gracious and the most merciful, who grants the useful wisdom, where this work would not be possible without his blessing.

Looking back at my stay in Belgrade, I see a number of people who have helped me in this endeavor. I would like to take this opportunity to express my sincere gratitude to all of them.

My appreciation and thanks are extended especially to my supervisors Dr. Željko Đurišić and Dr. Aleksandar Savić for their directions and supervision of this thesis.

Dr. Aleksandar Savić, I have always considered myself to be very fortunate to have had you as my supervisor. I have learned a lot from you. Your enthusiasm and energy have been the source of my motivation and inspiration all throughout my journey through graduate school.

For helping me and standing with me, the first who I knew at the university, Prof. Dr Stevica Graovac, my deepest thanks and great gratitude to you.

I would like to thank all the staff at the Faculty of Electrical Engineering at the University of Belgrade and special thanks to all the doctors who taught me all the courses.

Finally, I owe the deepest gratitude to my family, for their understanding and encouragement throughout this work.

Chapter 1. Introduction

The distribution system is a very important part of any an electric power system. Its role is to ensure that the end users are provided with a safe and reliable supply of the quality electrical energy. However, owing to the permanent growth of the load, market requirements and constraints, and connection of distributed generation (DG) units, this may become a very complicated and difficult task. One of the methods of ensuring that operation of a distribution network is safe and reliable is control of the reactive power flow. Building-in shunt capacitors is an efficient way of accomplishing that. By determining optimum locations and installed powers of shunt capacitors it is possible to improve voltage profile of the network, reduce active power and energy losses, and release the line capacity.

In recent years many methods and algorithms have been proposed to solve the optimal capacitor placement problem. The minimisation of active power losses, minimisation of voltage profile deviation, and minimization of costs are the main optimisation criteria found in the literature. An efficient approach for capacitor allocation in radial distribution systems in order to determine the optimal locations and sizes of capacitors with an objective of reduction of power loss and improving the voltage profile is presented in [1]. In [2] the authors presented a new mixed integer nonlinear programming approach for capacitor placement in radial/mesh distribution systems with an objective of reducing the power loss and investment capacitor costs. Lee et al. [3] proposed a particle swarm optimisation (PSO) approaches with operators based on Gaussian and Cauchy probability distribution functions to solve the optimal

capacitor placement problems. Bacterial foraging oriented by particle swarm optimisation algorithm for fuzzy optimal placement of capacitors in the presence of nonlinear loads in unbalanced distribution networks is proposed in [4]. For the purpose of solving the problems associated with the optimum distribution of shunt capacitors, the PSO method has also been used in [5-8]. In [9], a methodology is presented by using two parts. The first is sensitivity analysis to select the proper location for capacitor placement and the second is plant growth simulation algorithm for optimisation of the size of capacitors. The authors in [10] also presented a two-stage procedure. In the first stage, the loss sensitivity analysis is employed to select the most of candidate capacitors' locations. In the second stage, the ant colony optimisation algorithm is investigated to find the optimal locations and sizes of capacitors. Sensitivity analysis together with Gravitational Search Algorithm is used in [11]. In [12] Genetic Algorithm with special constraint handling procedure is proposed for the discrete optimisation problem of capacitor placement and sizing in a distribution system for cost reduction and power quality improvement. In [13-15] the problem of optimal capacitor placement has been modeled as a multiobjective optimisation problem and solved by applying Non-dominated Sorted Genetic Algorithm (NSGA-II).

Majority of the recent articles has been more focused on improving the optimisation procedure by applying different optimisation techniques and less on the improvement of the approach to solving the problems associated with optimum locations of capacitor banks. A bacteria foraging algorithm based on fuzzy logic theory is suggested in [16], differential evolution and pattern search in [17], cuckoo search algorithm in [18], a fuzzy set optimisation approach in [19], Monkey Search Algorithm in [20], and the hybrid honey bee colony optimisation algorithm in [21]. Harmony Search Algorithm is used in [22-24].

In all mentioned references, consumption within a network has been modeled as a deterministic quantity. However, distribution systems are probabilistic in nature, leading to inaccurate deterministic solutions. Therefore, in order to obtain a better quality and more accurate solution, it is necessary to develop a probabilistic optimisation model to include the uncertainties associated with consumption in a distribution network. In addition, if the network also contains DG units, like wind turbines or solar panels, it is required that their productions, having distinctly

intermittent character, are included in the probabilistic model. Uncertainty modelling of active loads for optimal capacitor placement has been considered by a limited number of papers. Carpinelli et. al [25] proposed a new single-objective probabilistic approach based on the use of a micro-genetic algorithm. Two different techniques, one based on the linearized form of the equality constraints of the probabilistic optimisation model and the other based on the point estimate method (PEM), were tested and compared. In [26] the authors suggested a new stochastic method based on PEM to consider the uncertainty effects in the optimal capacitor placement problem. The proposed stochastic method captured the uncertainty associated with the forecast errors of active and reactive loads as well as the cost function coefficients. In [27] uncertainty in load variation is considered by using fuzzy interval arithmetic technique. Load variations are represented as lower and upper bounds around base levels. Both fixed and switchable capacitors have been considered and the results for standard test systems are presented. In [28] the authors also used fuzzy theory to model uncertainty of loads. In this paper the multiobjective optimisation includes three objective functions: decreasing active power losses, improving voltage stability for buses, and balancing current in system sections. In [29] a Modified Particle Swarm Optimizer (MPSO) based method is proposed for placement of multiple Wind Power Distributed Generators and capacitors. A Monte Carlo Simulation (MCS) based probabilistic load flow, considering uncertainty in load demand and wind generation, is developed.

This thesis proposes a method for determination of optimum location and installed power of shunt capacitors in a distribution network comprising wind turbines (WTs) and solar power plants (SPPs). The method is applied to modelling the uncertainties in active load demand and renewable DGs active power productions. The presence of DGs in a distribution network has a significant influence on the voltage profile. Production of DGs, like WTs and/or SPPs, has a distinctly stochastic character owing to the nature of the primary resource (wind speed and solar irradiation). For this reason, modelling these sources in a stochastic way is a key factor in obtaining a quality solution for the optimum location and installed power of the shunt capacitors. In addition, the proposed method takes into account the correlation between sets of random variables. Calculations in the analyzed network have been performed by using the MCS method, which is the reference method for these purposes [30].

The variables of the system may be dependent on each other. So, the variation of one variable affects the other variables, too. In the case of two variables with nonzero correlation, it is said that they are correlated. For load consumption in the distribution network, because of the normal distribution is commonly used distribution to model uncertainty in load consumption, the correlated sets of random variables will be generated with the normal distribution. On the other hand, there are some approaches to solve difficulties with correlations of the non-normal distribution. Some techniques are presented in [31] for wind speed data. Where the correlation between wind speeds at different locations has been focused on. The presented method can be successfully applied to other physical variables and other non-normal distributions. In this thesis, the method described in [31, 32] will be used for simulation of correlated wind speeds and solar irradiation.

The optimisation problem is modelled as simultaneous optimisation of two criterion functions. The goal of the first criterion function is advancing the voltage profile of the network by minimising the sum of square deviations of the expected voltage value from the reference value. The goal of the second optimisation is minimisation of the total installed power of the shunt capacitors. Since the criterion functions defined in this way are contradictory, i.e. smaller installed power of the shunt capacitors will result in an inferior voltage profile and vice versa, the simultaneous optimisation of these two criterion functions is fully justified. The simultaneous optimisation results in a set of compromise solutions indicating how the network voltage profile is dependent on the installed power of the shunt capacitors. In this way one obtains a more complete picture on how and to what extent one can realize an improvement of the voltage profile. An original method of selecting the final compromise solution from the set of obtained solutions which the most adequate for the analyzed network is proposed. The selected solution represents the basis for practical realization. The proposed method has been tested on a real distribution network comprising WTs and SPPs. The calculations were performed by using real data obtained by the corresponding measurements.

Overview of the Thesis

Chapter 1 presents an Introduction.

Chapter 2 presents Distribution networks: The load demand and load demand diagrams, The clustering methods for modeling demand diagrams, Shirmohammadi method for load flow calculations, Voltage quality, Reactive power compensation in ditribution networks, Shunt capacitive compesation and Distributed Generation (DG) units.

Chapter 3 presents Uncertainty in loads and DG units productions: Random variables, Probability distributions, Power load uncertainty, Uncertainty of wind turbine production, Uncertainty of solar power plant production, Monte Carlo Simulation and Correlation in random variables.

Chapter 4 presents Multiobjective optimisation: Theory, Pareto optimality, Genetic algorithms (GAs) for multi-criteria optimisation, Single Genetic Algorithms, Vector Evaluated Genetic Algorithm (VEGA), Multiobjective Genetic Algorithm (MOGA), Non-dominated Sorted Genetic Algorithm (NSGA-II) and Effect of the constraints on the optimal fronts.

Chapter 5 gives a description of New method for capacitor allocation: Description of method, The tested distribution network, Calculation, Algorithm and Results.

Chapter 6 presents Conclusions.

Chapter 2. Distribution networks

2.1. Introduction

Electric power is normally generated at 11-25 kV in a power station. To transmit the power over long distances through high voltage transmission lines, it is then stepped-up to 220 kV or 400 kV as necessary. Usually, these transmission lines run into hundreds of kilometers and deliver the power into a common power pool called the grid. The grid is connected to load centers through a sub-transmission network of 110 kV lines. These lines terminate into a substation, where the voltage is stepped-down to 6–35 kV for power distribution to load points through a primary distribution. Finally, the voltage is stepped-down to 400 V for secondary distribution. Figure 2.1 shows an example of the transmission and distribution networks.

Depending on the geographical location, distribution networks can be in the form of overhead lines or underground cables. Cables are commonly used in urban areas and overhead lines are adopted for rural areas. Different network configurations are possible in order to meet the required supply reliability.

Distribution networks are divided into two types, radial or loop (ring). In the radial systems, each consumer has one source of supply. But in the loop systems, each consumer has multiple sources of supply operating in parallel.

Radial distributions system (This means that, the distribution feeders simply radiate out from the supply source as seen in Figure 2.2) is popular because of low cost and simple design. Also, it is easy for monitoring and protection as well as in fast fault

localization and simple operational management. But it has one major drawback that in case of any feeder failure, the associated consumers would not get any power as there was no alternative path to feed the consumers. Radial systems are commonly used in rural or suburban areas. The voltages at buses decrease when moved away from the substation, also the losses are high.

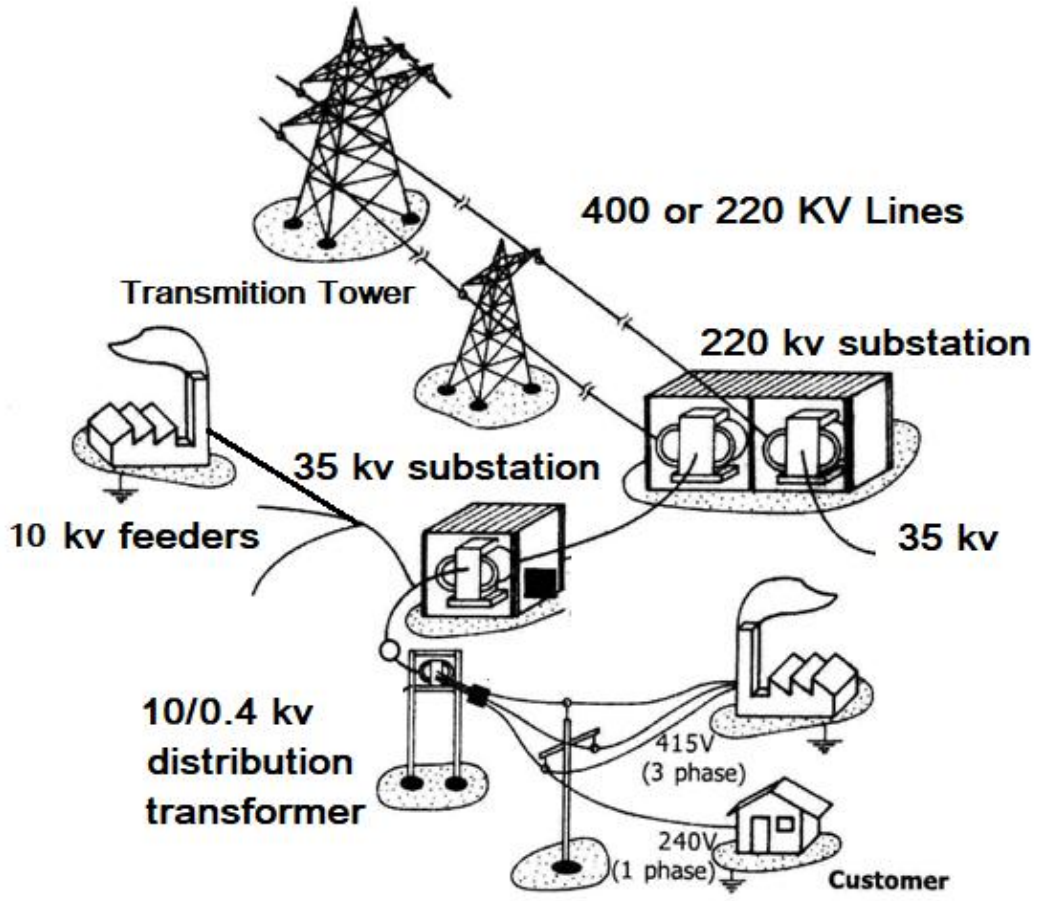

Figure 2.1. The transmission and distribution networks.

The loop system of distribution starts at the substation and is connected to or encircles an area serving one or more load centers. The conductor of the ring system returns to the same substation that it started from (as seen in Figure 2.3). This type is more reliable where each customer substation has dual supply and so a single circuit fault would not cause any supply interruption. However , operating loop networks, fault

localization and actions to attain a defined switching condition in cases of faults are always more complicated and more expensive than the radial network. This loop system also works in a radial way by breaking one section. But in case of fault on one section, consumers can be supplied by using an alternative path.

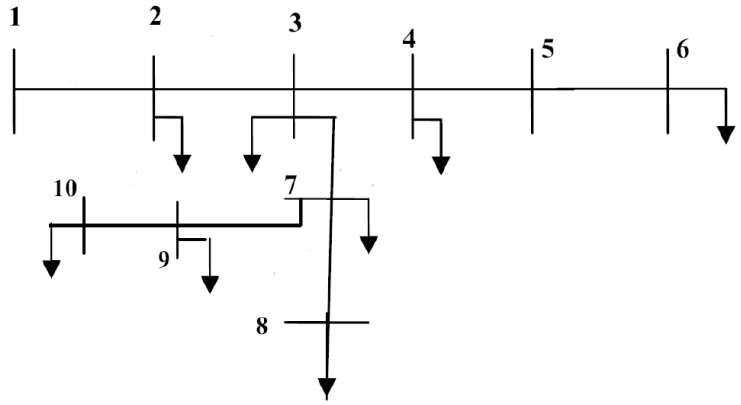

Figure 2.2. A radial electrical distribution system.

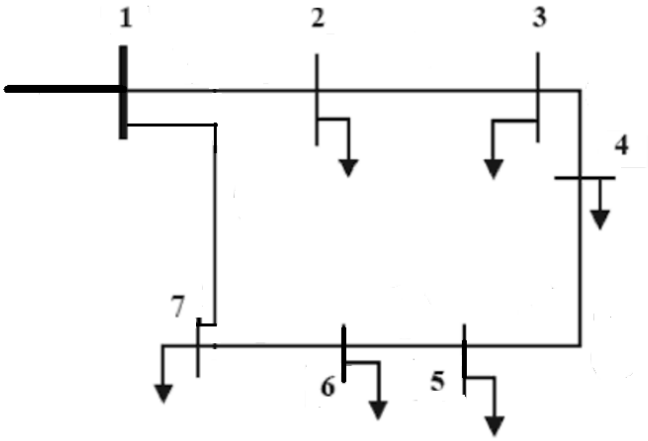

Figure 2.3. A loop electrical distribution system.

2.2. The load demand and load demand diagrams

Distribution systems obviously exist to supply electricity to end users, so loads and their characteristics are important. Utilities supply a wide range of loads, from rural areas to urban areas. A utility may feed houses on the same circuit with an industrial customer. The electrical load on a feeder is the sum of all individual customer loads.

Figure 2.4 shows the consumed load from multiple consumers and their total load. And, the electrical load of a customer is the sum of the load drawn by the customer's individual appliances. Customer loads have many common characteristics. Load levels vary through the day, sometimes reaching the peak in the afternoon or early evening.

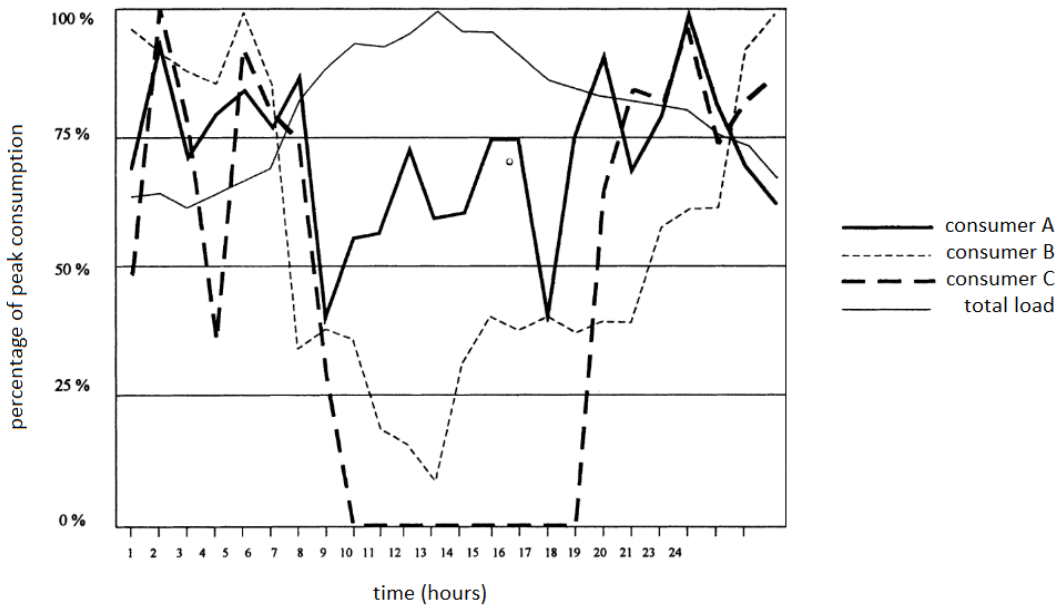

Figure 2.4. The consumed load from multiple consumers and their total load.

2.2.1. Load demand

Every 15 minutes (often 15, 20, or 30 minutes), the measured consumption as raw data represents the load demand. The load demand will vary according to customer type, temperature and seasons. These variations represent load demand for a specific period of time. Actual load demand can be collected at strategic locations to perform more detailed load analysis. Demand can be used to characterize active power, reactive power, apparent power, or current.

2.2.2. Load curve

The load curve is graphical plot showing the variation in load demand of the consumer with respect to time. The load is plotted along the y-axis while the time frame

of that load comes in the x-axis. It can be daily, weekly, monthly or yearly load curve. Figure 2.5 shows the daily load curve.

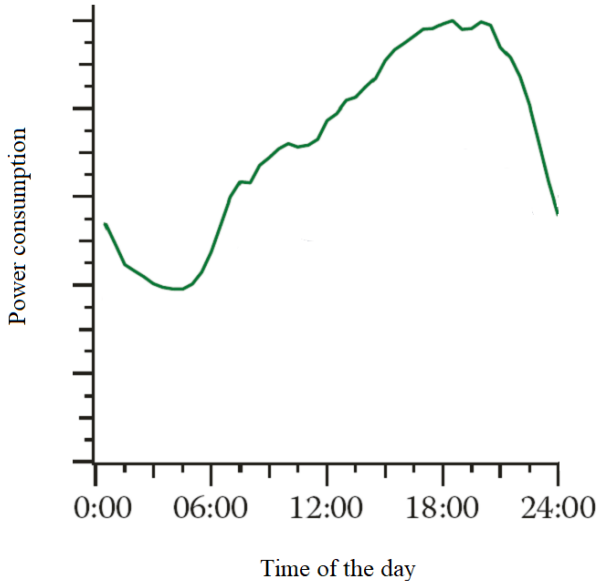

Figure 2.5. Daily load curve.

2.2.3. Load duration curve

If the points of the load curve are simply rearranged in a way where the highest demand comes first, and so on; we'll get a new curve known as the load duration curve. In other words, load duration curve illustrates the variation of a certain load in a downward form such that the greatest load is plotted in the left and the smallest one in the right. Figure 2.18 shows the load and load duration curves together.

2.3. The clustering methods for modeling demand diagrams

An actual load curve can be converted into a load duration curve expressed in per unit (a fraction with regard to the peak) as shown in Figure 2.6 to eliminate the chronology. Depending on the modeling technique and study purpose, the load curve or the load duration curve is used in system analysis. There are two types of load clustering.

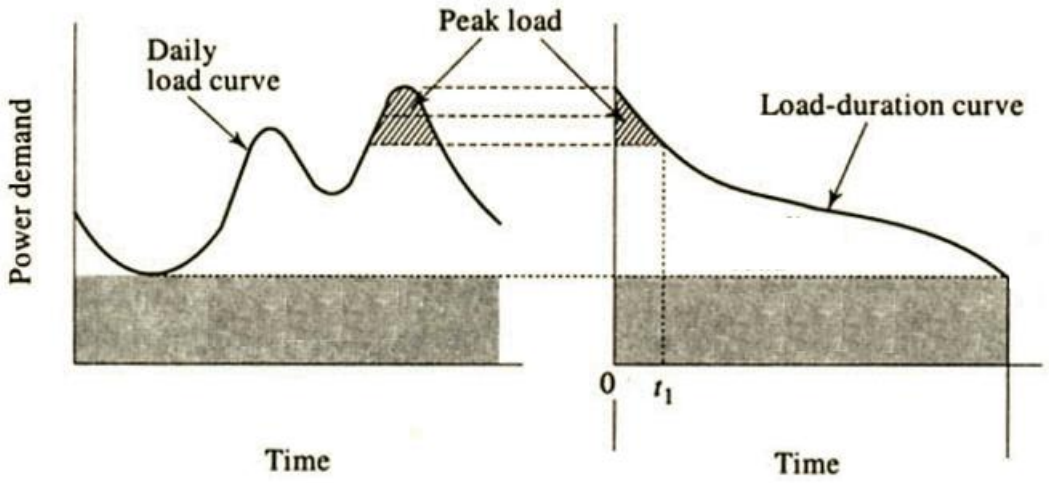

Figure 2.6. The load curve and the load duration curve.

2.3.1. Multistep Load Model

In this way, the load points in one or more load curves are clustered into several load-level groups. The K-mean clustering technique can be used to create a multistep load model, which is shown in Figure 2.7. It is assumed that a load duration curve is divided into *NL* load levels. This corresponds to grouping load points of the curve into *NL* clusters. Each load level is the mean value of those load points in a cluster. The load clustering is performed in the following steps [30]:

1. Select initial cluster mean M_i, where i denotes cluster i ($i = 1, \ldots, NL$).
2. Calculate the distance D_{ki} from each load point L_k ($k = 1, \ldots, NP$) (where NP is the total number of load points in the load curve) to the ith cluster mean M_i by

$$D_{ki} = |M_i - L_k|. \tag{2.1}$$

3. Group load points by assigning them to the nearest cluster based on D_{ki} and calculate new cluster means by

$$M_i = \frac{\sum_{k \in IC_i} L_k}{NS_i}. \tag{2.2}$$

where NS_i is the number of load points in the ith cluster and IC_i denotes the set of the load points in the ith cluster.

4. Repeat steps 2 and 3 until all cluster means remain unchanged between iterations.

The M_i and NS_i obtained are the load level (in MW) and the number of load points for the i^{th} step in the multistep load model, respectively. NS_i also reflects the length of the i^{th} step load level. The multistep load model can be easily expressed in per unit. The K-mean clustering technique can be extended to the case of multiple load curves where each one represents a curve for a bus or bus group in a region [30].

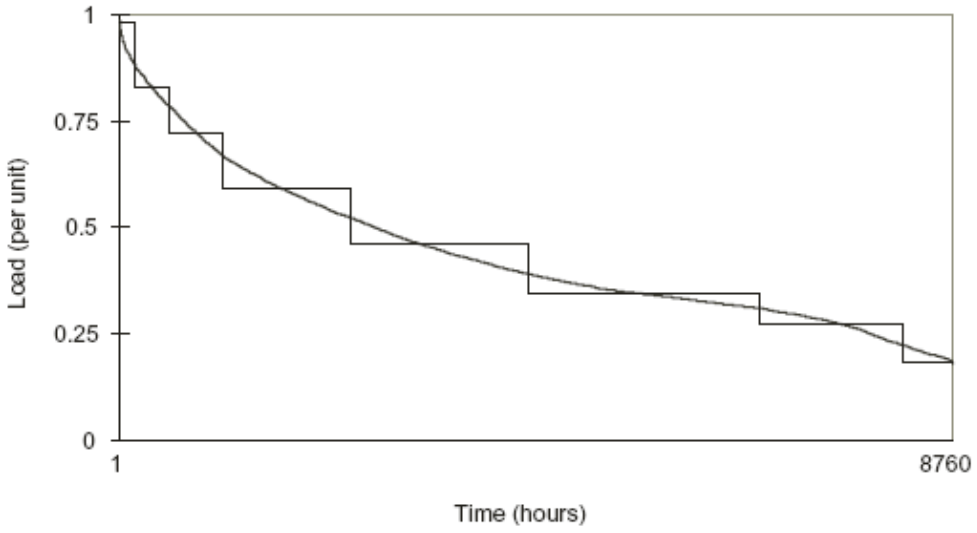

Figure 2.7. Load duration curve and its multistep model.

2.3.2. Load Curve Grouping

In this way, different load curves are clustered into several curve groups, in each of which load curves have a similar curve shape or time-varying load pattern. Sometimes in system analysis and reliability assessment, it is necessary to group load curves according to their similarity. A statistic-fuzzy technique can be used for this purpose with the following steps:

1. All load curves for clustering must be represented using their peak values to obtain the load curves in per unit.

2. Calculated the nearness coefficient between the two load curve vectors. The value of nearness coefficient is between [0,1]. The more the value of nearness coefficient approaches 1, the nearer the two load curves are.
3. A fuzzy relation matrix can be formed by using nearness relationships of all load curves.
4. An equivalent fuzzy matrix with transitivity can be obtained through consecutive self - multiplications of a resemblance fuzzy matrix.
5. A nondiagonal element in the last resulting matrix is selected as the threshold, and they are checked with transitive nearness coefficient. If a transitive nearness coefficient is equal to or larger than the threshold, then the corresponding load curves are classified in one cluster. A load curve that cannot be classified by this rule, if any, is in a cluster by itself.

Figure 2.8 shows Five load curves (in per unit) for a 24 hour period. The number of clusters and their load curves changes according to the selection of threshold value. With one value load curves (1, 2, and 5) can be in one cluster but load curves 3 and 4 in another. With another value for threshold, load curves are classified into three clusters: (1,2), (3,4), and (5) [30].

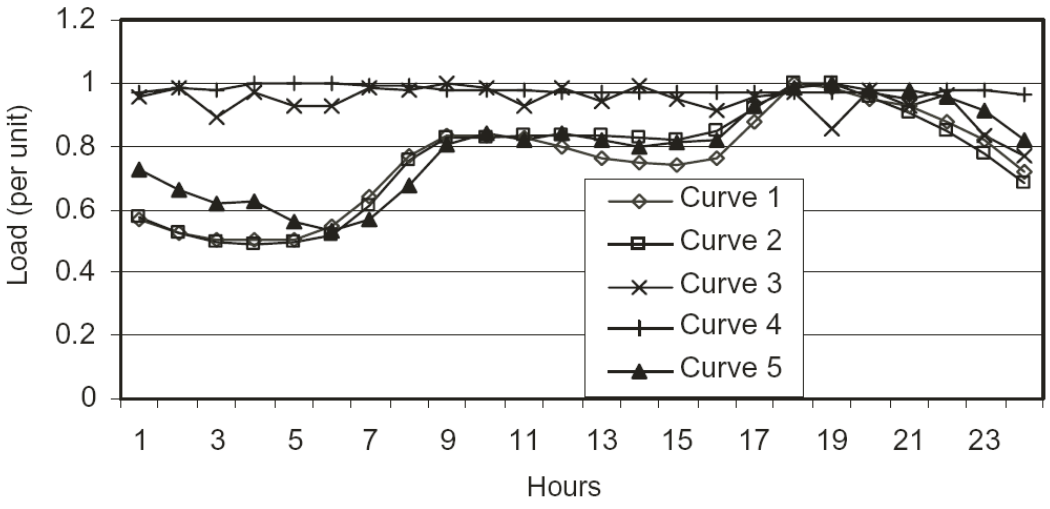

Figure 2.8. Daily load curves at fi ve substations (in per unit).

2.4. Shirmohammadi method for load flow calculations

Power flow calculations are the backbone for distribution systems studies. Therefore, an accurate, robust, and computationally efficient distribution power flow tool is highly demanded. Load flow is an important and fundamental tool for the analysis of any power system in operation as well as planning stages, particularly in the modern distribution system and optimization of the power system. The well-known characteristics of an electric distribution system are radial and meshed structures; the extremely large number of branches and nodes. Those features cause the traditional power flow methods used in transmission systems, such as the Gauss-Seidel and Newton-Raphson techniques, to fail to meet the requirements in both performance and robustness aspects in the distribution system applications [33].

Shirmohammadi et al. [34] have presented a compensation based power flow method for radial distribution networks and/or for the weakly meshed structure using a multi-port compensation technique and Kirchhoff's Laws. In the beginning, the meshed distribution network will be broken at number of breakpoints in order to convert it into one radial network. Then the radial part is solved by a straightforward two-step procedure in which the branch currents are first computed (backward sweep) and then bus voltages are updated (forward sweep). They said "***it is significantly more efficient than the Newton-Raphson power flow technique when used for solving radial and weakly meshed distribution and transmission networks***" [34]. This method includes numbering of all branches and nodes in the network. The numbering can be done as below:

If we have a typical radial distribution network as shown in Figure 2.9. This network has number of nodes and branches are n and $b = n$-1 consequently. There is a single voltage source at the root node.

The distribution system is divided into layers as shown in Figure 2.10. For numbering of branches, the branches is numbered away from the root node. The numbering of branches in one layer starts only after all branches in the previous layer have been numbered.

For numbering of nodes, the nodes is numbered stating from the root node (as showing in Figure 2.11). The numbering of nodes in the next layer starts after numbering of all present layer.

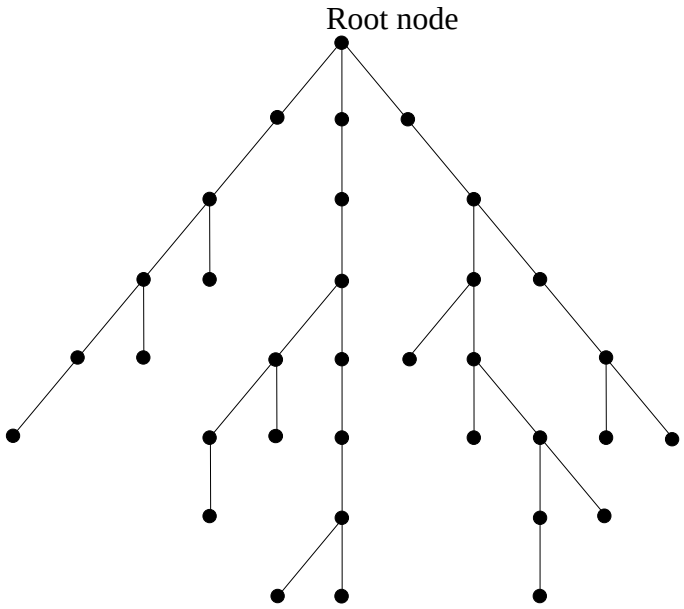

Figure 2.9. Example of radial distribution network.

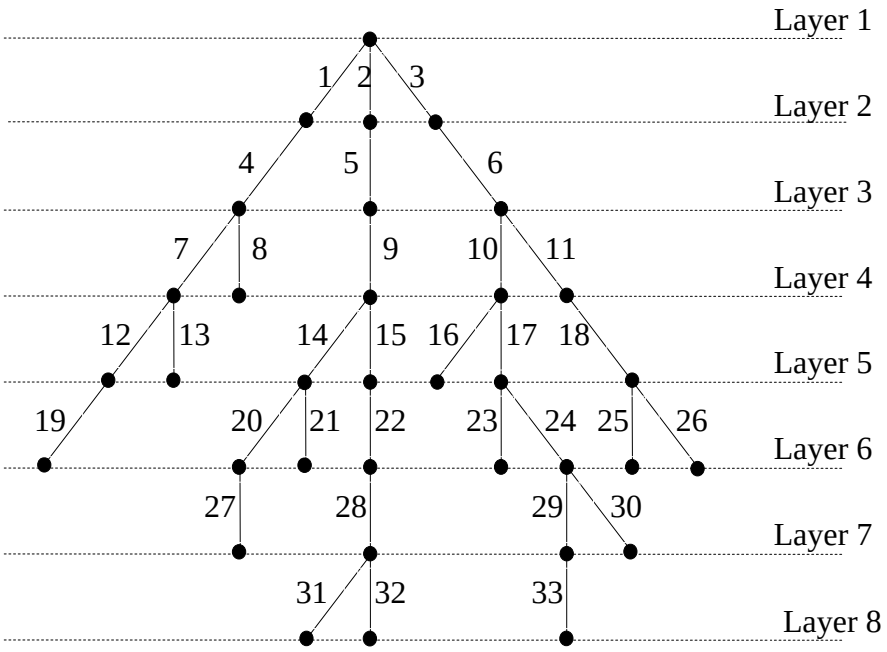

Figure 2.10. Branch numbering of the distribution network.

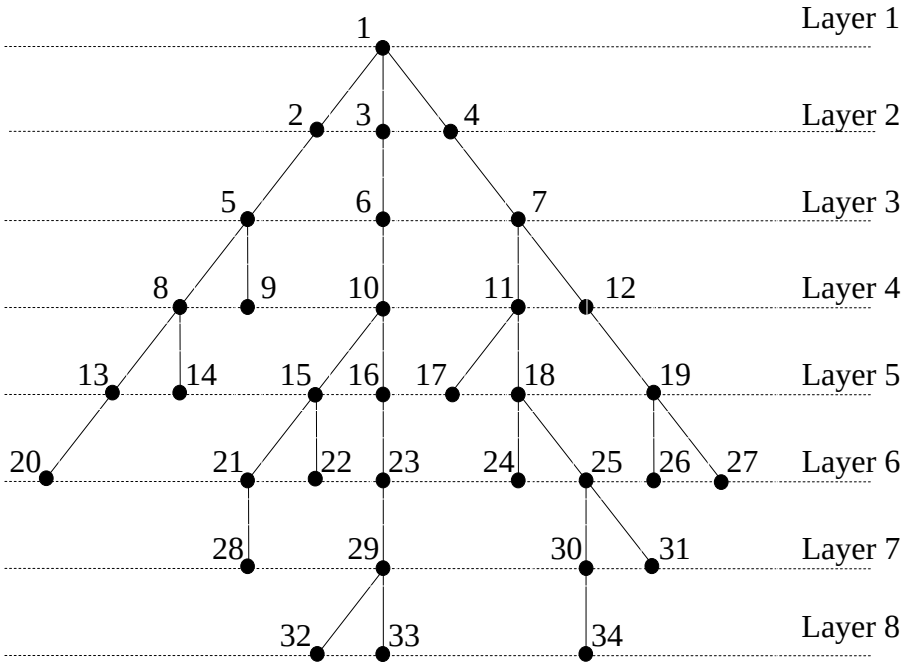

Figure 2.11. Node numbering of the distribution network.

For any branch L , the node which closed to the root node is denoted by L_1 and the other node by L_2 as shown in Figure 2.12.

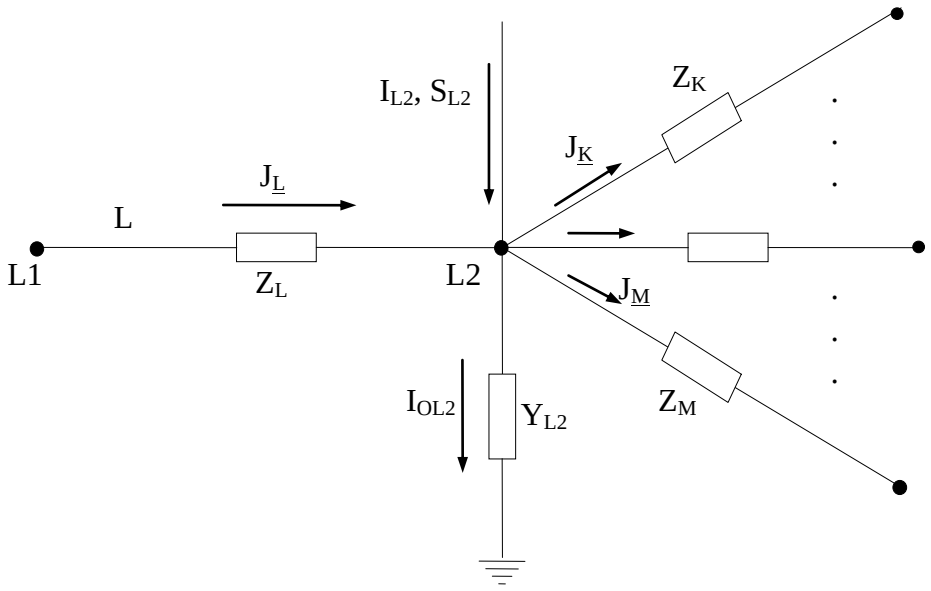

Figure 2.12. Currents in branch L.

The iterative solution algorithm consists the following steps:

a. Nodal current calculation:

The currents injection at node L_2 (at iteration k) is:

$$I_{L2}^{(k)} = \left(\frac{S_{L2}}{V_{L2}^{(k-1)}} \right)^* - V_{L2}^{(k-1)} Y_{L2}. \tag{2.3}$$

Where:

$V_{L2}^{(k-1)}$ is the voltage at node L_2 calculated during the $(k-1)^{th}$ iteration.

S_{L2} is the specified power injection at node L_2.

Y_{L2} is the sum of all the shunt elements at the node L_2.

b. Backward sweep:

Starting from the branches in the last layer and moving towards the branches connected to the root node, the current in branch L (at iteration k) is J_L where:

$$J_L^{(k)} = -I_{L2}^{(k)} + \sum_{\text{emanating from node } L_2}^{\text{currents in branches}}; \qquad \text{L} = \text{b}, \text{b-1}, ..., 1. \tag{2.4}$$

c. Forward sweep

Starting from the branches in the first layer towards those in the last layer, The nodal voltage (at iteration k) is:

$$V_{L2}^{(k)} = V_{L1}^{(k)} - Z_L J_L^{(k)}; \qquad \text{L} = 1, 2, ..., \text{b}. \tag{2.5}$$

Where:

Z_L is serial impedance of branch L.

After calculating the nodal currents and voltages, the maximum real and reactive power are used as convergence criterion. The power injection for node L_2 at k^{th} iteration is calculated as:

$$S_{L2}^{(k)} = V_{L2}^{(k)} \left(I_{L2}^{(k)} \right)^* - Y_{L2} \left| V_{L2}^{(k)} \right|^2. \tag{2.6}$$

Then, the real and reactive power mismatches at bus L_2 are calculated as:

$$\Delta P_{L2}^{(k)} = \text{Re}\left[S_{L2}^{(k)} - S_{L2}^{spec} \right] \le \varepsilon. \tag{2.7}$$

$$\Delta Q_{L2}^{(k)} = \text{Im}\left[S_{L2}^{(k)} - S_{L2}^{spec} \right] \le \varepsilon. \tag{2.8}$$

The basic idea of backward/forward sweep with compensation method proposed in reference [34] is shown in Figure 2.13.

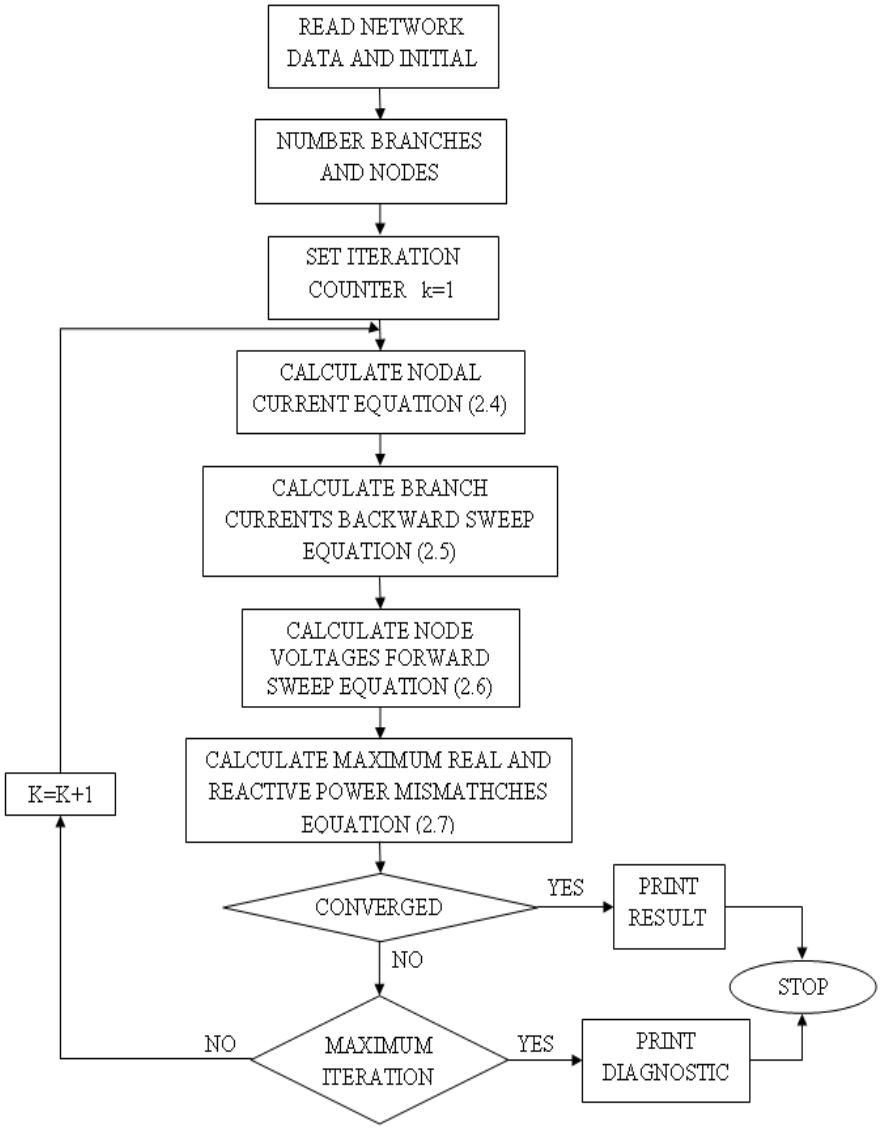

Figure 2.13. Power flow solution algorithm for the radial networks [34].

2.5. Voltage quality

In a modern power system, electrical power is generated at the power station far away from the consumer location and delivered to them through a network of transmission and distribution systems. The power systems can be well designed if they give a good quality of reliable supply. Good quality basically means the voltage levels maintained constant or within the permissible limit. As a result, no consumer supplied by those distribution systems suffers from high or low voltage (Figure 2.14 shows an ideal supply waveform). The principle cause responsible for voltage variation is the

change in loads (ON and OFF) and their power factors. Too wide variations of voltage may cause an irregular operation or fail of consumers' appliances. To safeguard the interest of the consumers, standards have been enacted in this regard. The allowable limits of the different types of voltage variations are given in Table 2.1 according to International Electromechanical Commission (IEC) or IEEE standards [35].

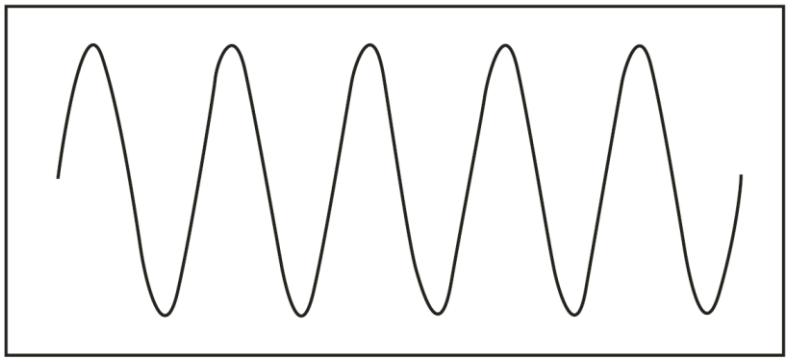

Figure 2.14. An ideal supply waveform.

Table 2.1. The limits of voltage variations.

Type of Voltage Variation	Allowable Limit of Accepted Power Quality Level	Reference
Voltage drop	Up to 33 kV: V_n ± 10% Above 33 kV: V_n ± 5% for normal case V_n ± 10% for emergency case	IEC 38/1983
Voltage unbalance	3%	IEEE 1159/1995
Voltage sag	10 – 90% of V_n from 3 s to 1 min 80 – 90% of V_n for duration >1 min	IEEE 1159/1995
Voltage swell	110 – 120% of V_n from 3 s to 1 min	IEEE 1159/1995
Overvoltage	110 – 120% of V_n for duration >1 min	
Voltage flicker	Duration: short period (up to 10 min), quality level 100%, MV 0.9, HV 0.8 Duration: long period (up to 2 h), quality level 80%, MV 0.7, HV 0.6	IEC 1000 - 3 - 7/1995
Frequency deviation	1% for nominal case 2% for emergency case	IEC 1000 - 2 - 4/1994

The voltage variations can be categorized as transient disturbances, fundamental frequency disturbances, and variations in steady state. The main types of voltage variations are described in the following.

2.5.1. Transient voltages

The transient is a sudden change of state which happening between two consecutive steady states during a short time interval. It can be a unidirectional impulse or an oscillatory wave. Figure 2.15 shows a transient event happened in the voltage wave.

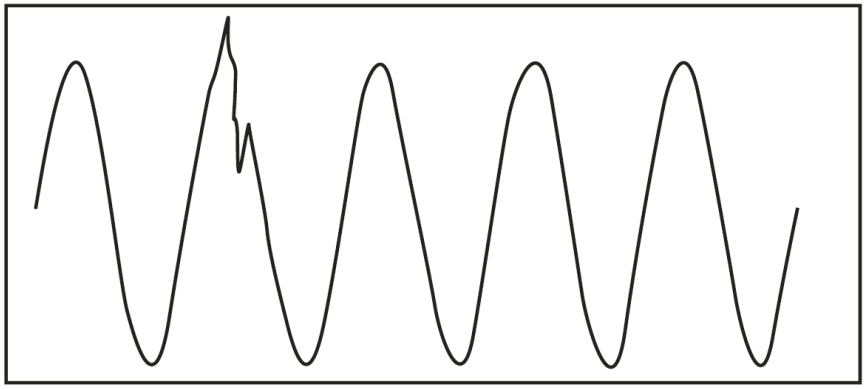

Figure 2.15. A voltage wave with a transient event.

2.5.2. Voltage sags (Dips)

The voltage sag is a decrease in root mean square (rms) voltage at power frequency for durations of 0.5 cycles to 1 min. Faults on neighboring feeders cause voltage sags, the duration of which depends on the clearing time of the protective device. The depth of the sag depends on how close the customer is to the fault and the available fault current. Faults on the transmission system cause sags to all customers off of nearby distribution substations. Figure 2.16 shows a voltage sag that caused the system voltage to fall.

2.5.3. Voltage swells

The voltage swell is a temporary increase in rms voltage of more than 10% of the nominal value at power system frequency, which lasts from 0.5 cycles to 1 minute. Figure 2.17 shows a momentary increase in voltage.

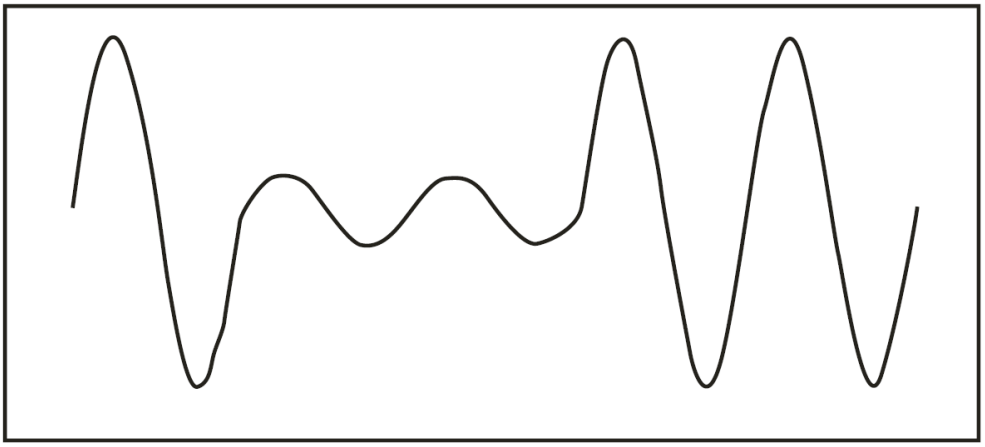

Figure 2.16. A voltage wave with voltage sag.

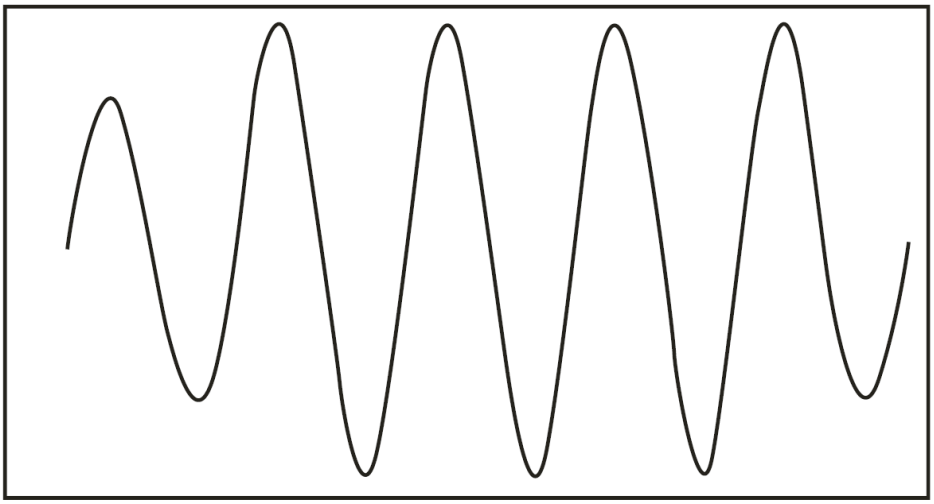

Figure 2.17. A momentary increase in the voltage.

2.5.4. Interruptions

The interruption is a complete loss of voltage (below 0.1 pu) on one or more phase conductors for a certain period of time. It can be one of the following: momentary interruptions (between 0.5 cycles and 3 sec.), temporary interruptions (between 3 and

60 sec.) and sustained interruptions (longer than 60 sec.). Figure 2.18 shows a momentary voltage interruption.

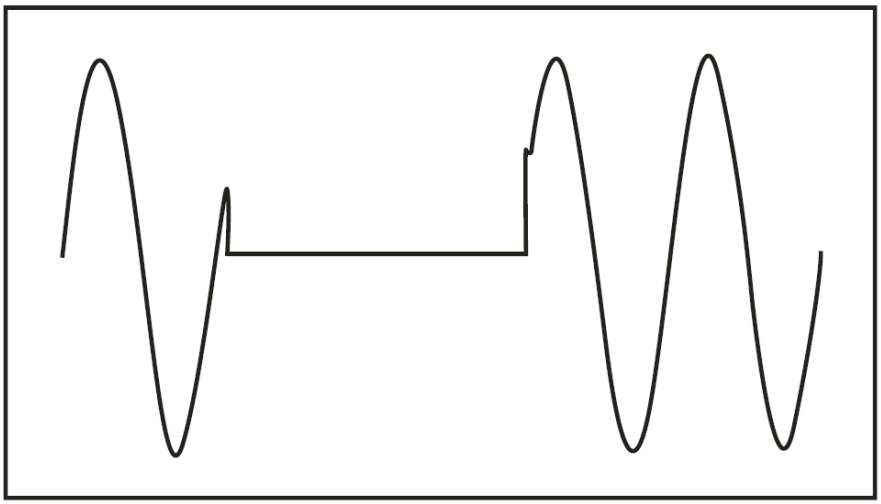

Figure 2.18. A momentary voltage interruption.

2.5.5. Voltage harmonics and interharmonics

The voltage harmonics are sinusoidal voltages having frequencies that are integer multiples of the fundamental power frequency. They are distortions repeated every cycle. Distorted waveforms are decomposed into a sum of the fundamental frequency wave and the harmonics. On the other hand, interharmonics voltages have frequencies that are not integer multiples of the fundamental power frequency. Figure 2.19 shows a distorted voltage waveform by harmonics.

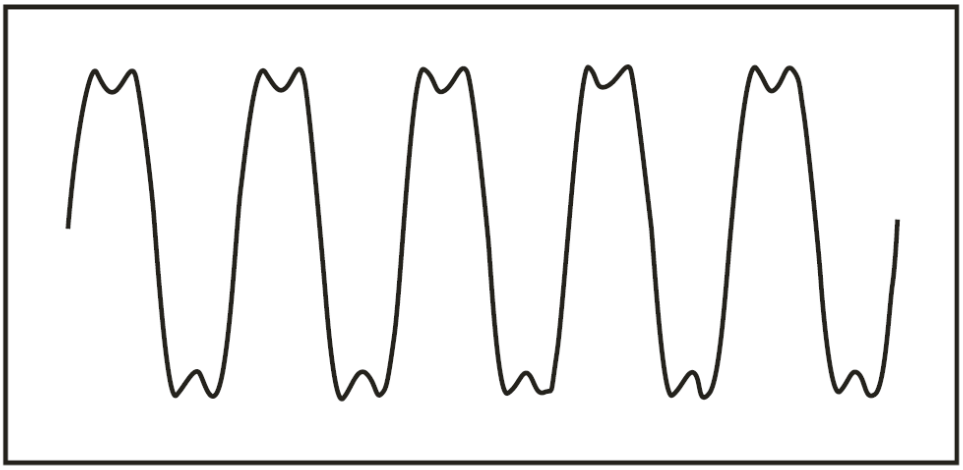

Figure 2.19. A Distorted voltage waveform by harmonics.

2.5.6. Voltage Flicker

The voltage flicker is fluctuations in voltage magnitude which happens randomly. These changes don't exceed voltage ranges of 0.9–1.1 pu. Figure 2.20 shows these fluctuations.

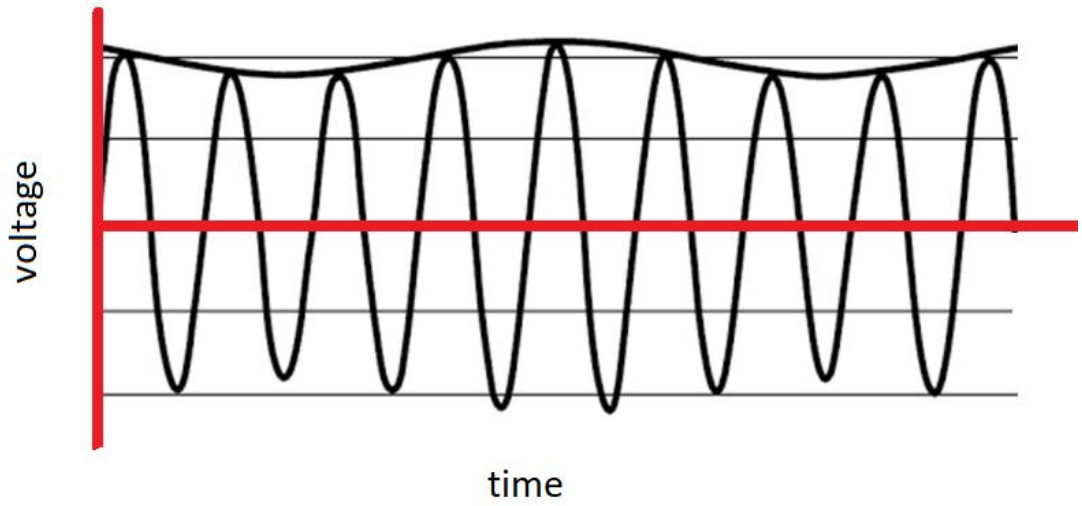

Figure 2.20. The fluctuations in voltage magnitude.

2.5.7. Undervoltages and Overvoltage

Undervoltage: It refers to a voltage having a value less than the nominal voltage for a period of time greater than 1 min. Typical values are 0.8–0.9 pu.

Overvoltage: It refers to a voltage having a value greater than the nominal voltage for a period of time greater than 1 min. Typical values are 1.1–1.2 pu.

Finally, one of a utility’s responsibilities is to deliver the electrical power to customers within a suitable voltage range. Therefore utilities must regulate the voltage. In distribution networks, voltage drops due to the current flowing through the line impedances. There are many ways to reduce voltage drop like increase power factor (adding capacitors) or use another conductor with a larger size, etc...

2.6. Reactive power compensation in ditribution networks

In recent years, there has been a greatly increased need for reactive power compensation in distribution networks owing to the growing use of electrical machines (inductive loads) and factories consuming a large reactive power which means low power factor. Low power factor causes losses, reduces the transmission capacity of lines and increases the cost. Therefore, it must be improved for several reasons.

2.6.1. Impacts of low power factor

There are many effects of low power-factor which are summarized as follows:

1. Low power factor will reduce the efficiency of the transmission lines and increase the transmission line losses, because it will have to carry more current at a low P.F. Also, low power factor increases the voltage drop.
2. The cross-sectional area of the busbars and the contact surface of the switch gears must be enlarged for the same power to be delivered at a low power factor.
3. The active power of the generators is lowered at the low P.F. Also, the power supplied by the exciter is increased as well as the generator copper losses are increased.
4. With low power factor the alternator develops more reactive power, so more energy is required to develop it which is supplied by the prime mover. Also, working at a low power factor decreases the efficiency of the prime mover.

2.6.2. Types of power factor compensators

For all practical purposes, the only way to improve the power factor is to reduce the reactive current component in the system. This is usually done using capacitors, synchronous motors and synchronous condensers.

i. Synchronous Motors

This motor can draw leading or lagging current. At the same time, it can supply mechanical power. Synchronous motors are available commercially in standard ratings of unity and (0.8) leading power factors. The unity power factor

motor costs less. It is more efficient for driving a given mechanical load and draws no lagging or leading current. The motors operate at leading power factor are used to improve the overall power factor of the system to which they are connected. If a very large load operates continuously with lagging power factor, synchronous motors with (1) or (0.8) leading power factor should be connected to it.

The synchronous motors deliver an increasing amount of (KVAR) as line voltage drops, raising the power factor and voltage. The synchronous motors, therefore, have the advantage of acting as a voltage regulator as well as a power factor controller. The main application of synchronous motors to improve power factor is in plants that require new large motor drives.

ii. Synchronous Condensers

A synchronous condenser is a rotating machine, some what, similar to the synchronous motor. The synchronous condenser, however, improves the power factor but drives no load. The use of synchronous condenser is rarely justified in industrial plants. The higher losses of synchronous condensers also make them undesirable on the basis of power factor correction alone.

iii. Capacitors

The use of capacitors is the simplest and the most economical method for improving power factor in plants that do not require additional large motor drives. In addition to their relatively low cost, capacitors have other properties such as:

1) Easy to installation.

2) Practically, need no maintenance.

3) Very low losses.

The capacitors used in power systems are connected in two ways: shunt and series (as shown in Figure 2.21). The reactive power in series capacitors is proportional to the square of the load current, where as in shunt capacitors it is proportional to the square of the voltage. The voltage rise across the capacitor is practically instantaneous, depending on the circuit parameters.

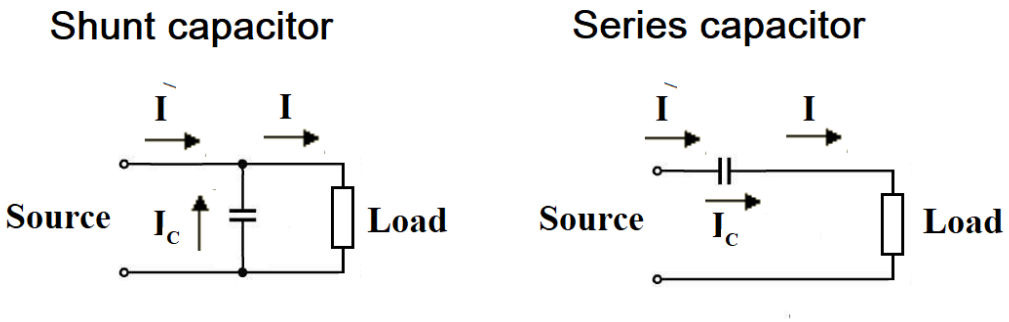

Figure 2.21. Shunt and series connections of capacitors.

There are many factors which influence the choice between the shunt and series capacitors. Also, there are certain unfavorable aspects of series capacitors. Generally speaking, the protective equipments for series capacitors are often more complicated. Therfore, the cost of installing a series capacitor is higher than that of a shunt capacitor. Due to various limitations in the use of series capacitors, shunt capacitors are widely used in distribution systems. They supply the reactive power required by an inductive load. Shunt capacitors are generally the cheapest way to improve the plant power factor, especially in existing plants. The shunt compensation equipments usually are installed near to the load.

2.7. Shunt capacitive compesation

Power factor correction is the main application for shunt capacitor units in the power system. Shunt capacitors supply reactive power when they are applied to the system. This improves the overall power factor. They also improve plants efficiency by reducing system losses and raising the voltage level, therefore additional loads can be added to the same system.

2.7.1. Location of shunt capacitors

It is more economical to install shunt capacitor banks in medium voltage (MV) and high voltage (HV) for powers greater than approximately 800 kvar [36]. Analysis of networks in various countries proves, however, that there is no universal rule. Reactive power compensation can be:

1. Global compensation: The shunt capacitor bank is connected at one location (the supply end) of the installation to be compensated and provides compensation for the entire installation. It is ideal for stable and continuous loads. Figure 2.22 shows this approach.
2. By sector: The shunt capacitor bank is connected at the supply end of the installation sector to be compensated. It is ideal when the installation is extended and contains workshops (industrial applications) with varying load systems. This type will not help reduce the losses in the primary circuit. An example to this approach is shown in Figure 2.23
3. Individual load compensation: The shunt capacitor bank is directly connected to the terminals of each load. This approach of power factor correction is mainly suitable for industrial loads and can be expensive.

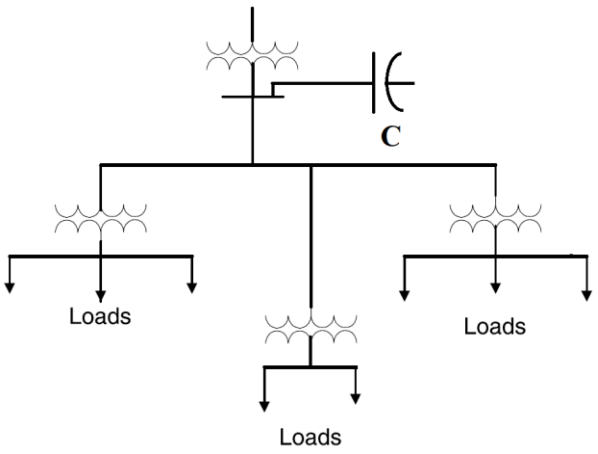

Figure 2.22. Global compensation.

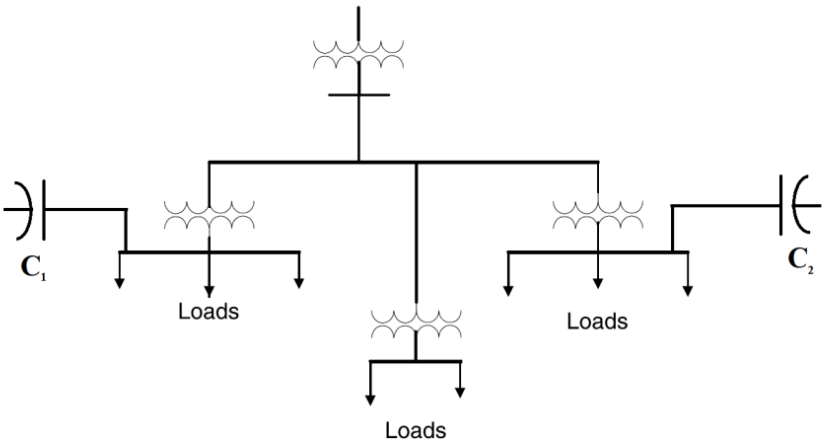

Figure 2.23. By sector compensation.

2.7.2. Mode of the operation of shunt compensation

The shunt capacitors are used for power factor correction by supplying reactive power. Their operation mode depends on the load conditions. It can be one of the following:

1. Fixed: by switching on/off a capacitor bank supplying a fixed amount of kvar. Sometimes no need for switching on/off if the load is constant for the 24-hour period.
2. Switched (Automatic): By switching on/off in steps. This approach is used if there is a big difference between the minimum load (base load) and the peak load. Figure 2.24 shows the required reactive power for a distribution system in a period of 24 hours. It is difficult to use a single fixed shunt capacitors to correct the power factor to the desired level and avoid the over-corrected condition of power factor. The installed shunt capacitors are divided into two or more parts. The first part of shunt capacitors is fixed capacitors to give the reactive power for the base load. The other part or parts of shunt capacitors can be switched on in steps during the peak load and switched off in steps during off-peak load. An automatic switching control is needed in this mode. This can provide the flexibility to control system voltage, power factor, and losses. Figure 2.25 shows an example of this mode.

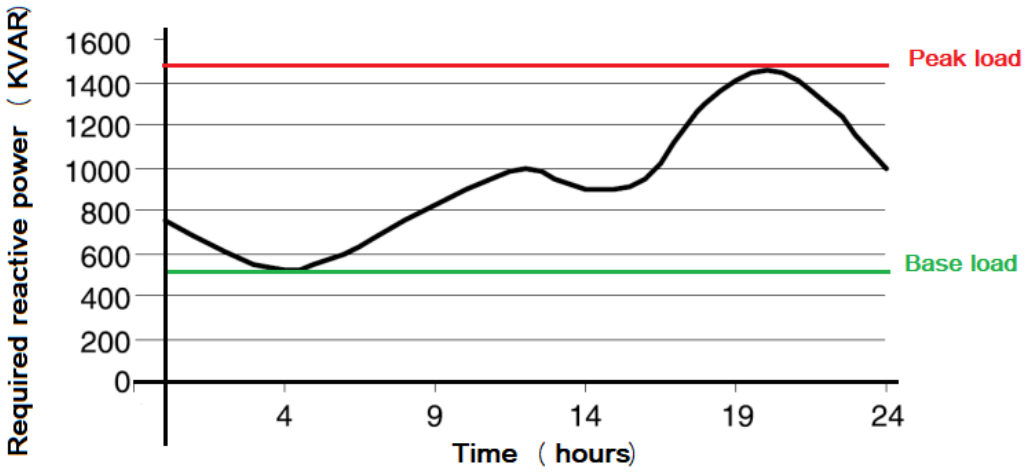

Figure 2.24. Reactive power requirement for a distribution system.

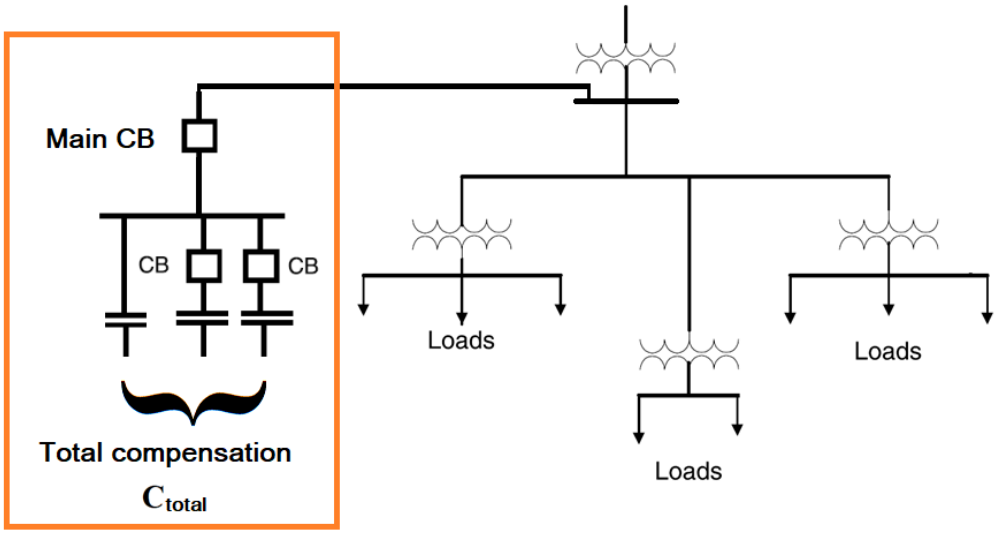

Figure 2.25. Configurations of the switched operation mode.

2.7.3. Benefits of improving the power factor by shunt compensation

If the power station works at a low power factor, the capital cost of the plant in generation, transmission and distribution systems are increased. Thus it is always advantageous to work at higher improved power factor. The following are the benefits of power factor improvement:

i. Voltage Improvement

Compensators raise the circuit voltage; it is rarely economical to apply them in industrial plants. The voltage improvement may be regarded as an additional benefit of power factor improvement.

ii. Reducing of Power System Losses

Although the financial return from conductor loss reduction alone is seldom sufficient to justify the installation of compensators, it is an attractive additional benefit, especially; in old plants with long feeders.

System conductor losses are proportional to current squared. This current is reduced with power factor improvement, and the losses are inversely proportional to the squared of the power factor. So; the percentage reduction in losses is given by:

$$\%\ \text{loss reduction} = \left(1-\left(\frac{PF_{Orginal}}{PF_{\text{Improved}}}\right)^2\right)\times 100\% \ . \qquad (2.9)$$

iii. Saving money

Improving power factor leads to important savings in power cost. Money is wasted in industrial plants if there is a lack of understanding of the benefits obtained from power factor improvement.

iv. Releasing System Capacity

The expression "release of capacity" means that as the power factor is improved, the current in the existing system will be reduced, and permitting additional load can be served by the same system. For example, Figure 2.26 can be used to determine the amount of additional system capacity obtained after a certain power factor correction. Select the current system power factor curve and follow it through to the new corrected power factor. Read the additional capacity to the system from the vertical axis.

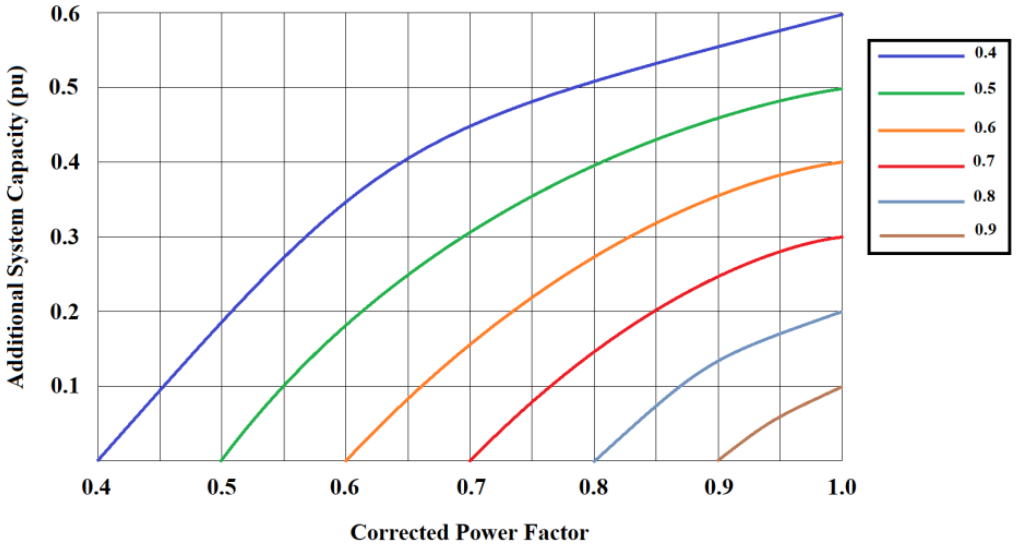

Figure 2.26. Additional system capacity after PF correction.

2.7.4. Determination of shunt compensation

The shunt compensation is determined by these followig steps [35]:

i. **Calculating reactive power:** The power to be installed is calculated from $cos\varphi_1$ or from $tan\varphi_1$ noted for the load. The aim is to move to a value of $cos\varphi_2$ or $tan\varphi_2$ thus improving the operation. *Qc* can be calculated by using tables or directly from this equation:

$$Q_c = P(\tan\phi_1 - \tan\phi_2) \ . \qquad (2.11)$$

where

Q_c is the required compensation power in kvar.

P is the active power of the load in kW.

$tan\varphi_1$ is the tangent of the phase angle (V, I) of the load.

$tan\varphi_2$ is the tangent of the phase angle (V, I) after installation of the shunt capacitor bank.

ii. **Choosing the compensation mode:** It can be global, by sector or individual load compensation.

iii. **Choosing mode of the operation of compensation:** The capacitor bank can be Fixed or switched.

iv. **Allowing for harmonics: C**are must be taken when applying capacitors in the presence of harmonics. This involves choosing the right equipment to avoid the effects of harmful harmonics on the installed capacitors.

2.8. Distributed Generation (DG) units

Distributed generation (DG) or embedded generation (the European term) refers to generation applied at the distribution level. Electric Power Research Institute (EPRI (1998)) defines distributed generation as the "utilization of small (0 to 5 MW), modular power generation technologies dispersed throughout a utility's distribution system in order to reduce transmission and distribution (T&D) loading or load growth and thereby defer the upgrade of T&D facilities, reduce system losses, improve power quality, and reliability" [37].

No exact size or voltages are accepted as definitions of distributed generation. A draft IEEE standard (IEEE P1547-D11-2003) applies to generation under 10 MW. Distribution substation generation is normally considered as distributed generation; sometimes subtransmission-level generation is also considered as DG since many of the application issues are the same. Related terms - non-utility generator (NUG) and independent power producer (IPP) - refer to independent generation that may or may not be at the distribution level. A broader term, distributed resources (DR), encompasses distributed generation, backup generation, energy storage, and demand side management (DSM) technologies [37].

DGs are improving in cost and efficiency. Moreover, they are available in modular units, characterized by ease of finding sites for smaller generators, shorter construction times, and lower capital costs. Simultaneously, there are many obstacles when building large power plants and transmission lines. Companies or end users can install DG quickly. This will reduce the need for large plants and transmission lines (TL). For companies, the need for local generation is for a) Overloaded circuits and b) Generation shortages.

Utilities must prepare for several scenarios and consider DGs as another tool for supplying end users with electric power. Although the installation of DGs to solve network problems has been debated in distribution networks, the distribution system operator (DSO) has no control about DG location and size in most cases. Renewable and nonrenewable DGs resources can be rotating devices (synchronous or asynchronous machines), or static devices. When connected to the power system, these DGs have different impacts on power system operation, control, and stability. Also, DG placement impacts critically the operation of the distribution network. Inappropriate DG placement may increase system losses and operating costs. On the contrary, optimal DG placement (ODGP) can improve network performance in terms of voltage profile, reduce flows and system losses, and improve reliability of supply.

There are several energy sources which drive distributed generators. And depending on how they connected to the system to convert the energy to electrical energy, they may be one of the following:

2.8.1. Synchronous Generator

Synchronous generators are used in interfacing to convert energy that produced from reciprocating engines and combustion turbines. In this type, because of the burn rate of the fuel/air mixture controls the power output, the real power output is controllable and responds to load changes.

Reciprocating engines and gas turbines above 500 kW nearly always interface with a synchronous generator. Most distribution generators are salient pole machines with four or six poles driven by 1800 or 1200 rpm reciprocating engines (with some even slower in larger units). Distribution gas turbines spin faster but are normally geared down to drive a salient-pole generator at 1800 rpm [37].

Most distributed synchronous generators use a voltage-following control mode. But there is a difference between them and large generators on the electric system which regulate the voltage (within the limits) by some controls. Also, they produce fixed power (at the utility voltage) sometimes at unity power factor.

2.8.2. Induction Generators

Induction generators are used when the speed of the prime mover varies as in some wind turbines (variable-speed), some microturbines and internal combustion engines. In these distributed generators, there are no exciters, voltage regulators, governors, or synchronizing equipment. Therefore, their cost and maintenance is lower than distributed synchronous generators. On the other hand, they have a disadvantage of not being able to provide reactive power control. Also, they can't operate as island generator because they cannot create voltage on its own. They need source of VARs and these powers can be supplied by the utility system or local capacitors.

The construction of induction generator is similar to the induction motor. Therefore, at starting, they draw inrush to 5 or 6 times their rating. Using of autotransformers can reduce this inrush. In starting of some induction generators, the utility may accelerate the prime mover to more than synchronous speed. If possible, the prime mover can accelerate the shaft to near synchronous speed before closing in; this softens the inrush when connecting. In addition, care must be taken to avoid damage the shaft and other equipment in reclosing the self-excited induction generator (SEIG) with local capacitors.

The SEIG is a good candidate for wind powered electric generation applications especially in variable wind speed and remote areas because the necessary exciting current can be supplied from excitation capacitors which connected across the stator terminals of the generator. This also requires that there is some residual magnetism in the rotors iron laminations when you start the turbine. A typical circuit for a induction generator is shown in Figure 2.27.

Most wind turbines in the world use induction generators to generate alternating current. The induction generator will increase or decrease its speed slightly if the torque varies. It is a very useful mechanical property. This will reduce depreciation on the

gearbox. This is one of the most important reasons for using induction generators on a wind turbines which is directly connected to the electrical grid.

The SEIG is a good candidate for wind powered electric generation applications especially in variable wind speed and remote areas, because they do not need external power supply to produce the magnetic field [38].

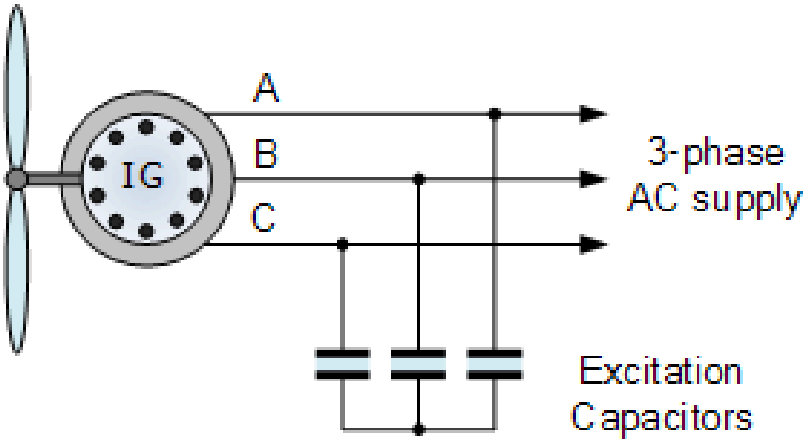

Figure 2.27. A typical circuit for a induction generator.

2.8.3. Inverters

Inverters are used for interfacing in many types of small power sources like photovoltaics and fuel cells those generate DC current. They used with some wind turbines and some microturbines which generate incompatible frequencies. The two main classes of inverters are line commutated and self-commutated.

Line-commutated inverter is the simplest and least-expensive. Thyristors in a full-wave bridge configuration convert from DC to AC by switching current. Figure 2.28 shows the bridge configuration of common three-phase line-commutated inverter. The inverter controls to turn on the thyristor and the thyristor is not turned off until the next current zero.

Since a line-commutated inverter draws currents in square waves, it creates large harmonics, primarily the 5^{th}, 7^{th}, 11^{th}, and 13^{th}. Line-commutated inverters require significant reactive power from the system, between 10% and 40% of the inverter rating. It is possible to use 12, 18, or 24-pulse bridge designs with phase-shifting transformers to reduce harmonics [37].

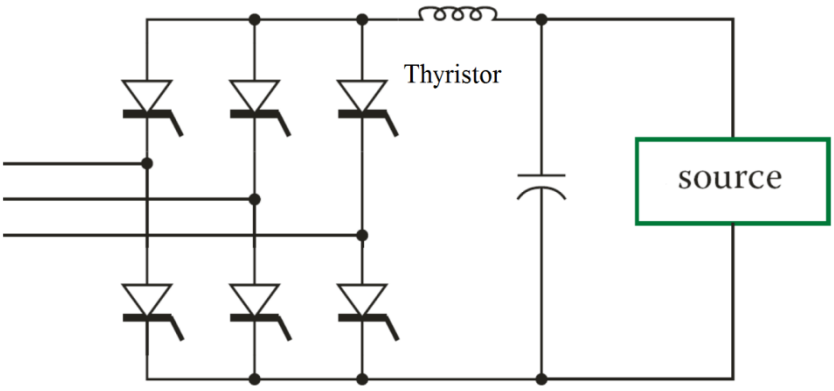

Figure 2.28. Configuration of three-phase line-commutated inverter.

Line-commutated inverter thyristors are switched on and off once per period. But Self-commutated inverters integrate electronic switches that are switched on and off a number of times per period, thus greatly reducing reactive power consumption and current harmonics. In lieu of thyristors, self-commutated inverters integrate the following elements that act as rapid electronic switches: Gate turn-off thyristors (GTOs), Bipolar solid state transistors, Power MOSFETs (power FETs with insulated gates) and Insulated gate bipolar transistors (IGBTs). These self-commutated inverters can either be voltage controlled or current controlled. The voltage-controlled inverter is simpler where the controller creates a reference voltage. The current-controlled inverter is more suitable for distributed generators where the controller uses the utility voltage as a reference and injects current at the proper angle (usually at unity power factor).

By using renewable energy (like wind and solar energy) as a source of DG to reduce greenhouse gas emissions and alleviate global warming, it is expected to provide a more secure and reliable power system if it is connected to the distribution system. Therefore, it will be worth utilizing these DG units for supporting utility distribution networks for both technical and economic reasons.

In wind energy, the movement of air mass is the source of mechanical kinetic energy produced by the wind turbine to drive the generator installed on the turbine shaft. To select the wind farm (a group of wind turbines) location, the sufficient rate and intensity of the wind over the year are necessary and not sufficient conditions. There are aspects such as the distance between the wind farm and the utility grid to be connected, topography and geography of the selected location.

It is important to collect accurate data about wind speed distribution hour by hour, day by day, and year by year to be able to determine the calm periods. Calm periods are the periods during which the wind speed is less than (3 m/s) and the wind system is completely stopped [35].

The total input mechanical power of the wind turbine $\boldsymbol{P}_{input}$ is:

$$P_{input} = \frac{1}{2}\rho A V^3. \tag{2.10}$$

Where:

ρ is the air density [kg/m^3].

A is the surface area swept by rotor blades [m^2].

V is wind speed.

The wind mechanical power is proportional to the wind speed cubed. A typical speed – power curve is shown in Figure 2.29.

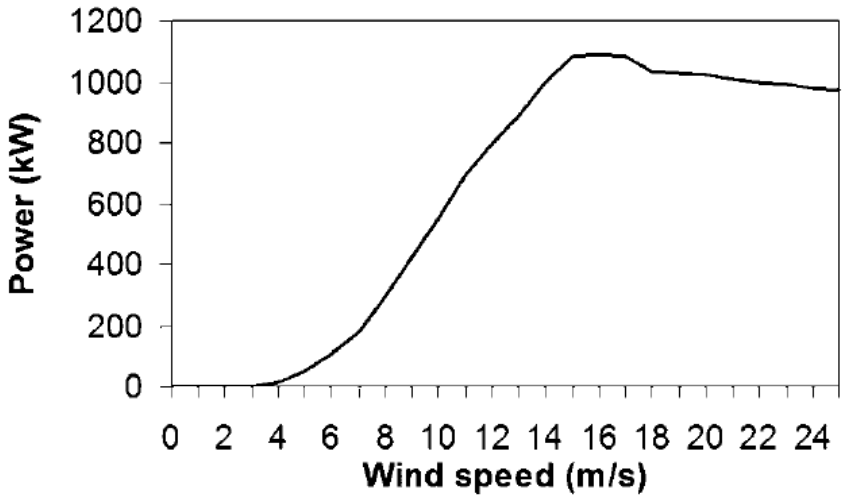

Figure 2.29. Typical speed–power curve of 1 MW wind turbine.

In solar energy, the sun is the source of solar radiation which converted to electric energy by solar cells. The operation of solar cells (also known as photovoltaic (PV) devices) convert solar radiation into electricity by light absorption based on photovoltaic effect. Each PV device delivers a voltage less than (1 V). So, these devices are connected in series and packaged into modules to deliver higher voltage. The

conversion efficiency of PV devices ranges from 13% to 16%. The PVs technology have received great interest because they have the following advantages [35]:

1. There is no noise, no pollution, and no mechanical moving parts.
2. Long lifetime.
3. Solar radiation is directly converted into electricity.
4. There is no cost and expense for energy source (the sun), which is also inexhaustible.
5. PV power ranges from microwatts to megawatts.
6. PV power sources are not limited to certain geographic locations compared with wind energy.

The output power of PV depends on the irradiance, which depends on the time of day and the day of the year. Therefore, the maximum power generated, and the length of operation achieved in the summer season. Also, local weather conditions result in power outputs with many spikes and troughs. The irradiance usually follows approximately a bell-shaped curve centered on midday, with a spread depending on the length of daylight. A PV bell-shaped curve during one day is shown in Figure 2.30.

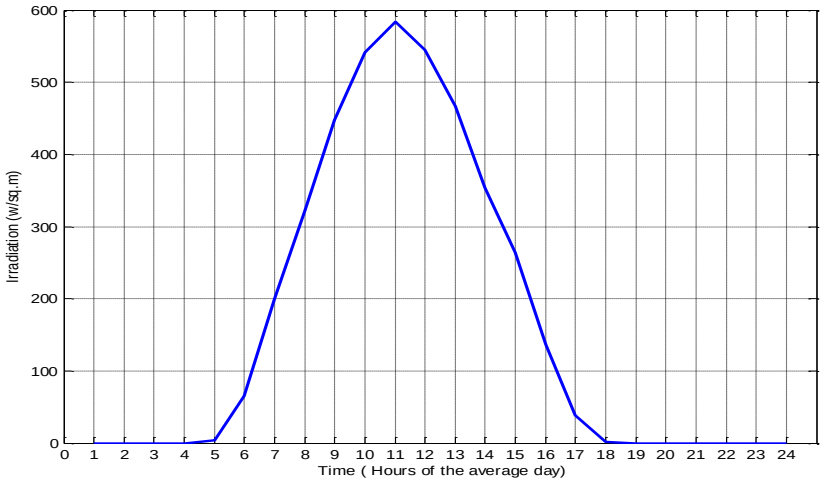

Figure 2.30. Diagram of one hour average of irradiation in the day.

PV systems applications are either stand – alone or connected to distribution networks. The applications may be DC power consumed without storage systems (in case of using PV during sunny periods only) or with storage systems (e.g., batteries) if power is needed in the evening or in cloudy weather. PV systems with inverters are used

for alternating current (AC) power applications. Large power PV systems can be connected to distribution networks through an inverter and the consumer's loads will be supplied from the utility grid. Figure 2.31 shows a PV system connected to the network.

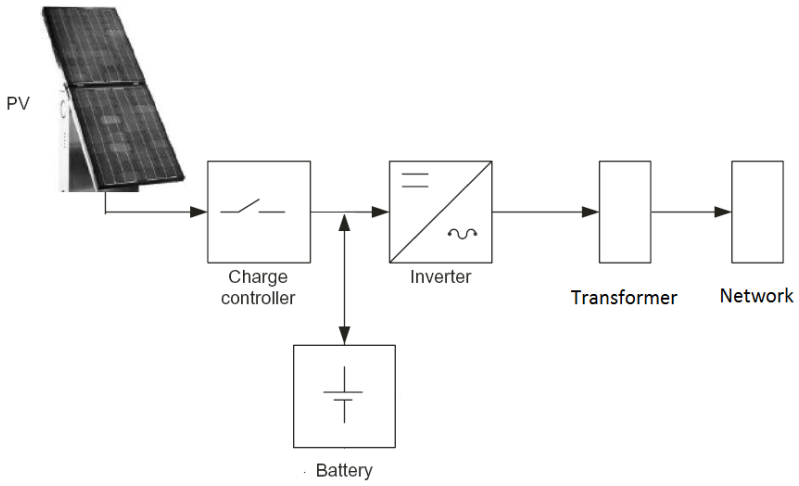

Figure 2.31. A PV system connected to network.

Chapter 3. Uncertainty in loads and DG units productions

3.1. Introduction

Actual distribution systems exhibit numerous parameters and phenomena that are nondeterministic and dependent on so many diverse processes that they may readily be regarded as nondeterministic or uncertain. Uncertainties of randomly varying system parameters cannot be analyzed by deterministic methods. Hence probabilistic methods are more suitable for this purpose. Generally, uncertainty can be modeled using mathematics definition and models. Uncertainty theory can start with random variables.

3.2. Random variables

A random variable is any variable determined by chance and with no predictable relationship to any other variable. The selection of the random variable is unpredictable and cannot be subsequently reproduced. A random variable generator is a tool for the generation of random variables. Actually, two methods are known to get the random variables [39]:

– Measuring a physical phenomenon that is expected to be random.

– Running a pseudorandom variable generator using computer algorithm.

Two examples of random numbers, generated by computer, are shown in Figure 3.1 and Figure 3.2. The first figure shows 100 and the second figure shows 1000 random numbers between 0 and 1. The visual comparison of these two cases shows that

the generated real numbers in larger quantities enable a higher degree of confidence that the generation is really random.

The most difficult is to prove that a number generator gives really a set of random numbers. The simplest tests can be done in a way to group the results of random experiments into the groups and evaluate the portion of the number of the event within one group versus all number of events. A large number of generated random numbers is a precondition for proving the randomness of the pseudorandom number generator. For example Table 3.1 shows the number of generated random numbers grouped in five intervals for 100, 1,000 and 10,000 random numbers.

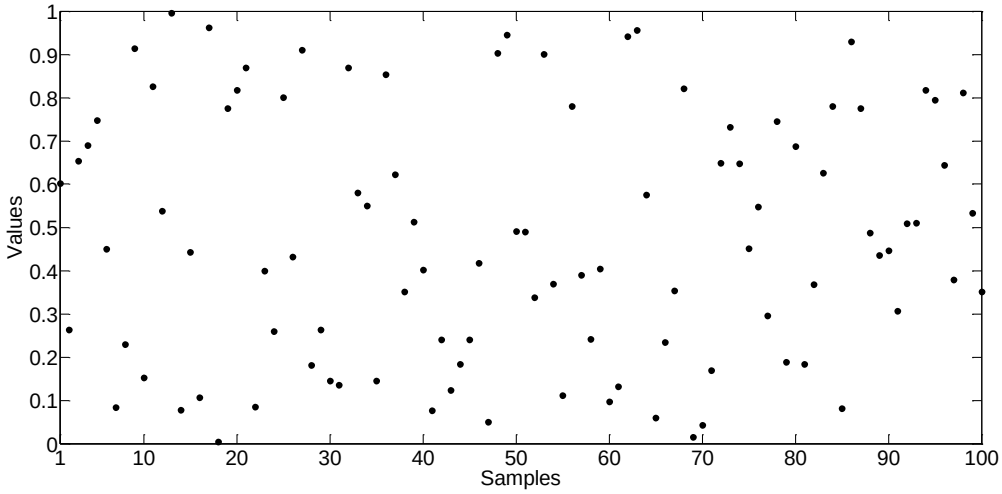

Figure 3.1. 100 random numbers between 0 and 1.

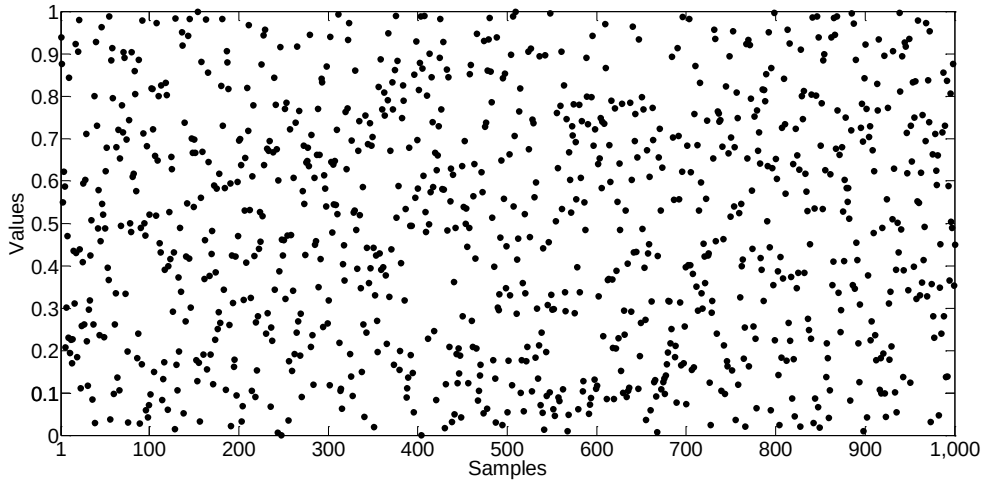

Figure 3.2. 1000 random numbers between 0 and 1.

Results in Table 3.1 show that the bigger set of random numbers meaning the bigger confidence that the generation of random numbers is really random.

Table 3.1. Random numbers grouped in five intervals.

	100 r. numbers		1,000 r. numbers		10,000 r. numbers	
x[0, 1]	samples	[%]	samples	[%]	samples	[%]
$0 < x \leq 0.2$	17	17	205	20.5	1985	19.85
$0.2 < x \leq 0.4$	25	25	192	19.2	2048	20.48
$0.4 < x \leq 0.6$	11	11	206	20.6	2008	20.08
$0.6 < x \leq 0.8$	23	23	177	17.7	1995	19.95
$0.8 < x \leq 1$	24	24	220	22.0	1964	19.64

3.3. Probability distributions

The probability distribution function describes the range of possible values that a random variable can attain and the probability that the value of the random variable is within any measurable subset of that range [39]. Probability distribution function can be discrete or continuous depending on the nature of the events that are considered. For discrete random variables, its probability distribution function is a discrete probability distribution function. If a random variable under investigation is a continuous variable, its probability distribution function is a continuous probability distribution function.

Cumulative distribution function (CDF) and the probability density function (PDF) are two functions that are representative for a distribution. Figure 3.3 shows the theoretical comparison of continuous and discrete distribution in terms of a probability density function.

For discrete random variables X with possible values x_1, x_2, ..., x_n, its distribution can be described by a function that specifies the probability at each of the possible discrete values for X. PDF for discrete variable is a function such that [40]:

$$f(x_i) \geq 0. \tag{3.1}$$

$$\sum_{i=1}^{n} f(x_i) = 1. \tag{3.2}$$

$$f(x_i) = P(X = x_i). \tag{3.3}$$

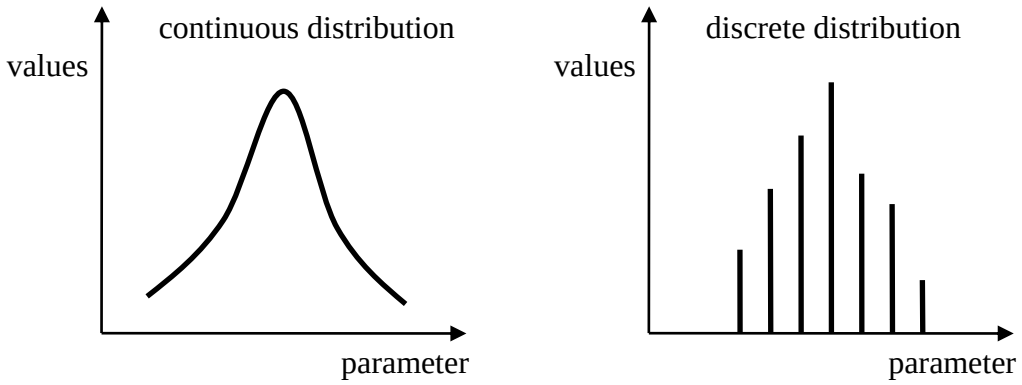

Figure 3.3. Ilustration of continuos and discrete PDF.

PDF is non-negative for all real x (eq. 3.1). The sum of all probabilities of PDF equals 1 (eq. 3.2). Probability for discrete variable x_i is given by equation (3.3).

For a continuous random variable X, a PDF is a function such that [40]:

$$f(x) \geq 0. \tag{3.4}$$

$$\int_{-\infty}^{+\infty} f(x)\,dx = 1. \tag{3.5}$$

$$P(a \leq X \leq b) = \int_{a}^{b} f(x)\,dx. \tag{3.6}$$

The function $f(x)$ is non-negative for all real x (eq. 3.4). The integral of the PDF equals 1 (eq. 3.5). The probability that x lays between two points a and b is calculated using equation (3.6).

The continuous probability density functions are defined for an infinite number of points over a continuous interval and the probability at a single point is zero. The probabilities are measured over intervals and the area under the curve between two distinct points defines the probability for that interval. The property of the continuous distribution that the integral must equal one is equivalent to the property for discrete distributions that the sum of all the probabilities must equal one.

Probability distributions are used in theory and in practice. The theoretical part is very mathematical. Practical applications are numerous. There are various probability distributions used in various different applications. Most commonly used probability distributions are [40]:

– Normal distribution or Gauss distribution.

– Lognormal distribution.

– Gamma distribution.

– Beta distribution.

– Weibull distribution.

– Uniform distribution.

– Exponential distribution.

In the following text definitions of terms that are important in statistics will be given. These definitions are necessary for defining the features of each distribution.

Arithmetic mean (μ) of a set of values is the quantity commonly called the average or the mean value. From a set of n discrete samples x_1, x_2, ..., x_n, the arithmetic mean is calculated as [40]:

$$\mu = \frac{1}{n}\sum_{i=1}^{n} x_i \,. \tag{3.7}$$

For a continuous function *f(x)* over the interval [a, b], the arithmetic mean is calculated as [40]:

$$\text{Mean} = \mu = \frac{1}{b-a}\int_a^b f(x)dx. \tag{3.8}$$

The expected value ($E(X)$) of a random variable X is defined by equation:

$$E(X) = \sum_{x:f(x)>0} xf(x). \tag{3.9}$$

Standard deviation (σ) is a measure of the dispersion of a set of data from its mean. If the data are more spread apart, the deviation is higher. Standard deviation is calculated as [40]:

$$\sigma = \sqrt{\frac{1}{n}\sum_{i=1}^{n}(x_i-\mu)^2}\,. \tag{3.10}$$

Variance (V) is a measure of the dispersion of a set of data points around their mean value. Variance is a mathematical expectation of the average squared deviations from the mean. The variance is the square of the standard deviation [40]:

$$V = \sigma^2 = \frac{1}{n}\sum_{i=1}^{n}(x_i-\mu)^2\,. \tag{3.11}$$

The variance of the random variable X with a finite mean μ is defined by the equation [40]:

$$V(X) = E[(X-\mu)^2] = E[X^2] - (E[X])^2. \quad (3.12)$$

The standard deviation of a random variable X is defined by equation [40]:

$$\sigma(X) = \sqrt{V(X)}. \quad (3.13)$$

A confidence interval is an interval in which a measurement or trial falls corresponding to a given probability. It is determined by a particular confidence level, usually expressed as a percentage. The confidence limits are the end points of the confidence interval [40].

3.3.1. Normal distribution or Gauss distribution

The normal distribution is the widely used model for the distribution in science. Repeated independent measurements with random uncertainties of almost any quantity follow this distribution. The PDF for this distribution defined for $-\infty < x < +\infty$ is given by equation [40]:

$$f(x) = \frac{1}{\sigma\sqrt{2\pi}} \exp\left[\frac{-(x-\mu)^2}{2\sigma^2}\right]. \quad (3.14)$$

where σ is the standard deviation of the variable X and μ is the mean value of the variable X. The notation $N(\mu, \sigma^2)$ is used to denote the distribution. The expected value and variance of the normal distribution are:

$$E(X) = \mu. \quad (3.15)$$

$$V(X) = \sigma^2. \quad (3.16)$$

Random variables with different means and variances can be modeled by normal PDF with appropriate choices of the center and width of the curve. The value of μ determines the center of the probability density function and the value of σ^2 determines the width. Figure 3.4 illustrates several normal PDFs with selected values of μ and σ^2.

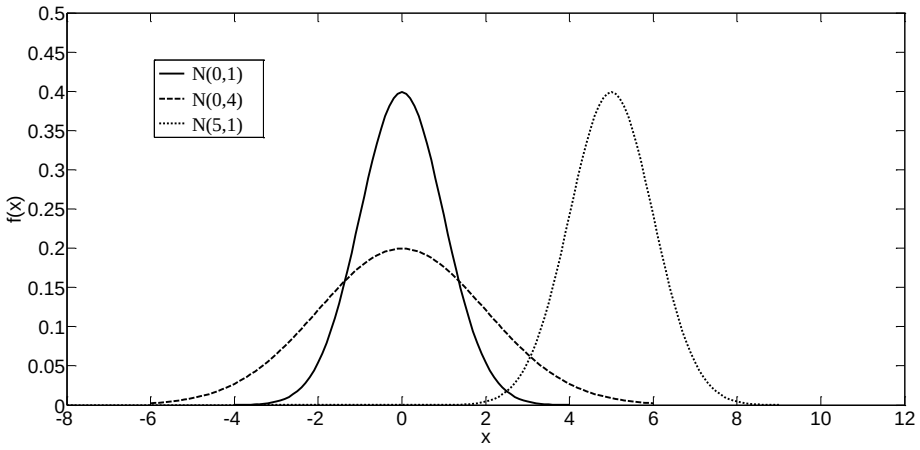

Figure 3.4. The normal PDFs with selected values of μ and σ^2.

3.3.2. Lognormal distribution

The lognormal distribution indicates that the logarithm of the random variable *X* is normally distributed. The PDF defined for *x* from $0 < x < +\infty$ is given by equation [40]:

$$f(x) = \frac{1}{x\sigma\sqrt{2\pi}} \exp\left[\frac{-(\ln(x)-\mu)^2}{2\sigma^2}\right]. \tag{3.17}$$

The scale parameter μ of the lognormal distributions equals to the mean value for the normal distribution. The shape parameter σ^2 of the normal and lognormal distributions equals to the standard deviation for the normal distribution. The mean value and variance of the lognormal distribution are:

$$\mu = E(X) = e^{\mu+\sigma^2/2}. \tag{3.18}$$

$$\sigma^2 = V(X) = e^{2\mu+\sigma^2}(e^{\sigma^2}-1). \tag{3.19}$$

Figure 3.5 illustrates the lognormal distributions for selected values of the parameters. The lognormal distribution is used for modeling the lifetime of a product that degrades over time. For example, this is a common distribution for the lifetime of a semiconductor laser.

3.3.3. Gamma distribution

The formula for the PDF of the gamma distribution for random variable is [40]:

$$f(x) = \frac{\beta^{\alpha} x^{\alpha-1} e^{-\beta x}}{\Gamma(\alpha)}. \tag{3.20}$$

where $\alpha > 0$ is the scale parameter, $\beta > 0$ is the shape parameter and $\Gamma(\alpha)$ is the gamma function given by equation:

$$\Gamma(\alpha) = \int_0^{\infty} x^{\alpha-1} e^{-x} dx. \tag{3.21}$$

The mean value and variance of the gamma distribution are:

$$\mu = E(X) = \alpha / \beta. \tag{3.22}$$

$$\sigma^2 = V(X) = \alpha / \beta^2. \tag{3.23}$$

Examples of the gamma distribution for several values of α and β are shown in Figure 3.6.

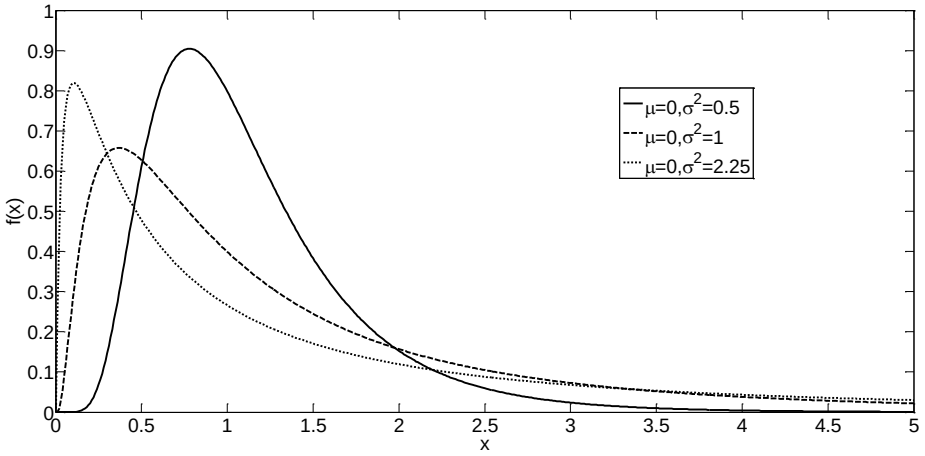

Figure 3.5. The lognormal distributions for selected values of the parameters.

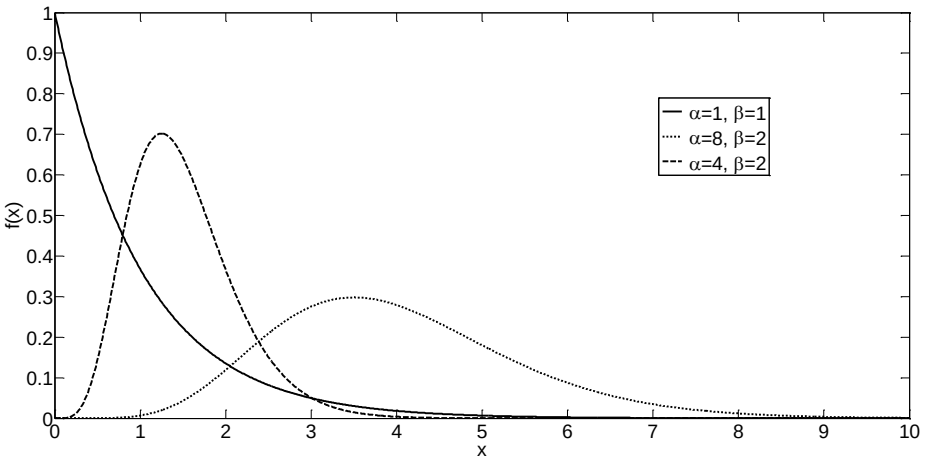

Figure 3.6. The gamma distribution for several values of α and β.

3.3.4. Beta distribution

The beta distribution is a continuous distribution that is flexible but bounded over a finite range. The proportion of solar radiation absorbed by a material or the proportion of the maximum time required to complete a task in a project are examples of continuous random variables over the interval [0, 1]. These cases can be modeled with the beta distribution. The formula for the PDF of the beta distribution for a random variable is [40]:

$$f(x)=\frac{\Gamma(\alpha+\beta)}{\Gamma(\alpha)\Gamma(\beta)}x^{\alpha-1}(1-x)^{\beta-1},\ x\in[0,1]. \tag{3.24}$$

where $\alpha > 0$ is the scale parameter, $\beta > 0$ is the shape parameter and $\Gamma(*)$ is the gamma function. The mean value and variance of the beta distribution are:

$$\mu=E(X)=\frac{\alpha}{\alpha+\beta}. \tag{3.25}$$

$$\sigma^2=V(X)=\frac{\alpha\beta}{(\alpha+\beta)^2(\alpha+\beta+1)}. \tag{3.26}$$

The parameters α and β allow the PDF to assume many different shapes. Some examples are shown in Figure 3.7. If $\alpha = \beta$ the distribution is symmetric about $x = 0.5$. The figure illustrates that other parameter choices generate nonsymmetric distributions.

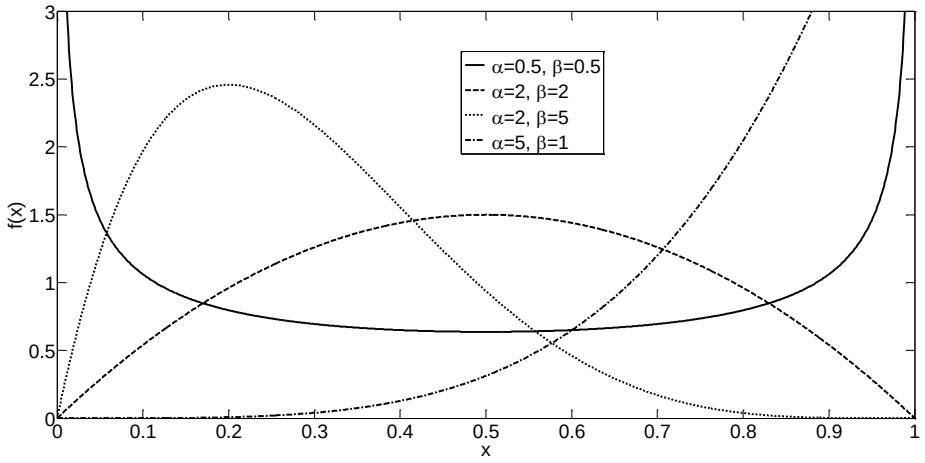

Figure 3.7. The Beta PDFs for selected values *α* and *β*.

3.3.5. Weibull distribution

The Weibull distribution is often used to model the time until failure of many different physical systems. The parameters in the distribution provide a great deal of flexibility to model systems in which the number of failures increases with time, decreases with time, or remains constant with time [40]. Also, the Weibull distribution is used to describe wind speed variations. The formula for the PDF of the Weibull distribution for a random variable is [40]:

$$f(x)=\frac{\beta}{\delta}\left(\frac{x}{\delta}\right)^{\beta-1}\exp\left[-\left(\frac{x}{\delta}\right)^{\beta}\right],\ x>0, \tag{3.27}$$

Where $\delta > 0$ is the scale parameter, $\beta > 0$ is the shape parameter. The mean value and variance of the Weibull distribution are:

$$\mu = E(X) = \delta\Gamma\left(1+\frac{1}{\beta}\right). \tag{3.28}$$

$$\sigma^2 = V(X) = \delta^2\Gamma\left(1+\frac{2}{\beta}\right)-\delta^2\left[\Gamma\left(1+\frac{1}{\beta}\right)\right]^2. \tag{3.29}$$

The flexibility of the Weibull distribution is illustrated by the graphs of selected PDFs in Figure 3.8. The Rayleigh distribution is a special case of the Weibull distribution when the shape parameter is 2 [40].

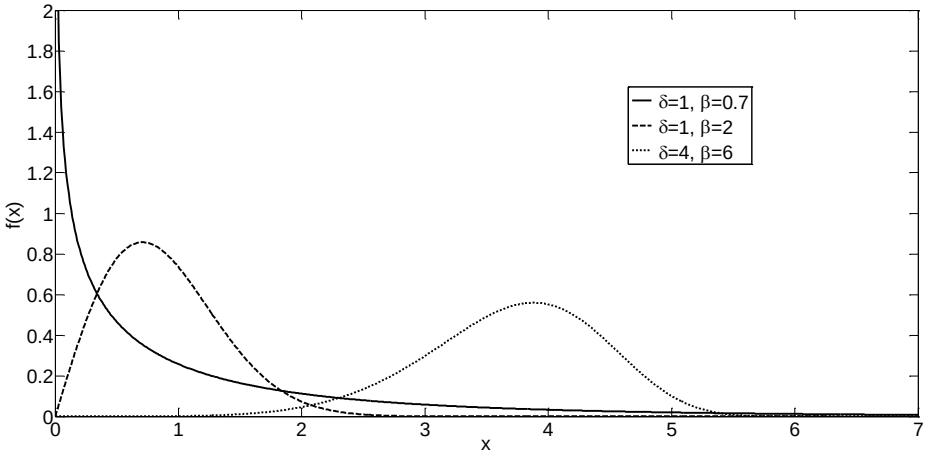

Figure 3.8. The Weibull PDFs for selected values of δ and β.

3.3.6. Uniform distribution

The uniform distribution is defined for values between two numbers. For others, it equals zero. The PDF of the uniform distribution for random variable is given by equation [40]:

$$f(x) = \frac{1}{b-a}, a < x < b. \tag{3.30}$$

The mean value and variance of the uniform distribution are:

$$\mu = E(X) = \frac{a+b}{2}. \tag{3.31}$$

$$\sigma^2 = V(X) = \frac{(b-a)^2}{12}. \tag{3.32}$$

The PDF of a continuous uniform random variable is shown in Figure 3.9.

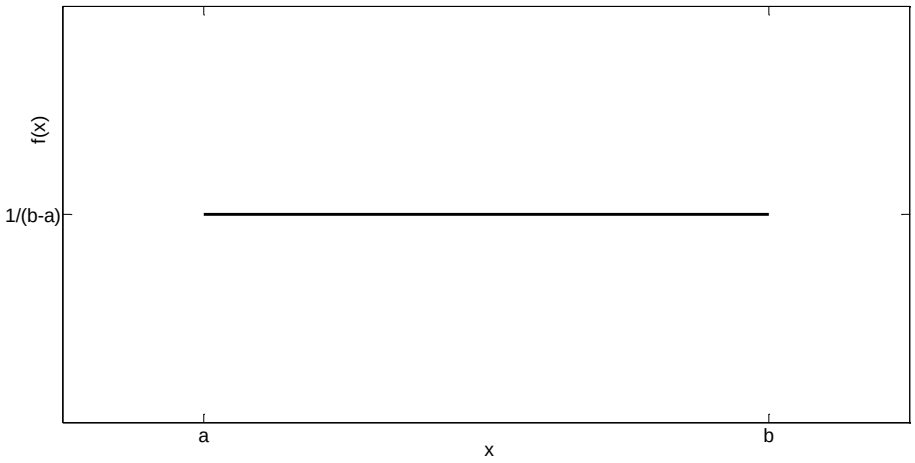

Figure 3.9. The PDF for uniform distribution.

3.3.7. Exponential distribution

The exponential distribution is widely used for modelling time to failure where t ≥ 0. The PDF for this distribution is given by equation [40]:

$$f(x) = \lambda e^{-\lambda x}, 0 < x < \infty. \tag{3.33}$$

The mean value and variance of the exponential distribution are:

$$\mu = E(X) = \frac{1}{\lambda}. \tag{3.34}$$

$$\sigma^2 = V(X) = \frac{1}{\lambda^2}. \tag{3.35}$$

Plots of the exponential distribution for selected values of are shown in Figure 3.10.

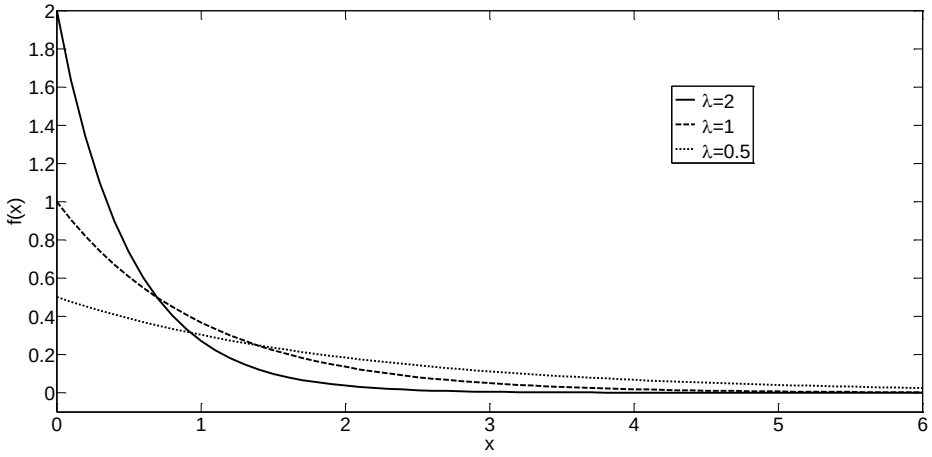

Figure 3.10. The PDF for exponential distribution for selected λ.

The exponential distribution is an excellent model for the long flat portion of the bathtub curve, because of its constant failure rate property.

3.4. Power load uncertainty

Generally speaking, there are two kinds of uncertainties in power systems operation and planning [41]:

1. Uncertainty in a mathematical sense, which means the difference between measured, estimated values and true values, including errors in observation or calculation.
2. Sources of uncertainty, including transmission capacity, generation availability, load requirements, unplanned outages, market rules, fuel price, energy price, market forces, weather and other interruption, etc.

Power loads especially residential loads are variable, exhibiting a very pronounced uncertainty. The power load is a function of time, weather conditions, market prices, and many other factors. Also, the variability of the electricity consumption of a single residential customer depends on the presence of the family members at home and on the time of using few high-power appliances with relatively short duration of use during the day. In such a way, it is impossible to predict the actual

load before its occurrence. Load forecasts, based on historical records of load variation, can predict a coarse picture of the probable situation. Thus instead of load representation by load levels, a probabilistic variation of loads would be a better representation.

Different probability distribution functions may be selected for the different kinds of uncertainty loads. However, the normal distribution is commonly the used distribution to model uncertainty in load consumption. Load uncertainty at specified load level can be modeled by using a normally distributed random variable according to the following equation:

$$P_\sigma = P(1+\sigma x)\,. \tag{3.36}$$

Where P is load level (mean value), σ is the standard deviation in percentage of load P and x is the random number with standard normal distribution. The standard normal distribution assumes a mean of zero and a variance of unity.

For illustration purposes, Figure 3.11 to Figure 3.13 show 10,000 samples, generated using equation (3.36), with the same mean value (P=100 kW) and different standard deviations. In Figure 3.11 samples generated with standard deviation σ = 0.1 (10%), in Figure 3.12 with σ = 0.05 (5%), and finally in Figure 3.13 with σ = 0.01 (1%). It is obvious that standard deviation plays the main role in sampling process for uncertainty modelling. With small values of standard deviation (Figure 3.13) all samples are near the mean value. In this case variations of loads are very small.

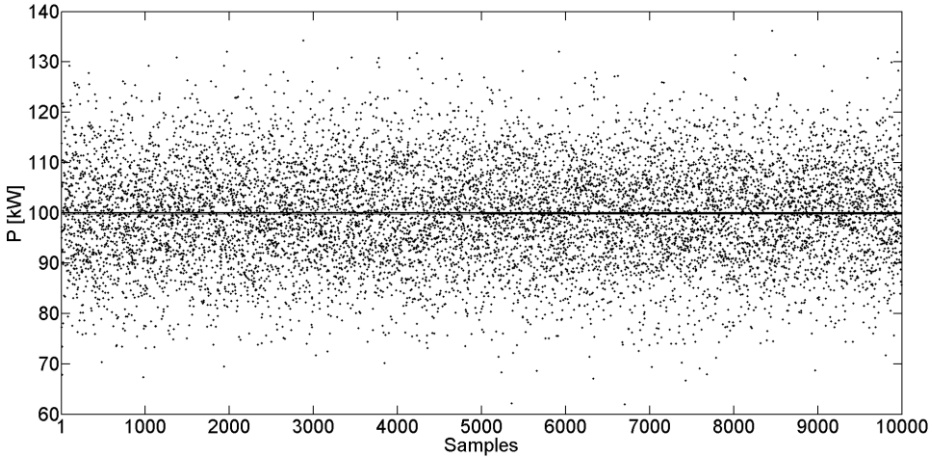

Figure 3.11. 10,000 samples with P=100 kW and σ=0.1 (10%).

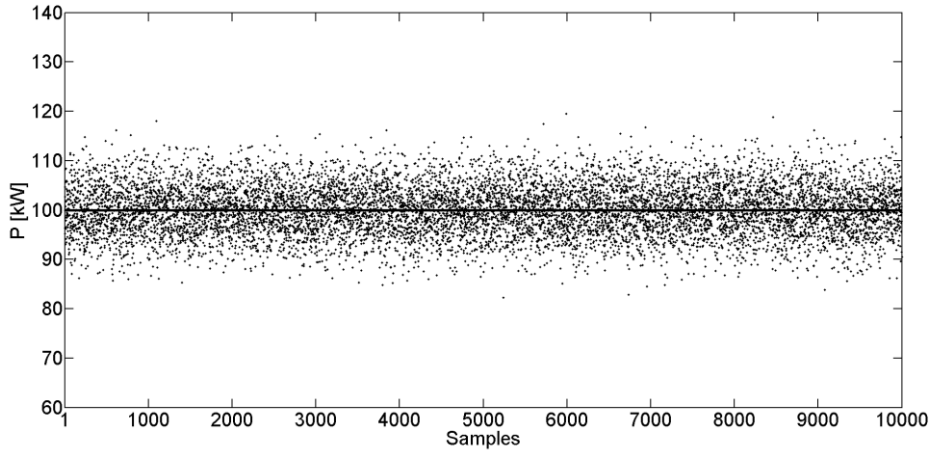

Figure. 3.12. 10,000 samples with *P*=100 kW and σ=0.05 (5%).

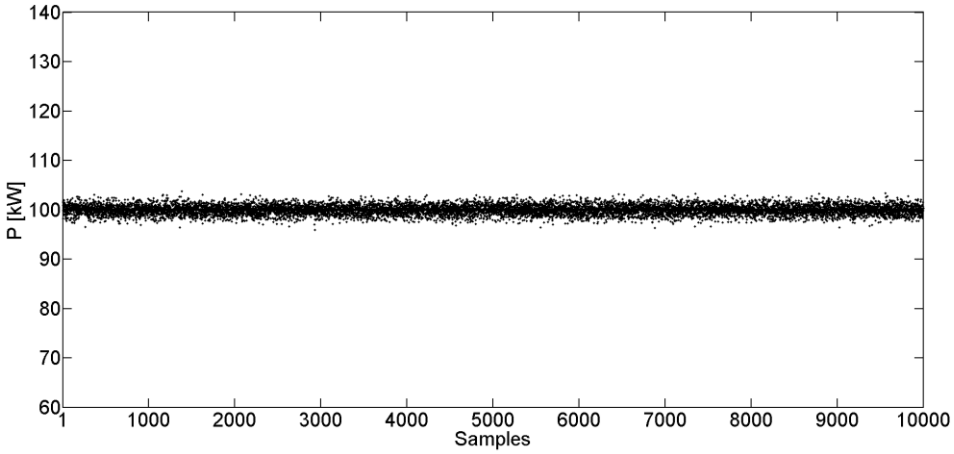

Figure 3.13. 10,000 samples with *P*=100 kW and σ=0.01 (1%).

3.5. Uncertainty of wind turbine production

Power generated by WTs depends on the wind speed that varies with time in a stochastic manner. Thus, in order to model wind speed properly, it is required to study the probabilistic wind power [42]. Wind speed random variations usually can be described by the Weibull PDF [40], which can be represented by this relation:

$$f(x)=\frac{\beta}{\delta}\left(\frac{v}{\delta}\right)^{\beta-1}\exp\left[-\left(\frac{v}{\delta}\right)^{\beta}\right],\ v>0. \tag{3.37}$$

Where v is the wind speed, δ is the scale parameter and β is the shape parameter. Equation (3.37) is the same as the equation (3.27) with the difference that the random variable x is replaced by the variable v, which represents the wind speed. The wind speed data should be obtained by measurements taken at the location to be analyzed.

The Weibull PDF parameters (the scale parameter δ and the shape parameter β) can be calculated using measured data. The parameters of the Weibull distribution define the distribution of the wind at the analyzed location.

For modelling a WT's output power uncertainty, the wind speed samples can be generated according to Weibull PDF. The generated wind speed samples can be transformed to the wind turbine output power by using the wind turbine power curve according to the following relation [42]:

$$P_{WT} = \begin{cases} 0, & 0 \le v < v_{cin} \\ \left(\dfrac{v - v_{cin}}{v_r - v_{cin}}\right) P_{rw}, & v_{cin} \le v < v_r \\ P_{rw}, & v_r \le v < v_{cout} \\ 0, & v \ge v_{cout} \end{cases}, \quad (3.38)$$

WTs are designed to start producing power at cut-in wind speed v_{cin}, arriving at its installed power P_{rw} at wind speed v_r. For wind speeds higher than v_r and less than v_{cout} the production stays at the installed power level. For safety reasons, WTs do not operate at wind speeds above the cut-out wind speed v_{cout} [42].

3.6. Uncertainty of solar power plant production

Solar radiation has a high degree of uncertainty. It is dependent on the time of day, the month of the year, the environmental conditions, the orientation of the photovoltaic (PV) panel with respect to solar radiation, etc [42]. Usually, solar radiation PDF is modeled by beta distribution function [40]:

$$f(x) = \frac{\Gamma(\alpha + \beta)}{\Gamma(\alpha)\Gamma(\beta)} R^{\alpha-1}(1-R)^{\beta-1}. \quad (3.39)$$

where R is solar radiation, and α, β are the shape parameters (α >0, β >0). Equation (3.39) is the same as the equation (3.24) with the difference that the random variable (x) is replaced by the variable R, which represents solar radiation. The beta PDF parameters (α and β) can be calculated using measured data of solar radiation taken at the analyzed location. The parameters of the beta distribution define the distribution of the solar radiation at the analyzed location.

For the purpose of modelling a PV panel output power uncertainty, the corresponding number of samples for the solar radiation, in accordance with the beta

distribution, can be generated. On the basis of the solar radiation values, the PV panel output power P_{SPP} can be calculated by means of the radiation-power curve [43]:

$$P_{SPP} = \begin{cases} P_{rs}(R^2 / R_{STD} R_C) & 0 \le R < R_C \quad , \\ P_{rs} \dfrac{R}{R_{STD}} & R_C \le R < R_{STD} \quad , \\ P_{rs} & R_{STD} \le R \quad . \end{cases} \tag{3.40}$$

Where R_{STD} is the standard solar radiation (usually 1000 W/m^2), R_C is a certain radiation point (usually 150 W/m^2) and P_{rs} is PV rated power.

3.7. Monte Carlo Simulation

Monte Carlo simulation (MCS) method is the computational algorithm that relies on repeated random sampling to obtain numerical results. MCS's essential idea is the using of randomness to solve the problems that might be deterministic in principle. In this view, MCS may be generally defined as a methodology for obtaining estimates of the solution of mathematical problems by means of random numbers. MCS is a powerful statistical analysis tool and it is widely used in both engineering fields and non-engineering fields. MCS method is also suitable for solving complex engineering problems because it can deal with a large number of random variables, various distribution types and highly nonlinear engineering models.

Credit for inventing the Monte Carlo method often goes to Stanislaw Ulam, a Polish born mathematician who worked for John von Neumann on the United States Manhattan Project during World War II. Ulam is primarily known for designing the hydrogen bomb with Edward Teller in 1951. He invented the MCS method in 1946 while pondering the probabilities of winning a card game of solitaire. Since the method is based on random numbers and probability, MCS is named after the city of Monte Carlo in Monaco which is famous for gambling such as roulette, dice, and slot machines.

MCS method has many advantages. MCS method allows a better understanding of the system, experimenting with the model of the system and preparation for unknown situations in the functioning of the system, enables detection of bottlenecks, assessment of different events and better preparation for decision making in risk conditions. The

fields of application within the energy sector can be the engineering economy, the forecast of consumption, the production planning, the network planning, the reliability and the risk assessment. The method can be applied in every calculation within the energy sector where variables are determined with a certain uncertainty. Also, the method is suitable for use with a calculation with variables measured with some error.

Unlike a physical experiment, MCS method performs random sampling and conducts a large number of experiments on the computer. Then the statistical characteristics of the experiments (model outputs) are observed, and conclusions on the model outputs are drawn based on the statistical experiments. In each experiment, the possible values of the input random variables $\mathbf{X} = (x_1, x_2, ..., x_n)$ are sampled according to their distributions (Gauss, Weibull, beta, etc.). Then the values of the output variable $\mathbf{Y} = (y_1, y_2, ..., y_m)$ are calculated through the performance function $\mathbf{Y} = f(\mathbf{X})$ by using the samples of input random variables. With a number of experiments carried out in this manner, a set of samples of output variable **Y** are available for the statistical analysis, which estimates the characteristics of the output variable **Y** (mean value, standard deviation, a confidence interval). The principle of the MCS method is shown in Figure 3.14.

MCS method can be summarized in next five steps:

Step 1: Create the mathematical model for the system, $\mathbf{Y} = f(\mathbf{X})$.

Step 2: Generate a set of random input variables, $x_{i1}, x_{i2}, ..., x_{in}$.

Step 3: Evaluate the model using function f and store the results, $y_{i1}, y_{i2}, ..., y_{im}$.

Step 4: Repeat steps 2 and 3 for $i = 1$ to N_{MCS}. N_{MCS} should be a large number, usually more than 10000.

Step 5: Analyze the results using histograms, summary statistics, confidence intervals, etc.

In Step 2 random variables are generated according to specified probability distributions. That process can be very easy using MATLAB software. For some probability distribution, the MATLAB functions are as follows [44]:

– *normrnd (mean, deviation,* 1, *N);* This function generates row vector of *N* random variables (samples), according the normal distribution with specified *mean* and *deviation*.

– *wblrnd* (*delta*, *beta*, 1, *N*); This function generates row vector of *N* random variables (samples), according the Weibull distribution with specified scale factor *delta* and shape factor *beta*.

– *betarnd* (*alfa*, *beta*, 1, *N*); This function generates column vector of *N* random variables (samples), according the beta distribution with specified scale factor *alfa* and shape factor *beta*.

Other probability distributions also have appropriate MATLAB functions for sampling random variables.

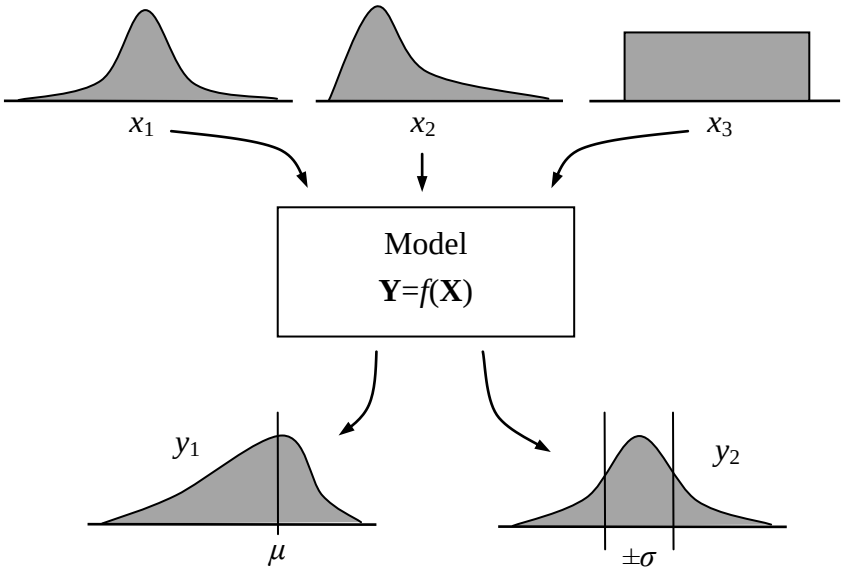

Figure 3.14. The basic principle behind MCS method.

The sampling process can be such that the series of random variables can be either independent or dependent. These aspects of the sampling process are discussed in the following section.

3.8. Correlation in random variables

The uncertain variables of the system may be dependent on each other or may not. When the variables are depending on each other, the variation of one variable affects the other variables, too. A common measure of the relationship between two series of variables is the *covariance* [40]. The covariance is defined for both continuous and discrete random variables by the same formula:

$$\mathrm{cov}(X,Y)=\sigma_{XY}=E[(X-\mu_X)(Y-\mu_Y)]=E(XY)-\mu_X\mu_Y\,. \tag{3.41}$$

Where X and Y are sets of random variables, $E(*)$ is expected value, μ_X and μ_Y are mean values of series X and Y, respectively.

In a practical view, series of variables can be obtained by simultaneous measurements. For example, by measuring load consumption at the network buses or by measuring wind speed on different locations.

The *Correlation* is another measure of the relationship between two random variables that is often easier to interpret than the covariance. The correlation coefficient between a set of random variables X and Y is calculated according to the following equation [40]:

$$\rho_{XY}=\frac{\mathrm{cov}(X,Y)}{\sqrt{V(X)V(Y)}}=\frac{\sigma_{XY}}{\sigma_X\sigma_Y}\,. \tag{3.42}$$

Where σ_X and σ_Y are the standard deviations for a set of random variables X and Y, respectively. The coefficient defined in this way is also called Pearson correlation coefficient.

Because $\sigma_X > 0$ and $\sigma_Y > 0$, if the covariance between X and Y is positive, negative, or zero, the correlation between X and Y is positive, negative, or zero respectively. For any two sets of random variables X and Y, it can be shown that:

$$-1\le\rho_{XY}\le 1. \tag{3.43}$$

The correlation just scales the covariance by the product of the standard deviation of each variable. Consequently, the correlation is a dimensionless quantity that can be used to compare the linear relationships between pairs of variables in different units [40]. The correlation coefficient is +1 in case of a perfect positive linear relationship, -1 in the case of a perfect negative linear relationship and some values in the range of [–1, +1] in all other cases, indicating the degree of linear dependence between the variables. Two random variables with nonzero correlation are said to be correlated. In Figure 3.15, the scatter diagrams for the two random variables with normal distribution X and Y are presented, corresponding to different correlations ranging from −1 to 1. Both series of random variables have 10000 samples with the mean values equal to 0 and the standard deviations equal to 1. As can be seen, while the correlation increases from 0 to 1, the random variables become more linearly dependent.

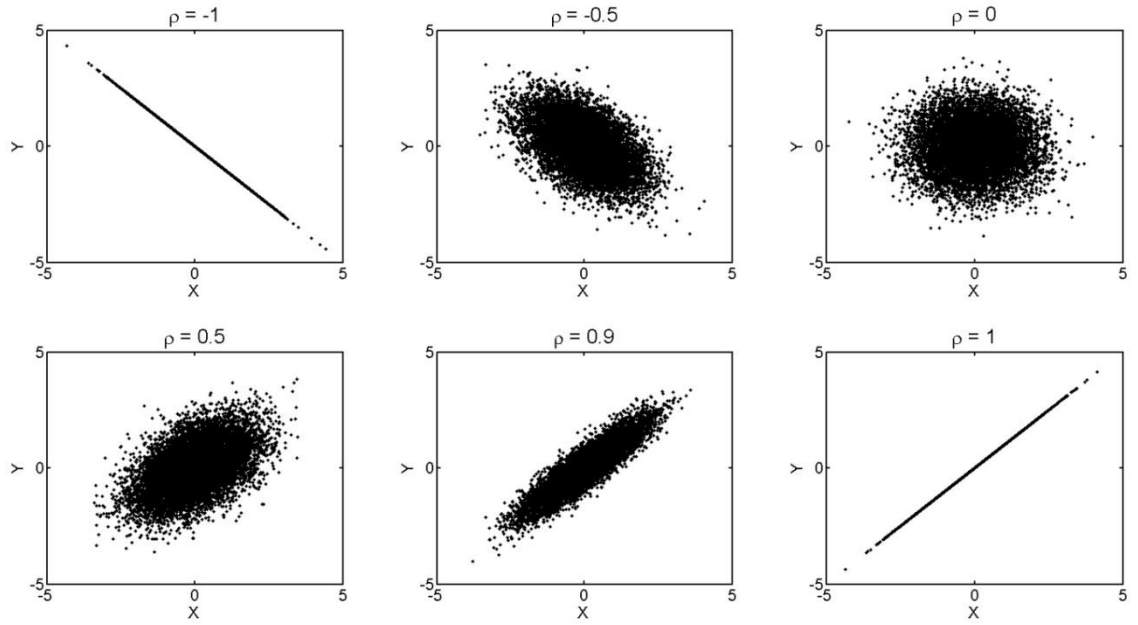

Figure 3.15. The scatter diagrams for two random variables with different correlations.

Generally, the correlation between K sets of random variables, say, $X_1, X_2, ..., X_K$, can be represented with the correlation matrix. The main diagonal elements of the matrix are unity and the off-diagonal elements ρ_{ij} are the correlations between X_i and X_j. The correlation matrix is given by the following equation:

$$\boldsymbol{\rho} = \begin{bmatrix} 1 & \rho_{12} & \cdots & \rho_{1K} \\ \rho_{21} & 1 & \cdots & \rho_{2K} \\ \vdots & \vdots & \ddots & \vdots \\ \rho_{K1} & \rho_{K2} & \cdots & 1 \end{bmatrix}. \tag{3.44}$$

Generating correlated sets of random variables will be shown first for random variables with normal distributions. Using the MCS method, K sets of random variables with standard normal distribution can be generated. Standard normal distribution implies the mean value equals 0 and the standard deviation equals 1. All generated samples can be represented by the matrix:

$$\mathbf{X} = \begin{bmatrix} x_{11} & x_{12} & \cdots & x_{1j} & \cdots & x_{1N} \\ x_{21} & x_{22} & \cdots & x_{2j} & \cdots & x_{2N} \\ \vdots & \vdots & \ddots & \vdots & \vdots\vdots & \vdots \\ x_{i1} & x_{i2} & \cdots & x_{ij} & \cdots & x_{iN} \\ \vdots & \vdots & \vdots\vdots & \vdots & \ddots & \vdots \\ x_{K1} & x_{K2} & \cdots & x_{Kj} & \cdots & x_{KN} \end{bmatrix}. \tag{3.45}$$

Where x_{ij} is j^{th} sample of i^{th} distribution, K is the number of sets of random variables (distributions) and N is the total number of MCS samples.

Correlated K sets of random variables can be obtained as follows:

$$\mathbf{Y} = \mathbf{L}\mathbf{X}. \tag{3.46}$$

Matrix **L** can be easily obtained through the Cholesky technique. The correlation matrix is decomposed into the product the lower triangular matrix **L** and its transposed matrix $\mathbf{L}^T$ as in equation (3.47).

$$\boldsymbol{\rho} = \mathbf{L}\mathbf{L}^T. \tag{3.47}$$

The matrix **Y** has a similar form like the matrix **X**. Rows of the matrix **Y** now represents set of random variables who are correlated. Obtained sets of random variables also have standard normal distribution (mean value equals 0 and standard deviation equals 1). Correlated sets with desired (specified) mean values $\mu_1, \mu_2, ..., \mu_K$ and standard deviations $\sigma_1, \sigma_2, ..., \sigma_K$, can be obtained as follows:

$$\mathbf{Z} = \boldsymbol{\mu}(1 + \boldsymbol{\sigma}\mathbf{Y}). \tag{3.48}$$

Where $\boldsymbol{\mu}$ is a diagonal matrix, $\boldsymbol{\mu} = diag(\mu_1, \mu_2, ..., \mu_K)$ and $\boldsymbol{\sigma}$ is diagonal matrix, $\boldsymbol{\sigma} = diag(\sigma_1, \sigma_2, ..., \sigma_K)$.

Finally, the matrix **Z** represents *K* correlated set of random variables with specified mean and standard deviations.

The normal distribution is commonly used distribution to model uncertainty in load consumption. Next few steps show how to generate correlated sets of random variables for load consumption in the network buses.

Step. 1. Based on the simultaneously measured load consumption in the network buses, calculate mean values, standard deviations, and correlated coefficients for analyzed busses. These values can be assumed if there are no measurements.

Step. 2. Generate sets of random variables with standard normal distribution using MCS method.

Step. 3. Generate correlated sets of random variables using equations (3.45)-(3.48).

For example, following Matlab code generates three correlated sets of load consumptions with normal distributions.

```
N=10000;                              % Number of MCS samples

M=diag([10 20 30]);                   % Mean value of load consumption in kW
D=diag([0.1 0.08 0.06]);              % Standard deviation (0.1 means 10% of mean)
R=[ 1   0.7  0.5 ;...                 % Correlation matrix
   0.7   1   0.2 ;...
   0.5  0.2   1  ];

for k=1:3                            % Three sets of random variables
    X(k,:)=normrnd(0,1,1,N);
end

L=chol(R,'lower');                    % Cholesky factorization of matrix R
Y=L*X;                                % Correlated sets of random variables
Z=M*(1+D*Y);                          % Correlated sets with mean and deviations
```

By executing this program code, the following results are obtained:

– correlation matrix:

$$\boldsymbol{\rho} = \begin{bmatrix} 1 & 0.702 & 0.505 \\ 0.702 & 1 & 0.205 \\ 0.505 & 0.205 & 1 \end{bmatrix}$$

– mean values:

$$\mu_1 = 9.9998 \text{ kW}$$
$$\mu_2 = 19.9990 \text{ kW}$$
$$\mu_3 = 30.0102 \text{ kW}$$

– standard deviation:

$$\sigma_1 = 1.005 \text{ kW } (10.05\%)$$
$$\sigma_2 = 1.5988 \text{ kW } (7.99\%)$$
$$\sigma_3 = 1.8108 \text{ kW } (6.03\%)$$

The described procedure can also be applied to other distributions. Thus, certain difficulties may arise. The conservation of the kind of distribution cannot be assured, as predicted by the Central Limit Theorem [40]. Also, the correlated value may have no physical meaning. For example, if the Weibull distribution is used to model wind speed, correlated values of wind speed can be negative. For a better understanding, the equation (3.46) can be expressed as follows:

$$\begin{bmatrix} y_{11} & y_{12} & \cdots & y_{1N} \\ y_{21} & y_{22} & \cdots & y_{2N} \\ \vdots & \vdots & \ddots & \vdots \\ y_{K1} & y_{K2} & \cdots & y_{KN} \end{bmatrix} = \begin{bmatrix} l_{11} & 0 & \cdots & 0 \\ l_{21} & l_{22} & \cdots & 0 \\ \vdots & \vdots & \ddots & \vdots \\ l_{K1} & l_{K2} & \cdots & l_{KK} \end{bmatrix} \cdot \begin{bmatrix} x_{11} & x_{12} & \cdots & x_{1N} \\ x_{21} & x_{22} & \cdots & x_{2N} \\ \vdots & \vdots & \ddots & \vdots \\ x_{K1} & x_{K2} & \cdots & x_{KN} \end{bmatrix}. \quad (3.48)$$

In (3.48) each row of matrix **X** can represent the random values of the wind speed at one wind park. The rows of matrix **Y** are sequentially calculated. By doing this to all the samples, the expected result is a set of values with the given correlation

matrix. The rows of matrix **Y** represents correlated wind speed data for certain wind park. During the process, negative values can appear, depending on the values of the matrix **L**. This is a problem because negative wind speed values do not exist. A number of negative values can be generally between 5 and 10% [31]. Also, the result of this procedure shows that the feature of the non-normal distribution is progressively lost as the subindex number of the row grows. So, if the initial distributions were Weibull distributions, then, the first row of the correlated variables will be a Weibull distribution, but the last row will be far from being one. This feature is in accordance with the Central Limit Theorem.

There are several different approaches to solve difficulties with correlations of wind speed data. A review of some techniques is presented in [31]. In this Ph.D. thesis, the method for simulation of correlated wind speeds described in [31, 32] will be used. Instead of Pearson's correlation, this method uses different correlation parameter, i.e. the nonparametric Spearman rank correlation. Spearman rank correlation is not calculated as a function of the values, but on the basis of the ranking of these values in the series.

The Spearman correlation coefficient is defined as the Pearson correlation coefficient between the ranked variables. Two series of data *X* and *Y*, that occur simultaneously, are converted into ranks *rgX* and *rgY* according to their values. After that, the Spearman correlation coefficient can be expressed as:

$$r_S = \rho_{rgX,rgY} = \frac{\mathrm{cov}(rgX, rgY)}{\sigma_{rgX}\sigma_{rgY}}. \tag{3.49}$$

Where ρ denotes the Pearson correlation coefficient, but applied to the rank variables, cov(*rgX*, *rgY*) is the covariance of the rank variables, σ_{rgX} and σ_{rgY} are the standard deviations of the rank variables. Only if all *n* ranks are distinct integers, it can be computed using the formula [32]:

$$r_S = 1 - \frac{6\sum_{i=1}^{n} d_i^2}{n(n^2-1)}. \tag{3.50}$$

Where $d_i = rgX_i - rgY_i$ is the difference between the two ranks of each sample, and *n* is the number of samples in one series of data.

The chosen method for simulation of correlated wind speeds can be summarized in next steps [32]:

1) Based on simultaneously measured wind speed data at different locations (wind farms), the Spearman rank correlation between all pairs of speed series is calculated. In this step, the Weibull scale parameter δ and shape parameter β for individual series of wind speed data are also calculated.

2) The Monte Carlo technique is used for generating the wind speed distributions corresponding to the different locations, based on calculated scale and shape parameters. These distributions are generated independently of each other. All generated samples can be represented by the matrix:

$$\mathbf{W} = \begin{bmatrix} w_{11} & w_{12} & \dots & w_{1j} & \dots & w_{1N} \\ w_{21} & w_{22} & \dots & w_{2j} & \dots & w_{2N} \\ \vdots & \vdots & \ddots & \vdots & \vdots\vdots\vdots & \vdots \\ w_{i1} & w_{i2} & \dots & w_{ij} & \dots & w_{iN} \\ \vdots & \vdots & \vdots\vdots\vdots & \vdots & \ddots & \vdots \\ w_{K1} & w_{K2} & \dots & w_{Kj} & \dots & w_{KN} \end{bmatrix}. \quad (3.51)$$

Where w_{ij} is j^{th} sample of i^{th} distribution, K is the number of distributions and N is the total number of MCS samples. Each row in the matrix **W** represents the distribution of wind speed for certain location (wind farm).

3) A number of independent uniform distribution functions coinciding with the number of distributions of the original problem are generated. The normal distribution would be equally valid. Also, the number of samples must coincide.

4) Calculate $\mathbf{Y} = \mathbf{LU}$, where **U** represents independent uniform distributions, **Y** is the vector of correlated uniform distributions and **L** is a lower triangular matrix obtained from the correlation matrix (Spearman indices) by means of the Cholesky technique. The matrices **U** and **Y** have a similar form and the same number of elements like the matrix **X.**

5) Some order of the elements is analyzed in each row of matrix **Y**. For example, if they are sorted by their values, a classification is established according to their ranks.

6) The same order is analyzed in the original distributions (rows of matrix **W**), and they are re-ordered according to a ranking similar to that obtained in step 5.

As a result, correlated distributions are obtained according to the rank correlation matrix desired and also keeping all features of the Weibull distributions. This is due to the fact that all their values are respected, and only their rank values (their positions in the series) are changed.

For example, following Matlab code generates three correlated sets of wind speed data with Weibull distributions using the described method.

```
N=10000;                                % Number of MCS samples

D=[  8    7     6  ];                  % Scale parameter delta
B=[  2   2.5   1.5 ];                  % Shape parameter beta
R=[ 1   0.9   0.7 ; ...                % Correlation matrix
   0.9   1    0.5 ; ...
   0.7  0.5    1  ];

for k=1:3                              % Three independent Weibull series
    W(k,:)=wblrnd(D(k),B(k),1,N);
end

for k=1:3                              % Three independent normal series
    X(k,:)=normrnd(0,1,1,N);
end

L=chol(R,'lower');                     % Cholesky factorization of matrix R
Y=L*X;                                 % Correlated normal distributions

for k=1:3
    [Ysort,Indx]=sort(Y(k,:));         % Sorting each row of matrix Y
    Wsort=sort(W(k,:));                % Sorting each row of matrix W
    Wcor(k,Indx)=Wsort;                % Reordering Wsort using order in Ysort
end
```

By executing this program code, the following results for correlated series of wind speeds are obtained:

– Spearman correlation matrix:

$$\mathbf{R}_S = \begin{bmatrix} 1 & 0.893 & 0.687 \\ 0.893 & 1 & 0.491 \\ 0.687 & 0.491 & 1 \end{bmatrix}$$

– scale parameters:

$$\delta_1 = 8.032, \delta_2 = 6.969, \delta_3 = 5.981 \text{kW}$$

– shape parameters:

$$\beta_1 = 2.007, \beta_2 = 2.528, \beta_3 = 1.491$$

The obtained values are very close to the target values. The Weibull parameters can be obtained using MATLAB function *wblfit()*.

For the given example, the Pearson parametric correlation matrix can be also calculated. The result is the next matrix:

$$\boldsymbol{\rho} = \begin{bmatrix} 1 & 0.897 & 0.686 \\ 0.897 & 1 & 0.487 \\ 0.686 & 0.487 & 1 \end{bmatrix}$$

It's obvious that it is the Pearson parametric correlation matrix is very close to Spearman rank correlation matrix. So, even if only Pearson parametric correlations are known, perhaps the use of this method can be advantageous, by assuming they are Spearman rank correlation values [32].

The presented method can be successfully applied to other physical variables (not only for wind speed) and other non-normal distributions (the beta distribution for example). Also, this method can be applied to generate correlated series of data between two or more different distributions (normal and Weibull, Weibull and beta, and so on).

Chapter 4. Multiobjective optimisation

4.1. Introduction

Historically, engineering optimisation problems were formulated as single objective problems and were solved with the use of gradient-based or direct search methods. Single objective optimisation may be defined as minimising (or maximising) a scalar function $f(X)$ where X is a set of variables, x_1, ..., x_n. However, real-world problems usually involve the simultaneous consideration of multiple performance criteria. For problems with multiple conflicting objectives, there is no one single optimal solution.

Multiobjective optimisation (known as multicriteria, multiperformance or vector optimisations) may be defined as minimizing (or maximising) number of components M of a vector function f of a vector variable $X = (x_1, x_2, ..., x_n)$ simultaneously, i.e., min $f(X)$ = [$f_1(X)$, ..., $f_m(X)$]. In other words, multiobjective optimisation could be defined as a process of systematic simultaneous optimisation of a set of objective functions with the presence of limitations that all permissible solutions must satisfy. Clearly, for this set of functions, it is unlikely that there is one ideal `optimal´ solution, rather a set of solutions for which an improvement in one of the design objectives will lead to a degradation in one or more of the remaining objectives. Such solutions are also known as Pareto-optimal or non-dominated solutions to the multiobjective optimisation problem.

Most optimisation problems which are encountered in practice involve multiple objectives that need to be considered. These objectives are mostly conflicting. For example, the decision on selecting a device to write text electronically. If the objectives are the most portable device and the most writing comfortable device, there are many devices that can be chosen. The first objective is determined by the value of the weight and volume. In other words, lighter and smaller devices are preferred. Therefore, the laptop is preferred over desktop Personal Computer (PC) and surely the smartphones and organizers with a tiny keyboard will be the more portable ones. In the same manner for the writing comfort criterion, the desktop (PC) is much easier to write than small keyboard of the portable organizer. Often, a compromise is made between mobility and writing comfort. This leads to a number of potential solutions and no single solution usually is simultaneously optimal with respect to these two objectives. Figure 4.1 illustrates the multiobjective optimisation on selecting a device to write text.

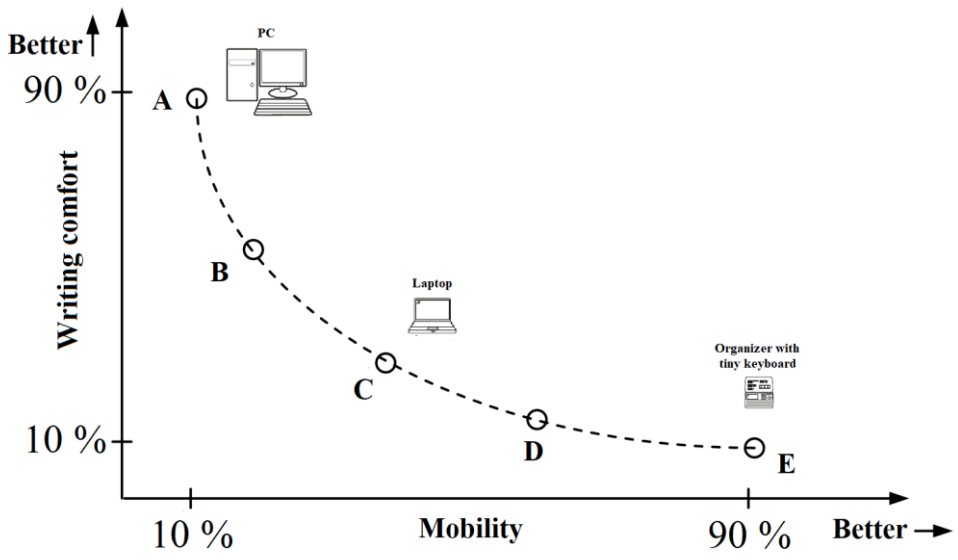

Figure. 4.1. Example of multiobjective optimisation.

4.2. Theory

Multiobjective optimisation problems have been intensively studied for several decades and the research is based on the theoretical background laid, for example, in (Edgeworth, 1881; Koopmans, 1951; Kuhn and Tucker, 1951; Pareto, 1896, 1906) [45]. It is characteristic that no unique solution exists, but a set of good solutions can be

identified (Pareto optimal solutions) as seen in Figure 4.2 for two objective functions. The idea of solving a multiobjective optimisation problem is understood as helping human decision makers (DMs) in considering the multiple objectives simultaneously and in finding a Pareto optimal solution that pleases them the most. Thus, the solution process needs some involvement of the DMs in the form of specifying preference information and the final solution is determined by thier preferences in one way or the other.

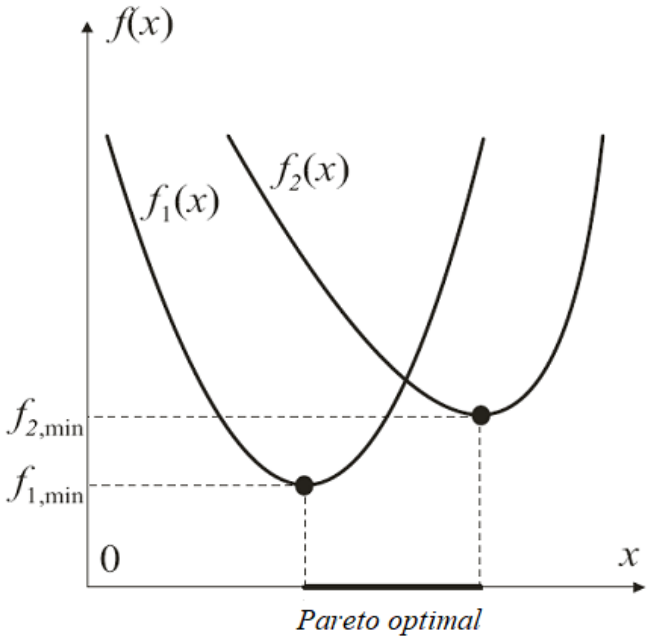

Figure 4.2. Parito optimal solutions.

There are number of objective functions $f_m(X)$ that be maximised or minimised in the multiobjective optimisation problem. Also, there are number of constrains. It can be stated in general form as [46]:

$$\left.\begin{array}{lll} \textit{Minimize/Maximize} & f_m(X), & m=1,2,\ldots,M; \\ \textit{subject to} & g_j(X)\geq 0, & j=1,2,\ldots J; \\ & h_k(X)=0, & k=1,2,\ldots,K; \\ & x_i^{(L)}\leq x_i\leq x_i^{(U)}, & i=1,2,\ldots,n. \end{array}\right\} \quad (4.1)$$

Where

$g_i(X)$ and $h_k(X)$ are constraint functions.

$x_i^{(L)}, x_i^{(U)}$ are lower and upper bounds of decision variables.

Any solution ***X*** is a vector of ***n*** decision variables (control variables): $X = (x_1, x_2, ..., x_n)^T$. The $x_i^{(L)}$ and $x_i^{(U)}$ bounds constitute a decision space (space of control variables ***S***). Also, ***M*** objective functions constitute a multi-dimensional space called the objective space **Z**. Every solution ***X*** in the decision space is represented by a point in the objective space. The feasible solution must satisfy all the constraints and all variable bounds. A set of all feasible solutions is called feasible region. Every solution ***X*** in the decision space is represented by a point in the objective space. Figure 4.3 illustrates these two spaces in the case of two variables and two criteria functions.

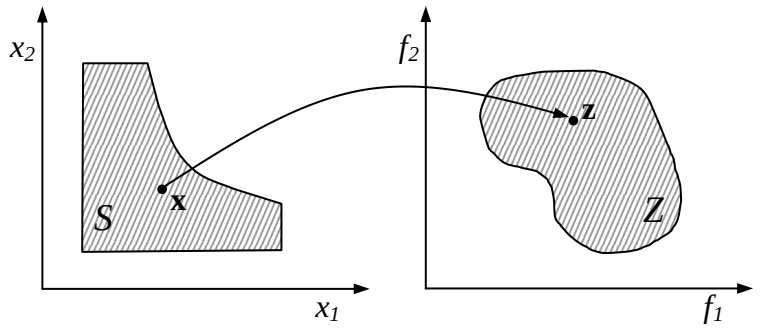

Figure 4.3. The space of the control variables and the corresponding area of the criterion functions.

4.3. Pareto optimality

Pareto Optimality is named after the famous Italian scientist, Vilfredo Pareto (born July 15, 1848, Paris, France, died August 19, 1923, Geneva, Switzerland). His concept was on mass and elite interaction (the selected part of the group is superior to the rest in terms of ability or qualities) as well as for his application of mathematics to economic analysis [47].

In the problem of multiobjective optimisation, generally there is no global solution - as in singleobjective optimization - and it is often necessary to determine a set of points (solutions) that all satisfy the definition of optimum. The concept of defining the optimal point is the Pareto optimality and can be defined in the following way:

″Pareto Optimal: A point, $\mathbf{x}^* \in \mathbf{X}$, is Pareto optimal iff there does not exist another point, $\mathbf{x} \in \mathbf{X}$, such that $\mathbf{F}(\mathbf{x}) \leq \mathbf{F}(\mathbf{x}^*)$, and $F_i(\mathbf{x}) < F_i(\mathbf{x}^*)$ for at least one function″ [48].

All Pareto optimal points (Pareto front) lie on the frontiers of the objective space Z. Often, there are algorithms which provide solutions that are not Pareto optimal solutions, but these solutions can satisfy other objectives and are important for practical applications. They called a weakly Pareto optimal solutions and can be defined as:

″Weakly Pareto Optimal: A point, $\mathbf{x}^* \in \mathbf{X}$, is weakly Pareto optimal iff there does not exist another point, $\mathbf{x} \in \mathbf{X}$, such that $\mathbf{F}(\mathbf{x}) < \mathbf{F}(\mathbf{x}^*)$″ [48].

Therefore, the solution is a Pareto optimal solution if there is no other solution that improves at least one objective function without degrading other objective functions. Figure 4.4 shows Pareto optimal and weakly Pareto optimal solutions for the case of minimising two objective functions. All points lie on the line AB are weakly Pareto optimal solutions. All points lie on the curve BC are Pareto optimal solutions.

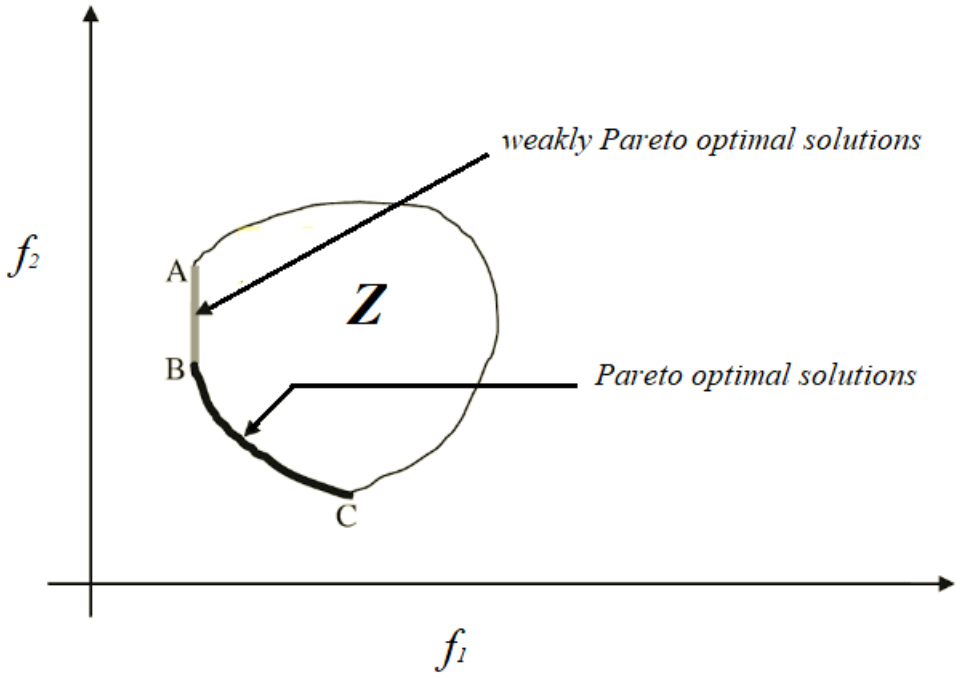

Figure 4.4. Pareto optimal and weakly Pareto optimal solutions.

Also, an additional definition is needed. It is the dominated and non-dominated solutions. For dominated solutions, when the solution (A) is no worse than the solution (B) in all objectives, and solution (A) is strictly better than the solution (B) in at least one objective, then the solution (A) dominates the solution (B). And for non-dominated solutions, a non-dominated solution is when none of both solutions are better than the other with respect to all objectives. All objectives are equally important. In other words:

″Non-Dominated and Dominated Points: A vector of objective functions, $\mathbf{F}(\mathbf{x}^*) \in Z$, is nondominated iff there does not exist another vector, $\mathbf{F}(\mathbf{x}) \in Z$, such that $\mathbf{F}(\mathbf{x}) \leq \mathbf{F}(\mathbf{x}^*)$ with at least one $\mathbf{F}_i(\mathbf{x}) < \mathbf{F}_i(\mathbf{x}^*)$. Otherwise, $\mathbf{F}(\mathbf{x}^*)$is dominated″ [48]. The goal of non-dominant sorting is to use a ranking selection method to emphasize good solutions and use a method to maintain stable population subpopulations of good solutions.

4.4. Genetic algorithms (GAs) for multi-criteria optimisation

The Genetic Algorithms (GAs) was introduced by Holand [48]. Genetic Algorithms (GAs), in essence, mimic the concept of evolution in nature. Therefore, It is a computational model inspired from the natural evolution of survivals. It is an optimisation procedure to find the optimal solution using natural selection process, in which stronger individuals of the population have the highest probability to reproduce based on their level of goodness. In other words, it is an optimisation technique, which tries to search in a set of input values that we got and find the best (optimal) value/values in that set.

GAs are more flexible than most search methods because they require only information concerning the quality of the solution produced by each parameter set (objective function values) and not like many optimisation methods which require derivative information, or worse yet, complete knowledge of the problem structure and parameters [49]. It is observed that, GAs methods differ from some optimisation methods in four ways:

- GAs work with a coding of the parameter set, not the parameters themselves. Therefore GAs can easily handle the integer or discrete variables.
- GAs search within a population of points, not a single point. Therefore GAs can provide a globally optimal solution.
- GAs use only objective function information, not derivatives or other auxiliary knowledge. Therefore GAs can deal with non-smooth, non-continuous and non-differentiable functions which are actually exist in a practical optimisation problem.
- GAs use probabilistic transition rules, not deterministic rules.

In addition to the fact that the genetic algorithm is simple, it is robust and can be applied to solve many optimisation problems from various areas. The following will give an overview of the genetic algorithm used to solve optimisation problems. But before reviewing GAs method for multiobjective optimisation, an overview of the genetic algorithm for single-objective optimisation will be given in order for better understanding. The basic principles, concepts and operators used in genetic algorithms for single-objective optimisation are also used in genetic algorithms for multiobjective optimisation. That means, the genetic algorithms for multiobjective optimisation use the same terms, principles, and operators as in genetic algorithms for single-objective optimisation.

In the late texts in this chapter, some advanced methods of genetic algorithms will be briefly discussed such as Vector Evaluated Genetic Algorithm (VEGA) and Multiobjective Genetic Algorithm (MOGA). Also, the used method (Non-dominated Sorted Genetic Algorithm (NSGA-II)) in this work will be briefly explained.

4.5. Single Genetic Algorithms

The genetic algorithms are part of the evolutionary algorithms family, which are computational models, inspired by Nature. Genetic algorithms are powerful stochastic search algorithms based on the mechanism of natural selection and natural genetics. GAs work with a population of a binary string, searching many peaks in parallel. By employing genetic operators, they exchange information between the peaks, hence reducing the possibility of ending at a local optimum. The Genetic Algorithms work by building a population of chromosomes which is a set of possible solutions to the optimisation problem. Within a generation of a population, the chromosomes are randomly modified in hopes of creating new chromosomes that have better evaluation scores. These new created chromosomes will be a part of the new population of chromosomes. The other chromosomes of the new population is randomly selected from the current generation based on the evaluation score of each chromosome.

4.5.1. GA steps

A simple Genetic Algorithm is an iterative procedure, which maintains a constant size population *P* of candidate solutions. During each iteration step (generation) three genetic operators (reproduction, crossover and mutation) are performing to generate new populations (offspring), and the chromosomes of the new populations are evaluated via the value of the fitness. Based on these genetic operators and the evaluations, the better new populations of candidate solution are formed. With the above description, a simple genetic algorithm is given as follow [49]:

1) Generate randomly a population of a binary string.
2) Calculate the fitness for each string in the population.
3) Create offspring strings through reproduction, crossover and mutation operation.
4) Evaluate the new strings and calculate the fitness for each string (chromosome).
5) If the search goal is achieved, or an allowable generation is attained, return the best chromosome as the solution; otherwise, go to step 3.

4.5.2. Chromosome coding and decoding

Each chromosome represents a potential solution for the problem and must be expressed in a binary form in the integer interval. We could simply code *X* in binary base. If we have a set of binary variables, a bit will represent each variable. For a multivariable problem, each variable has to be coded in the chromosome [50]. As an example, for a power system with 3-Generators, the active power generations P_{Gi} (in MW) for i=1, 2 and 3 with a length of 3-Digits (can be different) is shown in Table 4.1. If the chromosome is a binary string of: [100 101 011], then the candidate parameter set is: (153.568, 33.3, 27.99).

The first step of any genetic algorithm is to create an initial population of GAs by randomly generating a set of feasible solutions. A binary string of length *L* is associated to each member (individual) of the population. The string is usually known as a chromosome and represents a solution of the problem. A sampling of this initial population creates an intermediate population. Thus some operators (reproduction,

crossover and mutation) are applied to an intermediate population in order to obtain a new one, this process is called Genetic Operation. Finally, the decoding is the reverse procedure of coding.

Table 4.1. Coding of Active Power Generation.

	P_{G1}	P_{G2}	P_{G3}	CODE
0	0.00	0.00	0.00	000
1	38.392	6.66	9.33	001
2	76.784	13.32	18.66	010
3	115.76	19.98	27.99	011
4	153.568	26.64	37.32	100
5	191.96	33.3	46.65	101
6	230.352	39.96	55.98	110
7	268.744	46.62	65.31	111

4.5.3. Genetic Operation-Crossover

Crossover is the primary genetic operator, which promotes the exploration of new regions in the search space. For a pair of parents (as seen in Figure 4.5) selected from the population the recombination operation divides two strings of bits into segments by setting a crossover point. In single point crossover, the segments of bits from the parents behind the crossover point are exchanged with each other to generate their offspring. The mixture is performed by choosing a point of the strings randomly and switching the left segments of this point. The new strings belong to the next generation of possible solutions. The strings to be crossed are selected according to their scores. Thus, the strings with larger scores have more chances to be mixed with other strings because all the copies have the same probability to be selected [49].

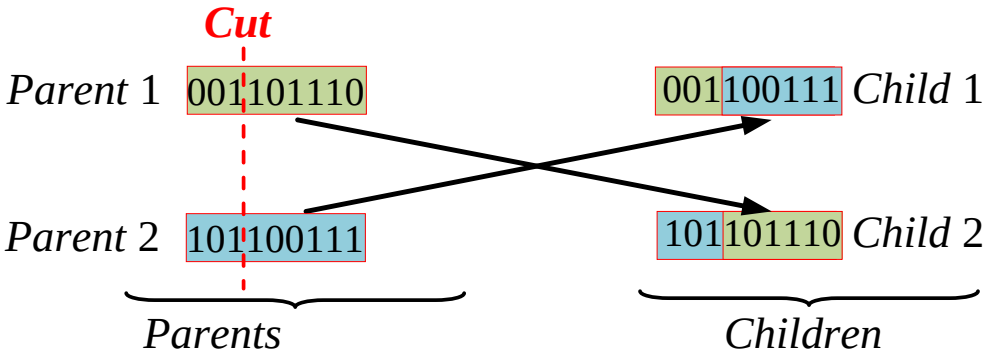

Figure 4.5. The single point crossover.

4.5.4. Genetic Operation-Mutation

Mutation is a secondary operator; it prevents the early stopping of the algorithm in a local solution. This operator can be made by a random bit value change in a chosen string with a low probability. All strings and bits have the same probability of mutation. For example, in this string [100 1**0**1 011], if the mutation affects underlined bit, the string obtained is [100 1**1**1 011] and the value of P_{G2} change from 33.3 to 46.62 MW.

4.5.5. Genetic Operation - Reproduction

Reproduction is an operation whereby an old chromosome is copied into a Mating pool according to its fitness value. Highly fit chromosomes (closer distances to the optimal solution mean highly fit) receive higher number of copies in the next generation. Copying chromosomes according to their fitness means that the chromosomes with a higher fitness value have the higher probability of contributing one or more offspring in the next generation.

4.5.6. Evaluation - Candidate solutions fitness

In the evaluation, suitability of each of the solutions from the initial set as the solution of the optimisation problem is determined. For this function called “fitness function” is defined. This is used as a deterministic tool to evaluate the fitness of each chromosome. The optimisation problem may be minimisation or maximisation type. In the case of maximisation type, the fitness function can be a function of variables that have direct proportionality relationship with the objective function. For minimisation type problems, the fitness function can be a function of variables that have inverse proportionality relationship with the objective function or can be reciprocal of a function of variables with direct proportionality relationship with the objective function. In either case, the fitness function is so selected that the fittest solution is the nearest to the optimum point.

A standard GA procedure for solving the optimal power flow problem is summarized in Figure 4.6 [51].

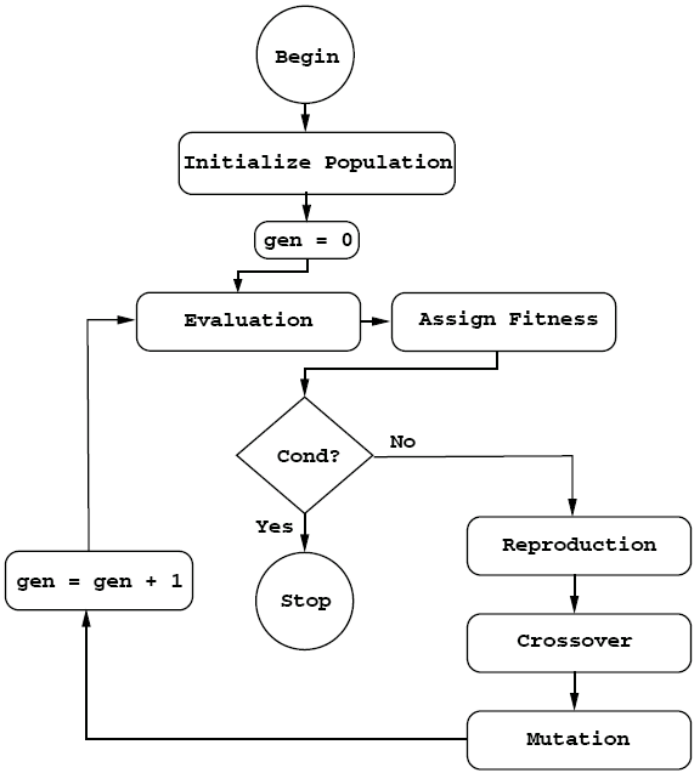

Figure 4.6. A Simple flow chart of the GAs.

4.5.7. Merits and Demerits of Genetic Algorithm

The Merits of Genetic Algorithm are summarized and given below:

1) GAs can handle the Integer or discrete variables.
2) GAs can provide a globally optimum solution as it can avoid the trap of local optimum solution.
3) GAs can deal with the non-smooth, non continuous, non-convex and non differentiable functions which actually exist in practical optimisation problems.
4) GAs has the potential to find solutions in many different areas of the search space simultaneously, there by multiple objectives can be achieved in single run.
5) GAs are adaptable to change, ability to generate large number of solutions and rapid convergence.
6) GAs can be easily coded to work on parallel computers.

And the Demerits are:

1) GAs are stochastic algorithms and the solution they provide to the problem is not guaranteed to be optimum.
2) The execution time and the quality of the solution, deteriorate with the increase of the chromosome length, i.e., the problem size. If dimension of the optimisation problem is increasing, the GA approach can produce more infeasible offsprings which may lead to wastage of computational efforts.

4.6. Vector Evaluated Genetic Algorithm (VEGA)

David Schaffer (1985) proposed an approach called as Vector Evaluated Genetic Algorithm (VEGA), and that differed of the simple genetic algorithm (GA) only in the way in which the selection was performed. This operator was modified so that at each generation a number of subpopulations were generated by performing proportional selection according to each objective function in turn. Thus a problem with k objectives and a population with a size of *M*, *k* subpopulations of size *M*/*k* each would be generated. These subpopulations would be shuffled together to obtain a new population of size *M*, on which GA would apply the crossover and mutation operators in the usual way [52]. It should be noted that the concept of Pareto's dominance in this way is not directly included in the selection process. It is a simple genetic algorithm with a modified selection mechanism. This mechanism of VEGA is shown in Figure 4.7.

4.7. Multiobjective Genetic Algorithm (MOGA)

Fonseca and Fleming proposed the Multiobjective Genetic Algorithm (MOGA), which was one of the first in using Pareto dominance to rank solutions. With this method, the ranking of the solutions depends on the number of solutions in the current population t_1 that dominate it. First, all nondominated solutions are assigned rank 1. then each solution is checked for its domination in the current population. Finally, the rank of the solution X^i equals to one plus the number of p_i solutions that dominate solution X^i as in next equation:

$$(X^i, t) = 1 + p_i \ . \tag{4.2}$$

Figure 4.8 shows the case of two objective functions minimisation where the solutions marked with empty circles are dominated solutions by a number of other solutions. Their ranking must have an additional amount. And solutions marked with full dark circles are the nondominated solutions. The rank of these solutions is 1.

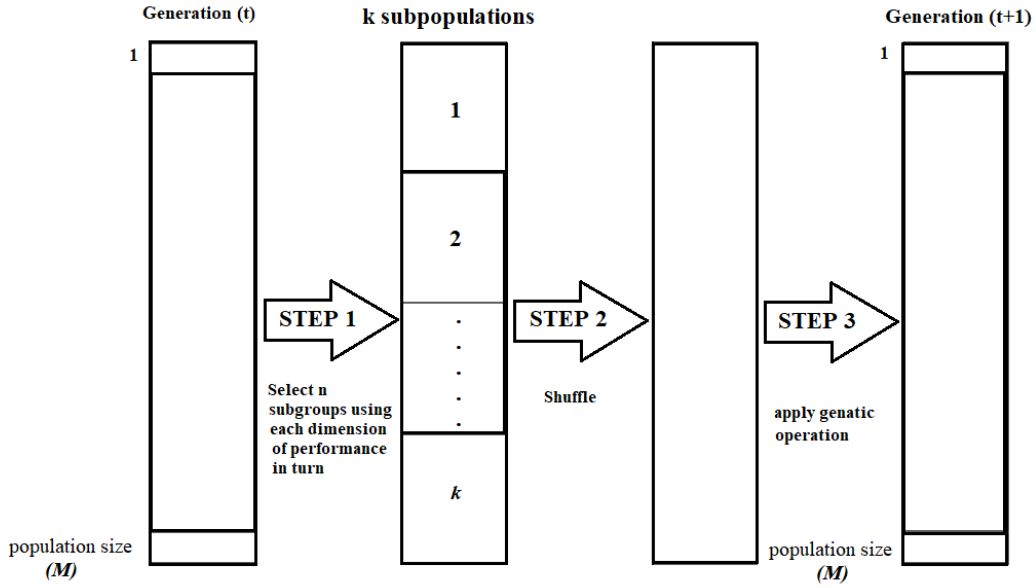

Figure 4.7. The mechanism of VEGA.

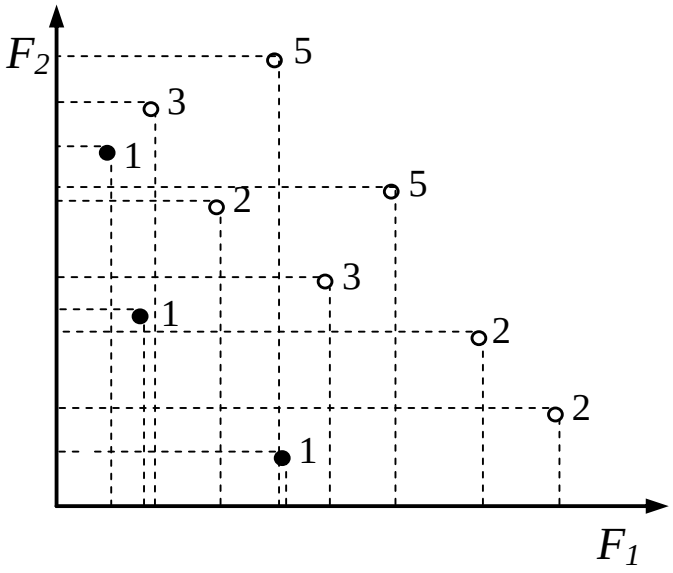

Figure 4.8. Rank determination by MOGA method for minimisation of two objective functions.

4.8. Non-dominated Sorted Genetic Algorithm (NSGA-II)

In 1994, Srinivas and Deb proposed The Nondominated Sorting Genetic Algorithm (NSGA). NSGA allows for a good search of various nondominated solutions regions and leads to a convergence of the population toward such regions where nondominant solutions are identified and a significant value is set for their fitness. Then these solutions are shared with their fitness values to maintain diversity in the population. These solutions are then temporarily ignored. Now, the second nondominated front for the rest of the population can be determined and a value of fitness smaller than the minimum shared fitness of the previous front is given to them. Finally, this process continues until the population is fully classified on several fronts. Solutions on the first front always get more copies than the rest of the population because they have the maximum fitness value [53][54].

NSGA has some criticisms like the high computational complexity of nondominated sorting, lack of elitism and need for specifying the sharing parameter. In [55], Kalyanmoy Deb addresses all of these issues and propose an improved version of NSGA, which he named it NSGA-II. He said NSGA-II is distinguished in finding a diverse set of solutions and in converging near the true Pareto-optimal set. He suggests a simple constraint-handling strategy that encourages the application of NSGA-II to more complex and real-world multiobjective optimisation problems.

NSGA-II method for finding Pareto optimal solutions for multi-criteria optimisation has three basic characteristics: using the principle of elitist, using a diversity mechanism for the solutions and keeping solutions in populations that are not dominated by other solutions.

The NSGA-II method algorithm is carried out as follows. Firstly, the basic population of $\boldsymbol{P_t}$ is generated, consisting of N solutions to the optimisation problem. Based on the $\boldsymbol{P_t}$ population, a new population of $\boldsymbol{Q_t}$ is generated using conventional genetic operators (selection, crossover and mutation). The two populations $\boldsymbol{P_t}$ and $\boldsymbol{Q_t}$ are combined and form together a new population of $\boldsymbol{R_t}$ with a number of $2\boldsymbol{N}$ solutions. Figure 4.9 shows schematically the combination of the two populations $\boldsymbol{P_t}$ and $\boldsymbol{Q_t}$.

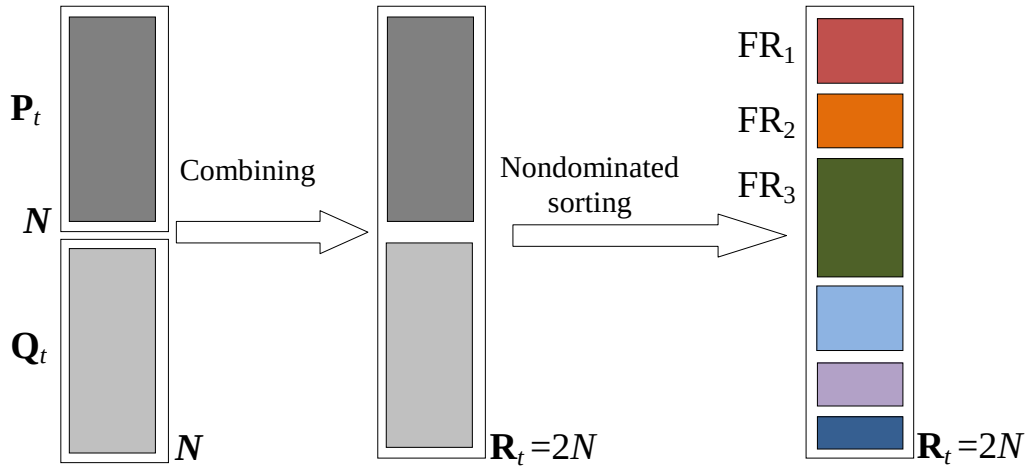

Figure 4.9. The combination for P_t and Q_t in one population.

Subsequently, by sorting population $\boldsymbol{R_t}$ according to the concept of nondomination [55], a new population is performed. For each solution in the old $\boldsymbol{R_t}$ population, according to the concept of nondomination, comparison with other solutions in the population is carried out. In this way, it is determined whether certain solutions dominate or not in relation to other solutions. For example, in the case of minimizing two objective functions with a population of 10 solutions, the principle of sorting the solutions in the $\boldsymbol{R_t}$ population is given in Figure 4.10. The solutions, which are not dominated by any member of the population, are called solutions of the first level. In Figure 4.10, they are solutions 2, 5, 7 and 8. For these solutions, it can be said that they lie on the best front FR_1, or on the front, which is not dominated by the remaining solutions of the population.

If the solutions from the first dominant front are removed for a moment (ignored momently) and simultaneously if the sorting principle according to nondomination is applied to the remaining solutions, the next dominant front FR_2 is obtained. It forms solutions 1, 3, 4 and 6. The process continues until all the solutions in the population are processed. Figure 4.10 shows the 10 solutions classified in 3 nondominant fronts (FR_1 – FR_2 - FR_3).

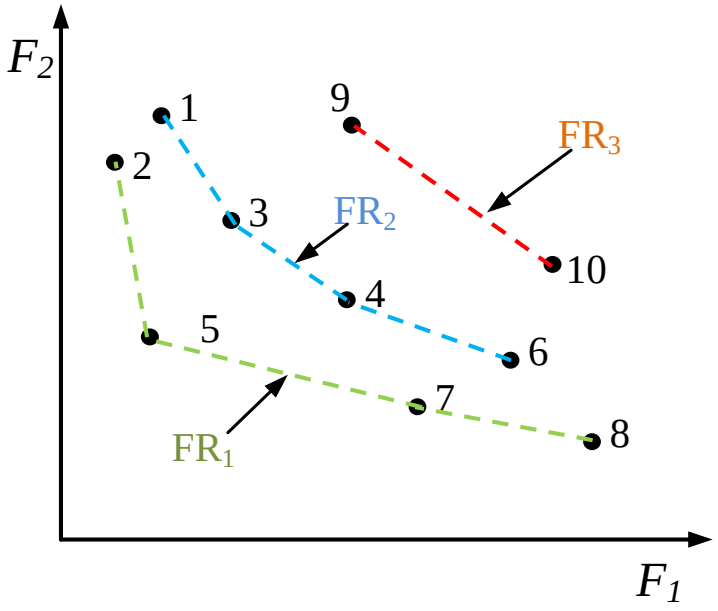

Figure 4.10. Fronts by application of nondomination concept in NSGA-II.

After sorting according to domination, the new population is filled with solutions belonging to solution fronts. Filling up a new population starts with the first best front, continues with the second best front, etc. The fronts that cannot enter into the new population are simply deleted. Figure 4.11 shows schematically that fronts FR_1 and FR_2 (as in our example) directly enter the next generation $\boldsymbol{P}_{t+1}$. Since the current population $\boldsymbol{R}_t$ has $2\boldsymbol{N}$ solutions, it is clear that not all solutions can be placed in $\boldsymbol{N}$ available locations in the new population $\boldsymbol{P}_{t+1}$. The last front (FR_3 as in our example) that enters the new population may have a number of solutions more than the remaining solutions' locations of the new population $\boldsymbol{P}_{t+1}$. Therefore, a sorting according to each other's distance is done to select the necessary number of solutions from the last front FR_3 those enter the new population $\boldsymbol{P}_{t+1}$. This sorting is called (crowding distance) and allows a choice of solutions that extend on that front. The sorting principle is shown in Figure 4.12. "*To get an estimate of the density of solutions surrounding a particular solution in the population, we calculate the average distance of two points on either side of this point along each of the objectives*" [55]. For each solution in front FR_3, for all objective functions, its total distance to adjacent solutions is calculated. In the case of two objective functions, the total distance of solution $\boldsymbol{i}$ of the considered front FR_3 and the adjacent solutions ($\boldsymbol{i}$-1) and ($\boldsymbol{i}$+1) in the same front FR_3 forms a rectangle *ABCD* which is shown in Figure 4.12. The rectangle side d_1 represents the distance of the

solution ***i*** to adjacent solutions for the objective function F_1, and the side d_2 for the objective function F_2. The mean distance of the solution and adjacent solutions for certain objective functions is:

$$The\ mean\ distance = \frac{d_1+d_2}{2} \tag{4.3}$$

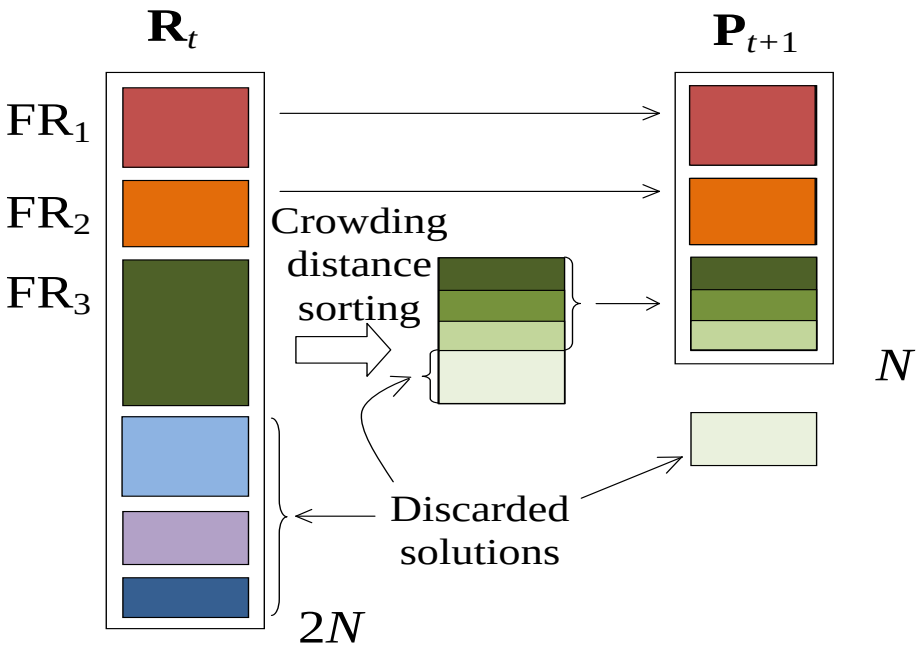

Figure 4.11. Principle of sorting in NSGA-II method.

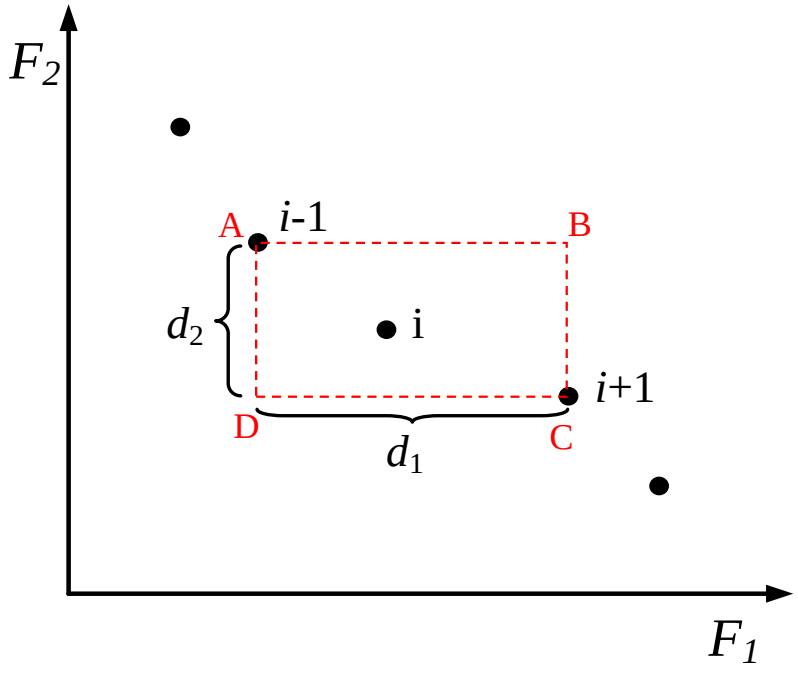

Figure 4.12. The principle of sorting according to mutual distance.

A descending sorting to all solutions of the front FR_3 is done according to the mean distance of the solution and adjacent solutions for certain objective functions, starting from the solution with the greatest distance value to the solution with the least distance value. This ensures even distribution of solutions across the front because close proximity solutions do not have the chance to enter the new population. In this way, a new $\boldsymbol{P}_{t+1}$ population was obtained with which we go to the next iteration. The procedure continues until meeting any stop criteria which usually be the maximum number of generations.

4.9. Effect of the constraints on the optimal fronts

In NSGA-II, the best solutions of the current population are kept and it can't happen that they disappear from the population in the process of crossing and mutations. This is because elitism is ensured by including the current population of $\boldsymbol{P}_t$ in the process of selection in addition to the population of $\boldsymbol{Q}_t$ formed by the application of genetic operators. But constraints often have a clear effect on optimal solutions. When there are constraints, the solutions may be either admissible or inadmissible (feasible or infeasible). Also, the definition of domination between two solutions will be modified. In comparing two solutions, there are three cases: both solutions are feasible, one solution is feasible and the other isn't feasible or both solutions are infeasible. Therefore, the domination principle is simply renamed to constrained-domination and redefined as [56]: a solution $\boldsymbol{x}^{(i)}$ is said to 'constrain-dominate' a solution $\boldsymbol{x}^{(j)}$ if any of the following three conditions is satisfied:

1. The solution $\boldsymbol{x}^{(i)}$ is feasible, and the solution $\boldsymbol{x}^{(j)}$ isn't feasible.
2. Both solutions $\boldsymbol{x}^{(i)}$ and $\boldsymbol{x}^{(j)}$ are infeasible, but the solution $\boldsymbol{x}^{(i)}$ violated the constraints to a lesser extent.
3. Both solutions $\boldsymbol{x}^{(i)}$ and $\boldsymbol{x}^{(j)}$ are feasible and the solution $\boldsymbol{x}^{(i)}$ dominates the solution $\boldsymbol{x}^{(j)}$ as in usual way.

This change in the definition of domination leads to some changes. These changes are illustrated in Figure 4.13 where the case of two objective functions minimization with and without the presence of constraints is shown. The feasible space is defined by constraints and is marked with a yellow surface. The figure also shows

non-dominated fronts for a population of 6 solutions. In the absence of restrictions, non-dominated fronts would be in order (1,3,5), (2,6) and (4). These fronts are marked with black broken lines. But in the presence of constraints, the fronts would be in the order of (4,5), (6), (2), (1), and (3). They are marked with red lines.

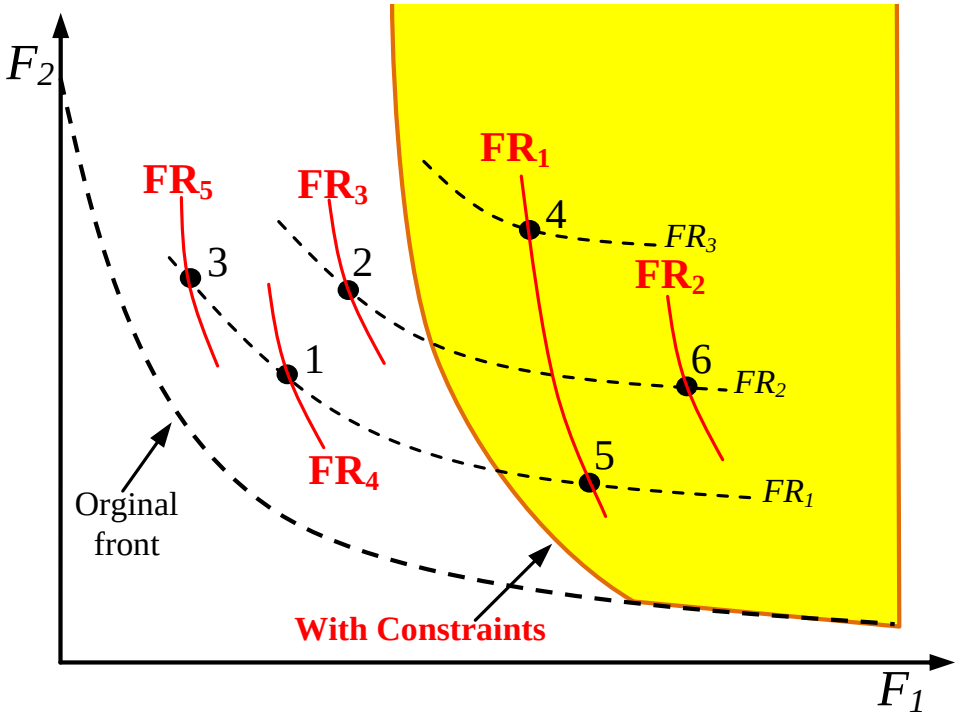

Figure 4.13. Non-dominated fronts with and without constraints.

Chapter 5. New method for capacitor allocation

5.1. Introduction

This thesis proposes a new method for determination of optimal location and installed power of shunt capacitors in a distribution network with wind turbines (WTs) and solar power plants (SPPs). The proposed method respects the uncertainties associated with load demand and renewable DGs active power productions. That is one of the main features of the proposed method. Also, the proposed method takes into account the correlation between stochastic variables like power demand and production of DGs. The methodology and calculations given below are published in part in [42].

The presence of DGs in a distribution network has a significant influence on the voltage profile. Production of DGs, like WTs and/or SPPs, has a distinctly stochastic character owing to the nature of the primary resource (wind speed and solar irradiation). For this reason, modelling these sources in a stochastic way is a key factor in obtaining a quality solution for the optimum location and installed power of the shunt capacitors [42].

Uncertainties of randomly varying system variables cannot be analyzed by deterministic methods; hence probabilistic methods are more suitable for this purpose.

One of the standard probabilistic methods is MCS. MCS method has been applied in many optimisation problems in distribution networks [57-61]. The MCS generates random values for uncertain input variables, and then they are used in deterministic routines to solve the problem in each simulation run [42].

5.2. The optimisation task

The optimisation task, in the proposed method, is a determination of optimal locations and installed powers of the shunt capacitors in order to improve voltage profile throughout the distribution network. The optimisation problem is modelled by two criterion functions [42].

The first criterion function is the sum of square deviations of the expected values of node voltages from the reference values and can be described by the following equation [42]:

$$f_1 = \sum_{i=1}^{N_N} \left[U_{ref} - E(U_i) \right]^2 . \tag{5.1}$$

Where

– U_{ref} is the reference voltage value.

– $E(U_i)$ is the expected voltage value at node i.

– N_N is the number of nodes in the network.

The goal of the first criterion function is to improve voltage profile of entire distribution network.

The second criterion function represents the sum of installed powers of the shunt capacitors [42]:

$$f_2 = \sum_{k=1}^{N_{SC}} Q_k . \tag{5.2}$$

Where

– Q_k is installed power of shunt capacitor k,

– N_{SC} is the number of installed shunt capacitors.

Capacitor power is modeled as a discrete variable changing in steps of 50 kvar. Total installed power of the shunt capacitors is limited to 4 Mvar. The goal of the

second criterion function is the minimization of the total installed power of the shunt capacitors.

Having in mind the defined criterion functions, the optimisation problem can be described by the following equation [42]:

$$\min(f_1, f_2). \tag{5.3}$$

The approach chosen for solving this problem is simultaneous optimisation of the assigned criterion functions. Since the criterion functions defined in this way are contradictory, i.e. smaller installed power of the shunt capacitors will result in an inferior voltage profile and vice versa, global minimum of both criterion functions cannot be attained. For that reason, the simultaneous optimisation is a logical choice. The result of this simultaneous optimisation is a set of optimum solutions, known in the literature as Pareto set of optimum solutions [46]. For solving the optimisation problem defined by equation (5.3) an evolutionary algorithm, known as "Non-dominated Sorted Genetic Algorithm II" or NSGA-II [55], is used. This algorithm is selected because it presents one of the standard procedures for solving the multi-criteria optimisation problems. NSGA-II algorithm has been widely used for solving the problem of optimum placement of shunt capacitors [13–15].

NSGA-II algorithm is based on a population consisting of chromosomes. Each chromosome represents a potential solution of the optimisation problem. Flow chart of the computational procedure is shown in Figure 5.1 [42].

The calculations start by forming the initial population of $\boldsymbol{N}_h$ chromosomes. The chromosomes are formed by the binary coding of the control variables (locations and installed powers of the shunt capacitors). The structure of a single chromosome is shown in Figure 5.2.

In the current generation i for each chromosome P_k (k=1,…,N_h) N_{MC} samples of the active load and DG power production are generated. For each sample calculation of the power flows in the distribution network is carried out by applying the Backward/Forward algorithm, which is a standard method for calculation of power flows in a radial network [34]. The goal of this calculation is a determination of voltages at all nodes. On the basis of the obtained node voltages for N_{MC} samples, the expected node voltage values are obtained by statistical analysis. In the next step, values of the criterion functions are determined for chromosomes P_k. Upon determination of values

of the criterion functions for all chromosomes, by applying the principles of NSGA-II algorithm, a new improved population of chromosomes, i.e. potential solution, is obtained. The calculations are carried out for a pre-assigned number of generations N_g [42].

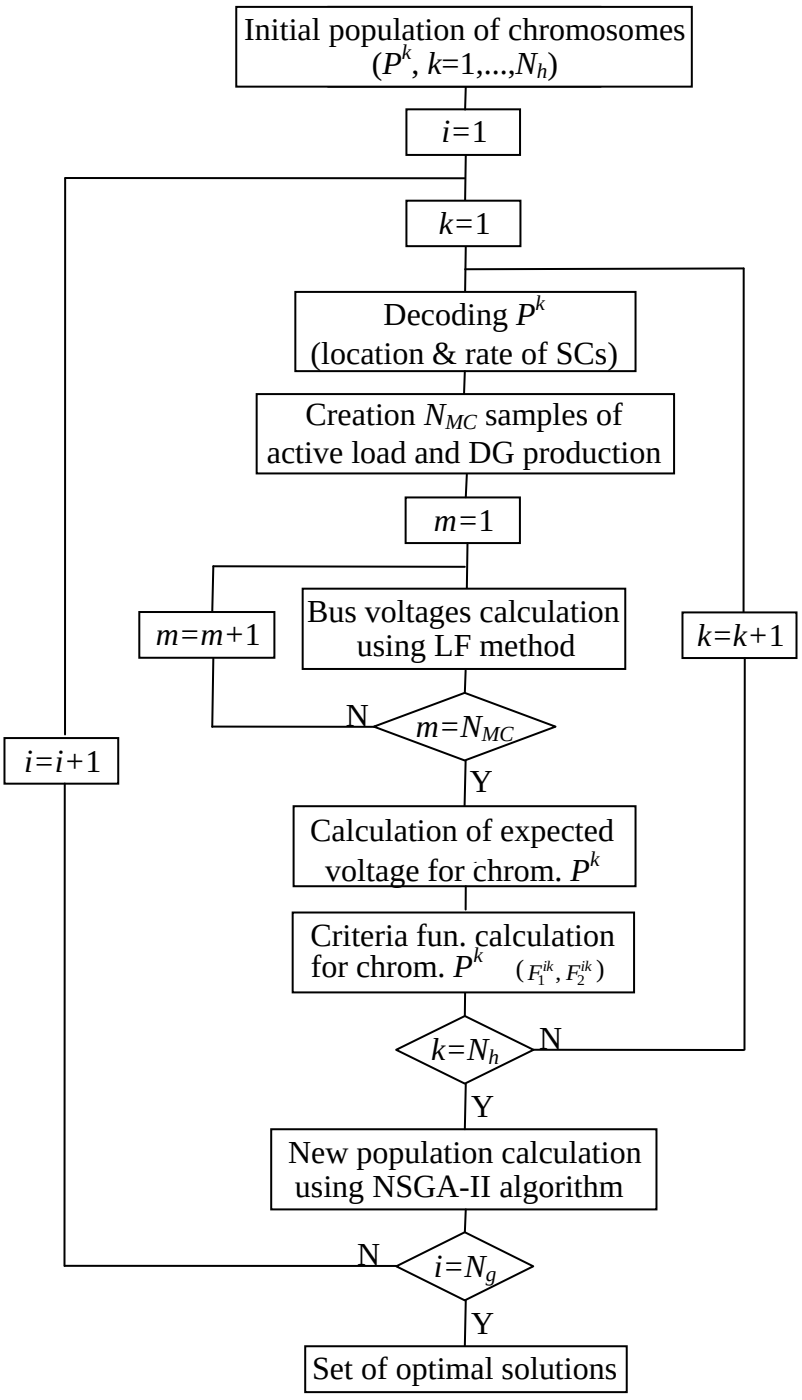

Figure 5.1. Flow chart of computational procedure.

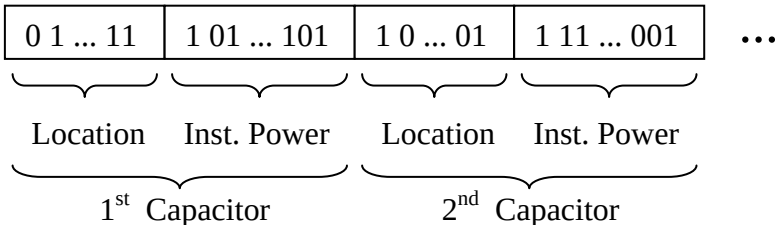

Figure 5.2. The structure of a single chromosome.

5.3. The tested distribution network

The proposed method is tested by using a real medium voltage distribution network supplying several small communities in the region of Banat in the Republic of Serbia. Single line diagram of the analyzed network is presented in Figure 5.3 [42].

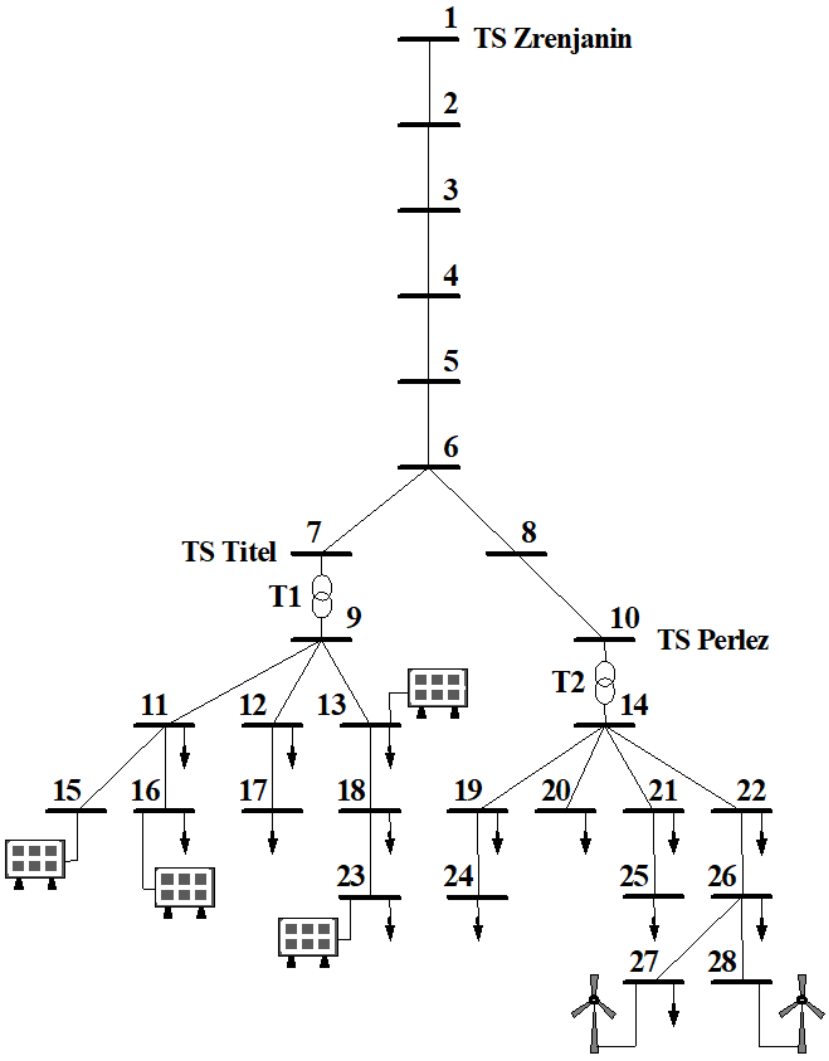

Figure 5.3. Single line diagram of the analyzed network.

The distribution network is radial, supplied from a 110/35 kV substation in node 1. All transmission lines are overhead lines with standard Aluminium Conductor Steel Reinforced of various sizes. Transformer T_1 has installed power S_{n1}=8 MVA and turns ratio 35/10 kV/kV, while Transformer T_2 has installed power S_{n2}=8 MVA and turns ratio 35/20 kV/kV. The network contains two WTs and four SPPs. Data of maximum active powers (P_{Dmax}) at individual nodes are given in Table 5.1. Data of installed powers of WTs (P_{WT}) and SPPs (P_{SPP}) are given in Table 5.2. The parameters of the network are given in Table 5.3 [42].

Table 5.1. Maximum active powers.

Node	P_{Dmax} [MW]	Node	P_{Dmax} [MW]
11	0.98	21	0.60
12	0.74	22	0.78
13	0.98	23	0.50
16	0.50	24	0.48
17	0.74	25	0.60
18	0.50	26	0.72
19	0.72	27	0.90
20	1.21		

Table 5.2. Installed powers of the renewable sources.

Node	P_{SPP} [MW]	P_{WT} [MW]
13	2.00	
15	4.00	
16	4.00	
23	2.00	
27		3.00
28		3.00

Table 5.3. The parameters of the network presented in Figure 5.3.

Nodes of line connection	Voltage level [kV]	Length of line [km]	Conductor cross section [mm^2]	Resistance [Ω]	Reactance [Ω]
1-2	35	0.7	3x50	0.4	0.24
2-3	35	4.1	3x70	1.7	1.44
3-4	35	5.4	3x240	0.64	1.9
4-5	35	13.4	3x70	5.5	4.7
5-6	35	1.9	3x50	1.2	0.7
6-7	35	5.0	3x50	3	1.77
6-8	35	2.0	3x95	0.6	0.7
8-10	35	0.4	3x150	0.1	0.07
9-11	10	1.5	3x50	0.91	0.57
9-12	10	1	3x70	0.43	0.37
9-13	10	1	3x70	0.43	0.37
11-15	10	2	3x70	0.87	0.73
11-16	10	2	3x50	1.21	0.75
12-17	10	2	3x50	1.21	0.75
13-18	10	2	3x70	0.87	0.73
14-19	20	1.5	3x70	0.65	0.55
14-20	20	1.5	3x70	0.65	0.55
14-21	20	2	3x70	0.87	0.73
14-22	20	1	3x70	0.43	0.37
18-23	10	1.5	3x50	0.91	0.57
19-24	20	1.5	3x50	0.91	0.57
21-25	20	1.5	3x50	0.91	0.57
22-26	20	2.5	3x70	1.08	0.92
26-27	20	2	3x70	0.87	0.73
26-28	20	3	3x95	0.96	1.1

Despite the production from renewable energy sources, owing to several very long heavily loaded line-segments, there are significant voltage drops in the network

and considerable active power losses. One solution for improving voltage profile in the network is using the shunt compensation [42].

5.4. Model for power consumption uncertainty

For the purpose of modeling active power consumption at the nodes of the distribution network of Figure 5.3, one year measurements at the feeding transformer in TS Zrenjanin have been carried out. The measured data have been converted to the load duration curve, scaled to the maximum measured active power. By applying the K-mean clustering technique [30] the load duration curve is modeled by the multistep load model [42]. In the clustering process, it has been assumed that the load duration curve was split into *NL* load levels. This corresponds to grouping load points of the curve into *NL* clusters. Figure 5.4 shows the load duration curve and the multistep load curve obtained by the clustering process [42]. The load duration curve has been modeled by 6 load levels (*NL* = 6). Data on active power, relative, and absolute durations of individual load levels are presented in Table 5.4 [42]. This model is a simple presentation of the load duration curve. Also, this model enables the analysis of the influence of the shunt capacitor on the distribution network for different load levels.

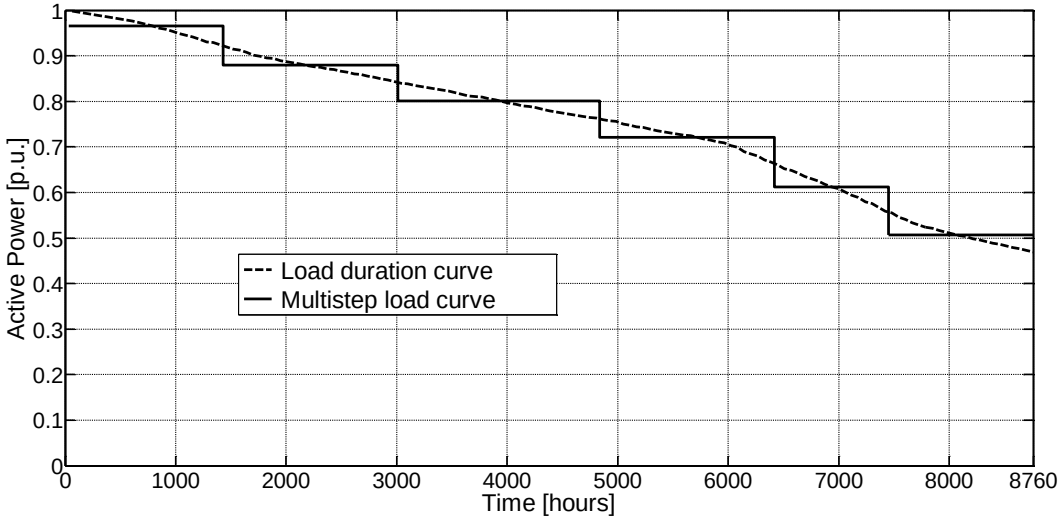

Figure 5.4. The load duration and multistep load curves.

Table 5.4. The load levels data.

Level	1	2	3	4	5	6
P_{step} [p.u.]	0.966	0.879	0.801	0.721	0.612	0.506
T_{step} [%]	16.0	18.1	20.8	18.0	11.8	15.3
T_{step} [hour]	1401	1586	1822	1577	1034	1340

It has been assumed that the load duration curves of all nodes were of the same form as the one shown in Figure 5.4. The multistep load curve of an arbitrary node in the distribution network is obtained by scaling the curve corresponding to the one shown in Figure 5.4 by the maximum active power consumption at that node [42]. The maximum powers of the nodes are given in Table 5.2.

Load uncertainty at each load level is modeled by using a normally distributed random variable according to the following equation [42]:

$$P_{\sigma i} = z_i \sigma_i + P_i \ . \tag{5.4}$$

Where:

– P_i is i^{th} load level in the multistep load model.

– z_i is the standard normal distribution random variable corresponding to i^{th} load level.

– σ_i is standard deviation representing the uncertainty of P_i.

– $P_{\sigma i}$ is random sample value around P_i.

It is necessary to say that for standard deviation for all nodes a value of 10% was adopted.

In this calculation, only the active power is modelled as a random variable. The reactive power changes with the active power according to constant power factor. For the power factor value 0.95 has been adopted.

5.5. Model for wind power production uncertainty

Data on wind speed have been obtained by the measurements taken at the location Belo Blato near Zrenjanin for the period of one year. Figure 5.5 shows the wind speed distribution obtained by the measurements [42].

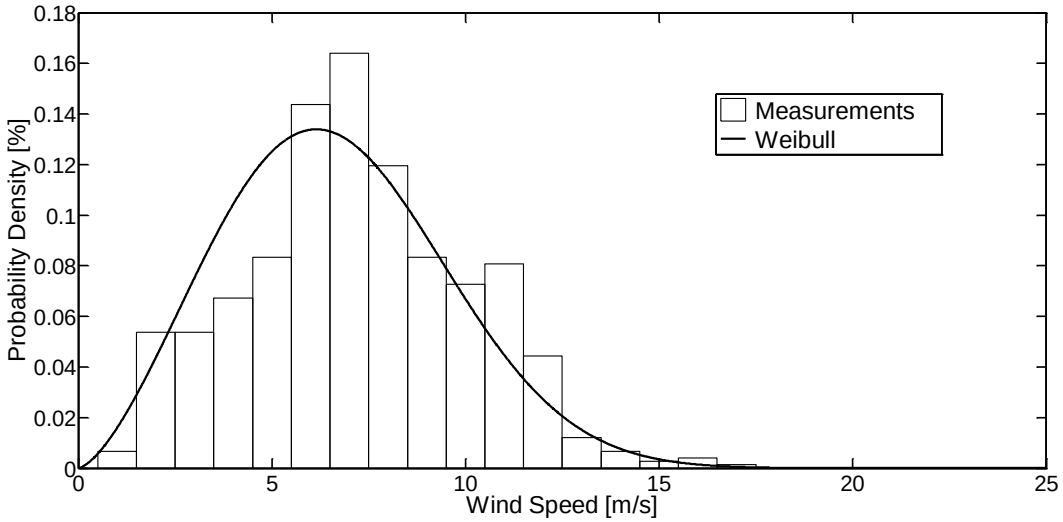

Figure 5.5. The histogram of wind data and Weibull distribution.

Wind speed random variations can usually be modeled by a Weibull PDF as described in Chapter 3. On the basis of the measured data, the Weibull PDF parameters are calculated as δ =7.54 m/s for scale parameter and β =2.5 for shape parameter. Figure 5.5 also shows the Weibull PDF corresponding to the measured data. It can be concluded that the Weibull PDF adequately models the measured data [42].

For modeling a WT's output power uncertainty, the wind speed samples are generated according to Weibull PDF. The generated wind speed samples can be transformed to the wind turbine output power by using the wind turbine power curve as described in Chapter 3.

5.6. Model for solar power plant production uncertainty

Data on solar radiation have been obtained by one year measurements at the location Belo Blato near Zrenjanin. Figure 5.6 shows the solar radiation distribution obtained by the measurements. Solar radiation random variations can usually be modeled by a Beta PDF as described in Chapter 3. On the basis of the measured data, the following shape parameters of Beta PDF have been obtained: α=0.151 and β=0.963. For the purpose of applying the MCS method, the corresponding number of samples for the solar radiation, in accordance with the Beta PDF has been generated. On the basis of the solar radiation values, the PV panel output power can be calculated by means of the radiation-power curve as described in Chapter 3.

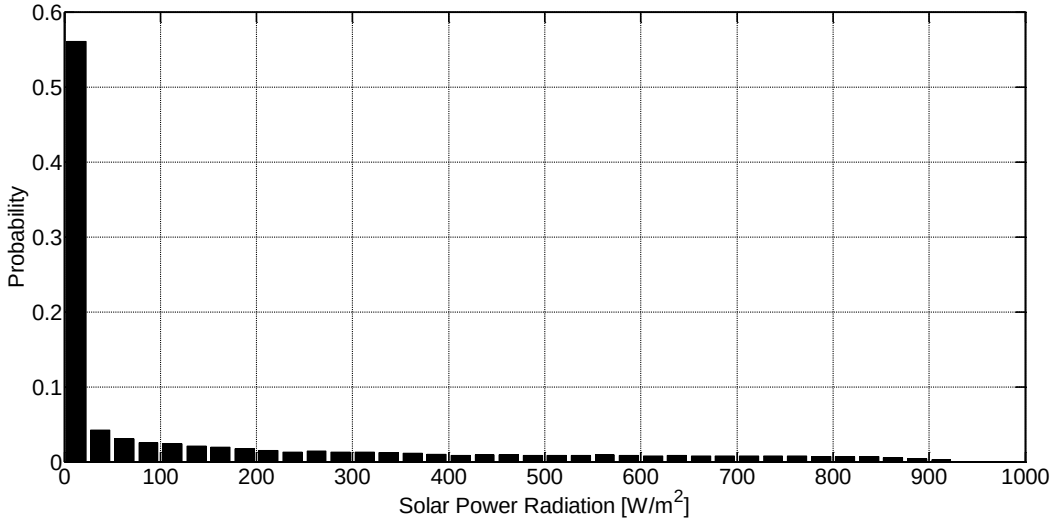

Figure 5.6. Solar radiation probability distribution.

For the purpose of calculating power flows within the distribution network, the WT and SPP output powers are modelled as negative loads in the corresponding node. Modern WTs and SPPs are connected to the grid via converters which can either absorb or generate reactive power within a declared range. Under such conditions, WTs and SPPs may participate in voltage regulation. The optimisation model presented in this work enables calculations even under conditions when the power factor is not unity, as is the case of a WT having an induction machine absorbing reactive power or modern SPPs and WTs capable of participating in voltage regulation. In this thesis, for the purpose of the analysis, it has been assumed that power factor of the operating WT and SPP was unity. This assumption has been introduced because the national technical rules do not require the use of DG units in voltage regulation. Also, owners of DG units wish to minimise losses in the interconnection lines through the operating DG units without exchange of reactive power with the distribution network [42].

5.7. The correlation between random variables

In stochastic calculations, it is important to take into account the correlation between the sets of random variables. The following correlations are considered in this calculation:

– the correlation between the active power consumptions.

– the correlation between WTs production.

– the correlation between SPPs production.

The correlations between active power consumption and DGs production are not considered in this calculation, although the proposed method allows it. There are many reasons for that. The measurements of power consumption, wind speed and solar radiation were not synchronized. It is therefore not possible to determine the correct correlation coefficients between them. Also, because of different nature, power consumption, wind speed and solar radiation do not have a strong correlation.

The following values for correlation coefficients are used in the calculation. The correlation coefficient between active power consumption for all nodes was 0.8, between WTs production was 0.9, and between SPPs production was also 0.9. The values for correlation coefficients are summarized in Table 5.5.

Table 5.5. The correlation coefficients.

	Power consumption	WTs production	SPPs production
Power consumption	0.8	-	-
WTs production	-	0.9	-
SPPs production	-	-	0.9

5.8. The results and discussion

Prior to the optimisation and determination of optimum locations and installed powers of the shunt capacitors, the basic calculation, i.e. the calculation without built-in capacitors, is carried out. The purpose of this calculation is to identify voltage profile of the network before the compensation. By applying MCS the calculation is performed for all 6 levels of consumption indicated in Figure 5.4. The calculation is performed for 10000 samples of active load, wind speed, and solar radiation. It should be mentioned that 10000 is the standard number of samples for the MCS method. To all 10000 samples, the Backward/Forward algorithm has been applied to calculate power flows. For each node, the expected voltage value has been obtained. Values of the expected node voltages for all 6 levels of consumption are given in Figure 5.7 [42].

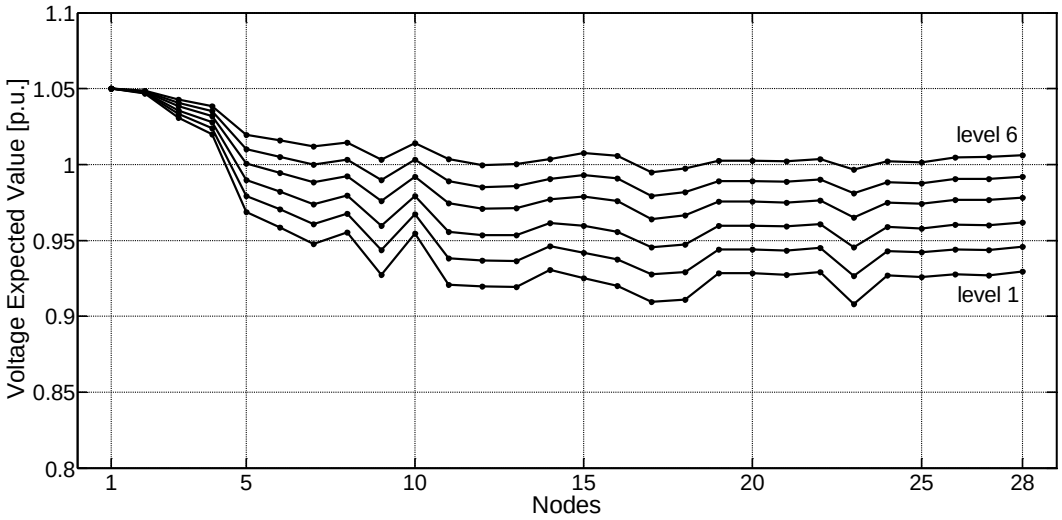

Figure 5.7. Voltage profile of the network before building-in the shunt capacitors.

From Figure 5.7 one can see that for the first and second load levels the expected voltage values of the majority of nodes are below 0.95 p.u. Since voltage value of the feeding node (node 1) is set at 1.05 p.u., it can be concluded that the expected values below 0.95 are not acceptable. For the purpose of improving this voltage profile application of the shunt, compensation is one of the realistic and efficient solutions [42].

Simultaneous optimisation of the proposed criterion functions by the proposed method has been carried out assuming three scenarios. In all scenarios, the calculations were performed for the highest analyzed load level in the network (level 1). In the calculations, the voltage value of the feeding node 1.05 p.u. was taken for the reference voltage value U_{ref}. For all scenarios, the number of samples for MCS was N_{MC}=10000. The calculations were performed assuming the population of 20 chromosomes and 200 generations. The first scenario analyzed the installation of only one shunt capacitor. In this scenario, two calculations were executed. The first calculation takes into account the correlation between the random variables. The second calculation was executed without correlation. The results of the optimisation for the first scenario are presented in Figure 5.8 in the criterion functions space.

The second scenario analyzed the installation of two shunt capacitors. Similar to the previous scenario two calculations were executed. The results of the optimisations in the criterion functions space for the second scenario are presented in Figure 5.9.

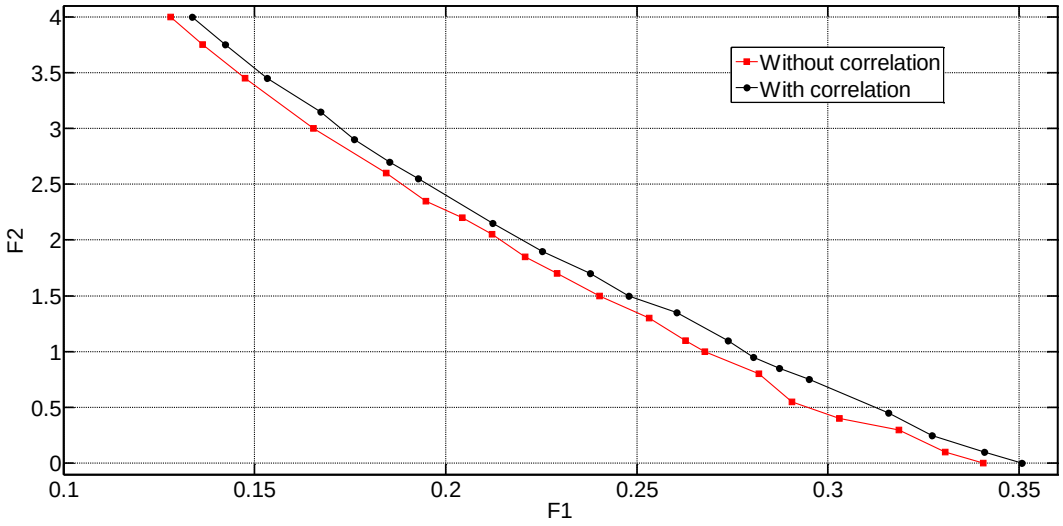

Figure 5.8. Results for the first scenario.

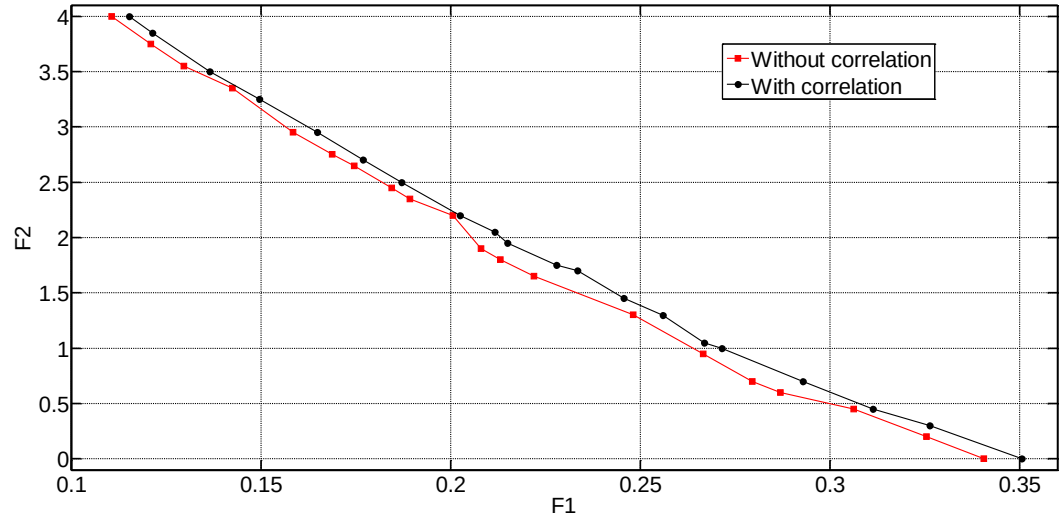

Figure 5.9. Results for the second scenario.

Figures 5.8 and 5.9 show that the results without correlation are better than the results with correlation. However, these results are not real because the correlation between the network variables exists. Figures 5.8 and 5.9 clearly indicate an error that occurs if the calculation does not take into account the correlation between random variables. In any case, it is clear that respecting the correlation between random variables is necessary. All further considerations will refer to the case when the correlation is considered.

The third scenario analyzed the installation of three shunt capacitors. In this scenario, only a calculation with a correlation between network variables was executed.

The results of the optimisations for all three analyzed scenarios are presented in Figure 5.10 in the criterion functions space. The results show how the installed power of the shunt capacitors affects voltage profile of the network. Figure 5.10 indicates that the results accomplished by using two capacitors are best. The results with two shunt capacitors are significantly better than results with only one shunt capacitor. On the other hand, the results with three shunt capacitors are only slightly better compared to results with two shunt capacitors. For this reason scenario with two shunt capacitors has been taken for further analysis. For the purpose of clarity, Figure 5.11 shows the results only for this scenario.

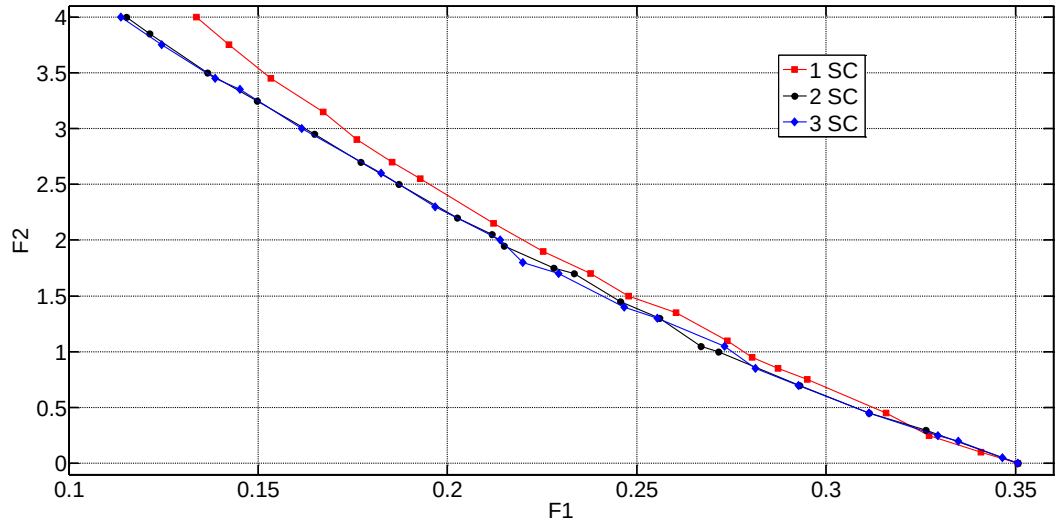

Figure 5.10. Comparative results for the three analyzed scenarios.

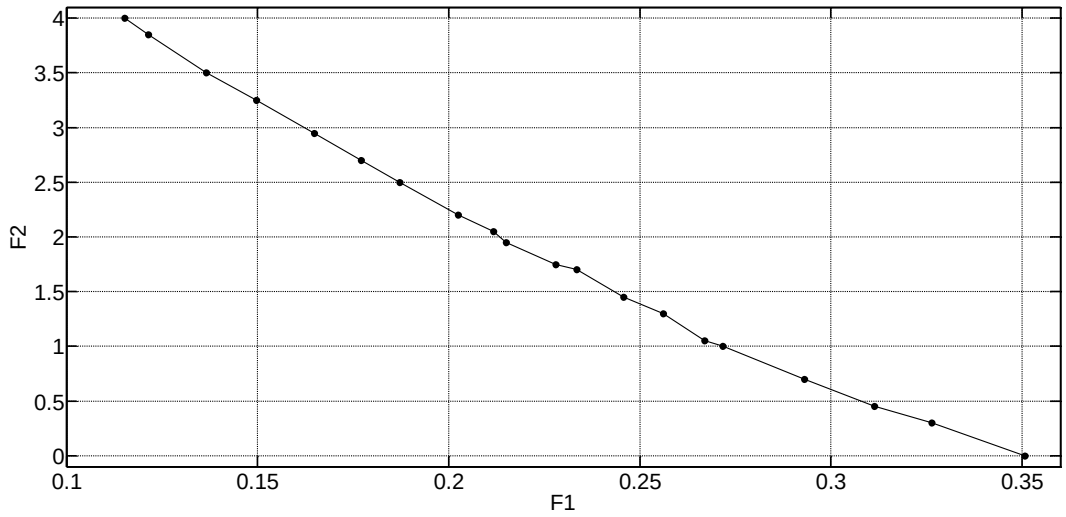

Figure 5.11. Results of optimisation for the scenarios with two shunt capacitors.

Table 5.6 shows data of the set of the obtained optimum solutions for the case of building-in two shunt capacitors. In addition to the locations and shunt capacitor powers, Table 5.6 also contains values of the criterion functions. It can be seen that in the optimization process the solution without built-in capacitors has been obtained (solution 20). This indicates that the space of control variables has been searched well by the selected algorithm. According to the theory of multi-criterion optimization, all obtained solutions are optimal therefore an additional analysis is required in order to select the corresponding solution for the analyzed distribution network [42].

Table 5.6. The obtained set of optimum solutions.

Solutions	Nodes (sizing in Mvar)	f_1	f_2
1	18 (2.00), 27 (1.00)	0.1153	4.00
2	18 (2.1), 27 (1.75)	0.1214	3.85
3	18 (2.00), 27 (1.50)	0.1366	3.50
4	18 (1.25), 27 (2.00)	0.1497	3.25
5	18 (1.95), 20 (1.00)	0.1648	2.95
6	18 (2.00), 26 (0.7)	0.1770	2.70
7	18 (1.50), 20 (1.00)	0.1872	2.50
8	18 (1.05), 20 (1.15)	0.2025	2.20
9	20 (1.00), 15 (1.05)	0.2117	2.05
10	20 (0.95), 23 (1.00)	0.2150	1.95
11	20 (0.65), 18 (1.10)	0.2280	1.75
12	18 (0.70), 23 (1.00)	0.2334	1.70
13	20 (0.45), 23 (1.00)	0.2457	1.45
14	20 (0.30), 23 (1.00)	0.2560	1.30
15	20 (0.35), 23 (0.70)	0.2668	1.05
16	20 (0. 50), 13 (0.50)	0.2716	1.00
17	20 (0.70), 26 (0.00)	0.2930	0.70
18	20 (0.45), 16 (0.00)	0.3114	0.45
19	18 (0.05), 15 (0.25)	0.3263	0.30
20	13 (0.00), 13 (0.00)	0.3506	0.00

With the aim of selecting a unique compromise solution, the minimum and maximum expected voltage values of the complete set of optimum solutions for both the highest (level 1) and the lowest (level 6) load levels have been analyzed. As far as exceeding voltage limits is concerned, for load level 1 the minimum limits are relevant, while for load level 6 the maximum limits are relevant [42]. These values for all obtained solutions are shown in Figure 5.12. For the remaining load levels (levels 2 to 5) the expected voltage values are between the two limits indicated in Figure 5.12. If value 0.95 p.u. is adopted for the minimum and 1.05 p.u. for the maximum permitted voltage value, it can be seen that solution 7 contains the least violations of the permitted limits when both considered load levels are taken into account. Ideally, the solution should contain no violation of the permitted limits, but here this is not the case. The expected voltage values of solution 7 are such that violations of the permitted limits are very small. Consequently, solution 7 can be taken as the selected one. This solution implies building-in one shunt capacitor of power 1.50 Mvar at node 18 and one shunt capacitor of power 1.00 Mvar at node 20.

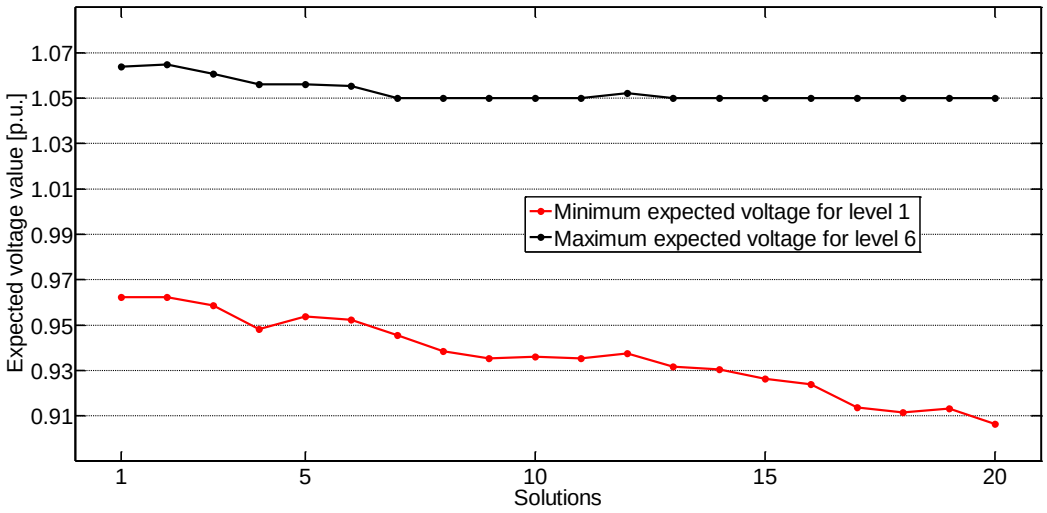

Figure 5.12. The minimum and maximum expected voltage values for levels 1 and 6, respectively.

Improving voltage profile in a network can be realized by using switched capacitors. The fixed and variable values when using switched capacitors can be selected on the basis of the obtained solutions shown in Table 5.6 and the expected voltage values for different load levels (level 1 to level 6). However, it should be mentioned that the solutions using switched capacitors are significantly more expensive [42].

The main goal of optimisation is to improve voltage profile of entire distribution network. However, the installation of the shunt capacitor significantly reduces the active power losses in the distribution network. Also, installation of the shunt capacitor reduces the load on heavy loaded lines in the distribution network. Figure 5.13 shows the active power losses in the distribution network for all solutions in Figure 5.11 and Table 5.6. Figure 5.14 shows relative line load of two most loaded lines of the distribution network for the same solutions. It is necessary to say that the results from the Figures 5.13 and 5.14 are given for the load level 1.

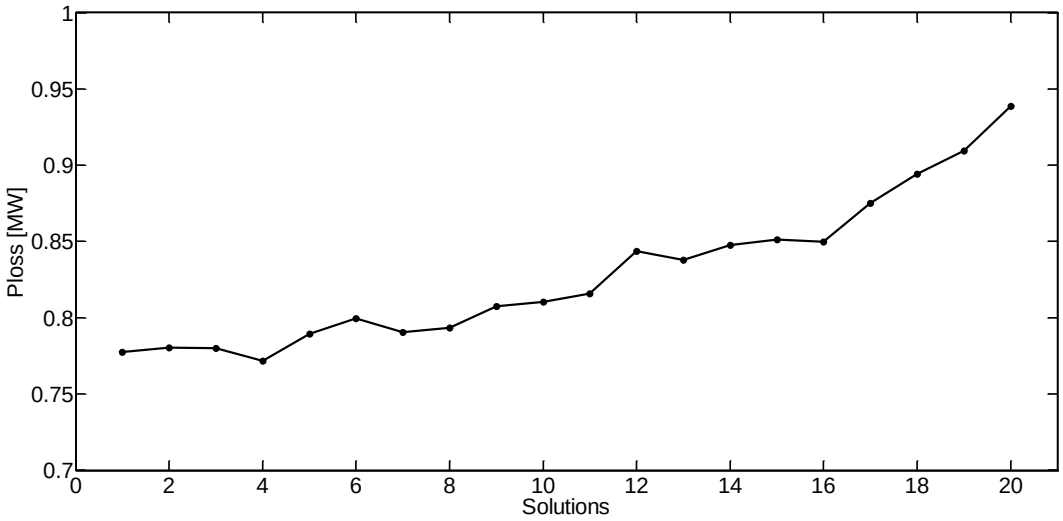

Figure 5.13. Active power losses in distribution network for the solutions in Figure 5.11.

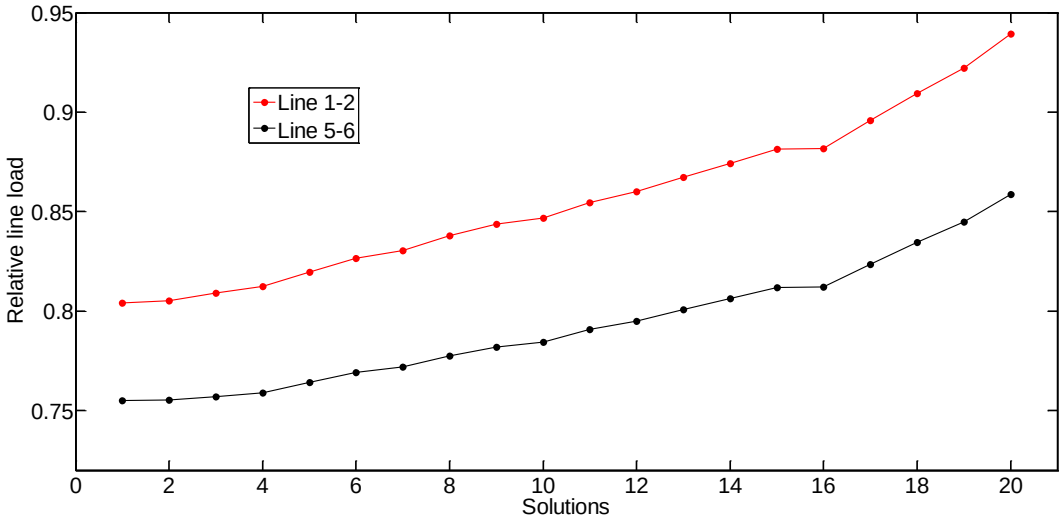

Figure 5.14. Relative line load for two most loaded lines for the solutions in Figure 5.11.

Concretely, building-in the suggested shunt capacitors (solution 7) reduces significantly the active power and energy losses. Table 5.7 shows the expected active power and energy losses prior to building-in shunt capacitors, while Table 5.8 shows the situation after building-in the suggested shunt capacitors (solution 7). Besides data concerning the individual load levels, the expected annual active energy losses are also shown. It can be seen from the tables that by building-in shunt capacitors one can expect annual active energy saving of 0.658 GWh. The average cost of (1 MWh) in the Republic of Serbia amounts (60 €). Consequently, the expected annual saving would be $658 \times 60 = 39480$ €. If one assumes that the average cost of building-in shunt capacitors is (4 €/kvar), the cost of building-in the suggested shunt capacitors would be $2500 \times 4 = 10000$ €. Obviously, this investment would pay off within several months.

Table 5.7. The expected active power and energy losses before the compensation.

Load level	1	2	3	4	5	6
$E(P_{loss})$ [MW]	0.942	0.736	0.579	0.453	0.338	0.254
$E(W_{loss})$ [GWh]	1.318	1.164	1.057	0.716	0.349	0.340
$E(W_{lossTot})$ [GWh]	4.944					

Table 5.8. The expected active power and energy losses after the compensation.

Load level	1	2	3	4	5	6
$E(P_{loss})$ [MW]	0.789	0.626	0.510	0.407	0.300	0.229
$E(W_{loss})$ [GWh]	1.105	0.993	0.929	0.642	0.310	0.307
$E(W_{lossTot})$ [GWh]	4.286					

Chapter 6. Conclusions

Electricity is very important in building any country, where electricity is indispensable for homes, factories or shops. In order for the electricity to reach the consumer, it passes through several stages. These stages are the generation, transmission and distribution. Distribution is carried out through electrical distribution networks. Distribution networks have great attention worldwide. Improve these distribution networks and work on the use of modern technology in them become very necessary. The increase in both power demand and the reactive power flow in distribution systems lead to increases the losses and reduces the line voltages. To avoid the expensive options, there is a need for reactive power compensation in the distribution systems to improve the voltage profile, reduce the power demand in the networks and other benefits. It is necessary to choose the correct location and size of the reactive power compensation. One of the reactive power compensation ways is the use of shunt capacitors. The main purposes of the shunt capacitors are to voltage profile improvement, maximize transmitted power flowing through the networks and improving the efficiency of distribution systems.

In this thesis, a new method for finding the optimal sizes and locations of the shunt capacitors in distribution networks with DG units has been introduced. The proposed method uses multiobjective optimisation and respects the uncertainties associated with load demand and DG power production by applying Monte Carlo Simulation methods. Also, it takes into account the correlation between sets of random variables. The probabilistic optimisation in this method allows a more comprehensive

approach to solving the problems of optimum locations of shunt capacitors compared to the deterministic models which are mainly met in the literature.

The optimisation problem is modeled by simultaneous optimisation of two objective functions with the aim of improving voltage profile in a network by optimal selection of the locations and installed powers of the shunt capacitors. The two objective functions are optimised simultaneously by applying the Non-dominated Sorting Genetic Algorithm II (NSGA-II). NSGA-II algorithm was chosen because it represents one of the standard procedures for solving multiobjective optimisation problems. Several feasible solutions can be resulted to select the appropriate solution from them.

The proposed method was applied to a real radial medium voltage distribution network which suffers from voltage drops and active power losses despite there is a power production from DGs in this distribution network. By applying this method to the distribution network in three scenarios, a set of optimal solutions were obtained for every scenario. The first and the second scenarios contain the installation of only one and two shunt capacitors respectively with and without taking into account the correlation between the random variables. The third scenario analyzes the installation of three shunt capacitors with taking into account the correlation between the random variables. It is clear that an error occurs if the calculation does not take into account the correlation between random variables. The active power consumption, the solar radiation and wind speed data for all scenarios have been modeled by using one-year measurements.

The set of optimal solutions represents a compromise between voltage profile in a distribution network and total installed power of the applied shunt capacitors. A method for selecting the final solution from this set of optimal solutions has been proposed. Even though the active power losses have not been the subject of optimization, calculation of the expected annual active energy losses was performed. The result indicates that the saving of active energy compared to the situation prior to building-in shunt capacitors is very significant. In view of the obtained results, it can be said that the proposed method can be successfully applied for identification of optimum locations and installed powers of the shunt capacitors built-in a distribution network containing DG units.

References

[1] Abul'Wafa, A.R.:'Optimal capacitor allocation in radial distribution systems for loss reduction: a two stage method', Elec. Power Syst. Res. 2013, 95, pp.168–174.

[2] Nojavan, S., Jalali, M., Zare, K.: 'Optimal allocation of capacitors in radial/mesh distribution systems using mixed integer nonlinear programming approach', Electr. Power Syst. Res., 2014, 107, pp. 119– 124.

[3] Lee, C-S., Ayala, H.V.H., Coelho L.S.: 'Capacitor placement of distribution systems using particle swarm optimization approaches', Int. J. Electr. Power Energy Syst., 2015, 64, pp. 839–851.

[4] Mohkami, H., Hooshmand, R., Khodabakhshian, A.: 'Fuzzy optimal placement of capacitors in the presence of nonlinear loads in unbalanced distribution networks using BF-PSO algorithm', Applied Soft Computing, 2011, 11, pp. 3634–3642.

[5] Chen, S., Hu, W., Su, C., et al.: 'Optimal reactive power and voltage control in distribution networks with distributed generators by fuzzy adaptive hybrid particle swarm optimisation method', IET Gener. Transm. Distrib., 2015, 9, (11), pp. 1096-1103.

[6] Razak, M.A.A., Othman, M.M., Shahidan, M.B., et al.: 'Optimal capacitor placement and sizing in an unbalanced three-phase distribution system using particle swarm optimization technique'. IEEE Proc. 8th International Power Engineering and Optimization Conference (PEOCO), Langkawi, Malaysia, March 2014, pp. 624-629.

[7] Sonwane, P.M., Kushare, B.E.: 'Optimal capacitor placement and sizing for enhancement of distribution system reliability and power quality using PSO'. International Conference for Convergence of Technology (I2CT), Pune, India, April 2014, pp. 1-7.

[8] Kanwar, N., Gupta, N., Swarnkar, A., et al.: 'New Sensitivity based Approach for Optimal Allocation of Shunt Capacitors in Distribution Networks Using PSO', Energy Procedia, 2015, 75, pp. 1153-1158.

[9] Rao, R.S., Narasimham, S.V.L., Ramalingaraju, M.: 'Optimal capacitor placement in a radial distribution system using Plant Growth Simulation Algorithm', Int. J. Electr. Power Energy Syst., 2011, 33, (5), pp. 1133–1139.

[10] Abou El-Ela, A.A., El-Sehiemy, R.A., Kinawy, A.M., et al.: 'Optimal capacitor placement in distribution systems for power loss reduction and voltage profile improvement', IET Gener. Transm. Distrib., 2016, 10, (5), pp. 1209-1221.

[11] Shuaib, Y.M., Kalavathi, M.S., Rajan, C.C.A.: 'Optimal capacitor placement in radial distribution system using Gravitational Search Algorithm', Int. J. Electr. Power Energy Syst., 2015, 64, pp. 384-397.

[12] Vuletić, J., Todorovski, M.: 'Optimal capacitor placement in distorted distribution networks with different load models using Penalty Free Genetic Algorithm', Int. J. Electr. Power Energy Syst., 2016, 78, pp. 174-182.

[13] Montoya, D.P., Ramirez, J.M., Zuluaga, J.R.: 'Multi-objective optimization for reconfiguration and capacitor allocation in distribution systems'. North American Power Symposium (NAPS), Pullman, USA, Sept. 2014, pp. 1-6.

[14] Gallano, R.J.C, Nerves, A.C.: 'Multi-objective optimization of distribution network reconfiguration with capacitor and distributed generator placement'. IEEE Region 10 Conference (TENCON), Bangkok, Thailand, Oct. 2014, pp. 1-6.

[15] Azevedo, M.S.S., Abril, I.P., Leite, J.C., et al.: 'Capacitors placement by NSGA-II in distribution systems with non-linear loads', Int. J. Electr. Power Energy Syst., 2016, 82, pp. 281-287.

[16] Tabatabaei, S.M., Vahidi, B.: 'Bacterial foraging solution based fuzzy logic decision for optimal capacitor allocation in radial distribution system', Electr. Power Syst. Res., 2011, 81, (4), pp. 1045–1050.

[17] El-Fergany, A.A.: 'Optimal capacitor allocations using integrated evolutionary algorithms', IET Gener. Transm. Distrib., 2013, 7, (6), pp. 593–601.

[18] El-Fergany, A.A., Abdelaziz, A.Y.: 'Capacitor allocations in radial distribution networks using cuckoo search algorithm', IET Gener. Transm. Distrib., 2014, 8, (2), pp. 223–232.

[19] Ramadan, H.A., Wahab, M.A.A., El-Sayed, A-H.M., et al.: 'A fuzzy-based approach for optimal allocation and sizing of capacitor banks', Electr. Power Syst. Res., 2014, 106, pp. 232– 240.

[20] Duque, F.G., de Oliveira, L.W., de Oliveira, E.J., et al.: 'Allocation of capacitor banks in distribution systems through a modified monkey search optimization technique', Int. J. Electr. Power Energy Syst., 2015, 73, pp. 420-432.

[21] Taher, S.A., Bagherpour, R.: 'A new approach for optimal capacitor placement and sizing in unbalanced distorted distribution systems using hybrid honey bee colony algorithm', Int. J. Electr. Power Energy Syst., 2013, 49, pp. 430–448.

[22] Ali, E.S., Abd Elazim, S.M., Abdelaziz, A.Y.: 'Improved Harmony Algorithm and Power Loss Index for optimal locations and sizing of capacitors in radial distribution systems', Int. J. Electr. Power Energy Syst., 2016, 80, pp. 252-263.

[23] Ali, E.S., Abd Elazim, S.M., Abdelaziz, A.Y.: 'Improved Harmony Algorithm for optimal locations and sizing of capacitors in radial distribution systems', Int. J. Electr. Power Energy Syst., 2016, 79, pp. 275-284.

[24] Muthukumar, K., Jayalalitha, S.: 'Optimal placement and sizing of distributed generators and shunt capacitors for power loss minimization in radial distribution networks using hybrid heuristic search optimization technique', Int. J. Electr. Power Energy Syst., 2016, 78, pp. 299-319.

[25] Carpinelli, G., Noce, C., Proto, D., et al.: 'Single-objective probabilistic optimal allocation of capacitors in unbalanced distribution systems', Electr. Power Syst. Res., 2012, 87, pp. 47–57.

[26] Kavousi-Fard, A. Niknam, T.: 'Considering uncertainty in the multi-objective stochastic capacitor allocation problem using a novel self adaptive modification approach', Electr. Power Syst. Res., 2013, 103, pp. 16– 27.

[27] Mukherjee, M., Goswami, S. K. : 'Solving capacitor placement problem considering uncertainty in load variation', Int. J. Electr. Power Energy Syst., 2014, 62, pp. 90–94.

[28] Zeinalzadeh, A., Mohammadi, Y., Moradi, M.H.: 'Optimal multi objective placement and sizing of multiple DGs and shunt capacitor banks simultaneously considering load uncertainty via MOPSO approach', Int. J. Electr. Power Energy Syst., 2015, 67, pp. 336-349.

[29] Jain, N., Singh, S.N., Srivastava, S.C.: 'PSO based placement of multiple wind DGs and capacitors utilizing probabilistic load flow model', Swarm and Evolutionary Computation, 2014, 19, pp. 15–24.

[30] Li, W.: 'Probabilistic Transmission System Planning' (Wiley-IEEE Press, 2011).

[31] Andrés Feijóo, Daniel Villanueva, José Luis Pazos, Robert Sobolewski, 'Simulation of correlated wind speeds: A review', Renewable and Sustainable Energy Reviews 15 (2011) 2826– 2832.

[32] Andrés Feijóo, Robert Sobolewski, 'Simulation of correlated wind speeds', International Journal of Electrical Energy Systems Volume 1, Number 2, July-December 2009, pp. 99 – 106.

[33] B. Ravi Teja, V.V.S.N. Murty, Ashwani Kumar.: 'An Efficient and Simple Load Flow Approach for Radial and Meshed Distribution Networks', International Journal of Grid and Distributed Computing Vol. 9, No. 2, (2016), pp.85-102.

[34] D. Shirmohammadi, Hong, H.W., Semlyen, A., et al.: 'A Compesation-Based Power Flow Method For Weakly Meshed Distribution And Transmision Networks'. IEEE Trans. Power Syst., 1988, 3, (2), pp. 753-762.

[35] Abdelhay A. Sallam and O. P. Malik.: 'Electric Distribution Systems', Published by John Wiley & Sons, Inc., Hoboken, New Jersey, 2011, Canada.

[36] Schneider Electric, "Power factor correction and harmonic filtering", Electrical installation guide 2008, https://www.schneider-electric.nl/documents/producten-diensten/energiebeheer/zoekfunctie-isc-catalogus/Beeld/Catalogi/Electrical/EIG-L-power-factor-harmonic.pdf.

[37] T.A. Short.: 'Electric Power distribution handbook', (CRC Press LLC., 2004).

[38] http://www.alternative-energy-tutorials.com/wind-energy/induction-generator.html

[39] Marko Čepin, Assessment of Power System Reliability, Methods and Applications, Springer-Verlag London Limited 2011.

[40] Montgomery, D.C., Runger. G.C.: 'Applied Statistics and Probability for Engineers' (John Wiley & Sons, Inc., 5th edn. 2011).

[41] Jizhong Zhu, Optimization of Power System Operation, Second Edition, John Wiley & Sons, Inc., Hoboken, New Jersey, 2015.

[42] Jannat, M.B., Savić, A.S.: ‘Optimal capacitor placement in distribution networks regarding uncertainty in active power load and distributed generation units production’IET Gener. Transm. Amp Distrib., 2016, 10, (12), pp. 3060–3067.

[43] Aien, M., Rashidinejad, M., Firuz-Abad, M. F.: ‘Probabilistic optimal power flow in correlated hybrid wind-PV power systems: A review and a new approach’, Renewable and Sustainable Energy Reviews, 2015, 41, pp. 1437–1446.

[44] MATLAB, The MathWorks, Inc. ’Statistics Toolbox’, User’s Guide Version 3, November 2000.

[45] Jürgen Branke, Kalyanmoy Deb, Kaisa Miettinen and Roman Slowiński.: "Multiobjective Optimization: Interactive and Evolutionary Approaches" Springer, Germany, 2008, Online: https://books.google.rs/books. file:///C:/Users/asd/Downloads/Book_August_14_2008.pdf

[46] Deb, K.: ‘Multi-Objective Optimization Using Evolutionary Algorithms’, (Wiley, Chichester, UK, 2001).

[47] Online website : https://prateekvjoshi.com/2016/09/15/what-is-pareto-optimality/,, 13/11/2017.

[48] R.T. Marler, J.S. Arora.: "Survey of multi-objective optimization methods for engineering", Published online 23 March 2004, Springer-Verlag 2004.

[49] Tarek BOUKTIR, Linda SLIMANI, M. BELKACEMI .: “A Genetic Algorithm for Solving the Optimal Power Flow Problem”, Leonardo Journal of Sciences. ISSN 1583-0233, Issue 4, January-June 2004. Pages 44-58.

[50] James A. Momoh.: “Electric Power System Applications of Optimization”, Marcel Dekker, Inc. 2001.

[51] Kalyanmoy Deb.: “Genetic Algorithms for Optimization” Indian Institute of Technology Kanpur. E-mail: deb@ iitk.ac.in.

[52] Md. Saddam Hossain Mukta, T.M. Rezwanul Islam and Sadat Maruf Hasnayen.: “Multiobjective Optimization Using Genetic Algorithm”, International Journal of Emerging Trends and Technology in Computer Scince [IETTCS], Volume 1, Issue 3, September–October 2012, ISSN2278-6856, Web Site:www.ijettcs.org.

[53] N. Srinivas and Kalyanmoy Deb.: “Multiobjective Optimization Using Nondominated Sorting In Genetic Algorithms” Journal of Evolutionary compution, Vol. 2, No. 3, pages 221-248.

[54] A. Jaimes, S. Martınez and C. Coello.: ‘AN INTRODUCTION TO MULTIOBJECTIVE OPTIMIZATION TECHNIQUES‘, Chapter 1, pages 1-26, Nova Science Publishers, Inc. 2009.

[55] Deb, K., Pratap, A., Agarwal, S., et al.: ‘A Fast and Elitist Multiobjective Genetic algorithm: NSGA-II’, IEEE Trans. Evol. Comput., 2002, 6, pp. 182–197.

[56] K. Deb.: ’Single and Multi-objective Optimization Using Evolutionary Computation Genetic Algorithms: NSGA-II’, KanGAL Report Number 2004002, Indian Institute of Technology, Kanpur, India.

[57] Šošić, D., Žarković, M., Dobrić, G.: ‘Fuzzy-based Monte Carlo simulation for harmonic load flow in distribution networks’, IET Gener. Transm. Distrib., 2015, 9, (3), pp. 267-275.

[58] Yu, L., Gao, S., Liu, Y.: ‘Pseudo-sequential Monte Carlo simulation for distribution network analysis with distributed energy resources’. 5th International Conference on Electric Utility Deregulation and Restructuring and Power Technologies (DRPT), Changsha, China, Nov. 2015, pp. 2684-2689.

[59] Lu, Q., Hua, Y., Shen, Y., et al.: 'Reliability evaluation of distribution network based on sequential Monte Carlo simulation'. 5th International Conference on Electric Utility Deregulation and Restructuring and Power Technologies (DRPT), Changsha, China, Nov. 2015, pp. 1170-1174.

[60] Goerdin, S.A.V., Smit, J.J., Mehairjan, R.P.Y.: 'Monte Carlo simulation applied to support risk-based decision making in electricity distribution networks'. IEEE PowerTech, 2015, Eindhoven, Netherlands, July 2015, pp. 1-5.

[61] Zio, E., Delfanti, M., Giorgi, L., et al. : 'Monte Carlo simulation-based probabilistic assessment of DG penetration in medium voltage distribution networks', Int. J. Electr. Power Energy Syst., 2015, 64, pp. 852-860.

Author Biography

Mohamed B. Jannat was born on 12/09/1975 in Benghazi (Libya). He finished secondary school in Misurata (Libya) on 1993. He was graduated from Faculty of Engineering at Garyounis University in Benghazi on 2000. he worked as a teacher in a secondary school between 2001–2003 and as an inspector in the secondary education from 2003 until 2008. Also, he worked as an electrical engineer in Misurata Company from 2008 until 2009. He had the master (M. Sc.) in Electrical Engineering on 2008 from Faculty of Engineering - Misurata University–Misurata (Libya). The master thesis titled "Reduction of Harmonics Generated by Electrical Arc Furnaces".

In September 2009, he started working at Faculty of Engineering-Misurata University as an assistant lecturer. In his work at the faculty, he was engaged in teaching in the subjects of Analysis of Power Systems, Electrical Machines, Electrical Materials Science, Electrical Circuits and High voltages. In addition to teaching activities, he participated in the supervising of several scientific projects for undergraduate students. He was promoted from Lecturer Assistant to Lecturer in 2013. He also served as the chairman of the receipt of maintenance committee at the University of Misurata on 2013.

He has some papers which were published in international conferences, an international journal and a number of papers published at domestic conferences.

ИЗЈАВА О АУТОРСТВУ

Потписани: Mohamed B. Jannat

Број уписа: 5055/2013

Изјављујем

да је докторска дисертација под насловом

Анализа оптималне снаге и локације оточних батерија кондензатора у активним дистрибутивним мрежама

- резултат сопственог истраживачког рада;
- да предложена дисертација у целини ни у деловима није била предложена за добијање било које дипломе према студијским програмима других високошколских установа;
- да су резултати коректно наведени и
- да нисам кршио ауторска права и користио интелектуалну својину других лица.

Потпис докторанда

У Београду, 21.8.2018. године

ИЗЈАВА О ИСТОВЕТНОСТИ ШТАМПАНЕ И ЕЛЕКТРОНСКЕ ВЕРЗИЈЕ ДОКТОРСКЕ ДИСЕРТАЦИЈЕ

Име и презиме аутора: Mohamed B. Jannat

Број уписа: 5055/2013

Студијски програм: Електротехника и рачунарство

Наслов рада: Анализа оптималне снаге и локације оточних батерија кондензатора у активним дистрибутивним мрежама

Ментор: др Жељко Ђуришић, доцент

Потписани: Mohamed B. Jannat

Изјављујем да је штампана верзија мог докторског рада истоветна електронској верзији коју сам предао за објављивање на порталу **Дигиталног репозиторијума Универзитета у Београду.**

Дозвољавам да се објаве моји лични подаци везани за добијање академског звања доктора наука, као што су име и презиме, година и место рођења и датум одбране рада.

Ови лични подаци могу се објавити на мрежним страницама дигиталне библиотеке, у електронском каталогу и у публикацијама Универзитета у Београду.

Потпис докторанда

У Београду, 21.8.2018. године

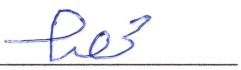

ИЗЈАВА О КОРИШЋЕЊУ

Овлашћујем Универзитетску библиотеку „Светозар Марковић“ да у Дигитални репозиторијум Универзитета у Београду унесе моју докторску дисертацију под насловом:

Анализа оптималне снаге и локације оточних батерија кондензатора у активним дистрибутивним мрежама

која је моје ауторско дело.

Дисертацију са свим прилозима предао сам у електронском формату погодном за трајно архивирање.

Моју докторску дисертацију похрањену у Дигитални репозиторијум Универзитета у Београду могу да користе сви који поштују одредбе садржане у одабраном типу лиценце Креативне заједнице (Creative Commons) за коју сам се одлучио.

1. Ауторство
2. Ауторство – некомерцијално
3. Ауторство – некомерцијално – без прераде
4. Ауторство – некомерцијално – делити под истим условима
5. Ауторство – без прераде
6. Ауторство – делити под истим условима

Потпис докторанда

У Београду, 21.8.2018. године